

Targeting the oncogenic signaling of the transcription factor STAT3 with potent and selective monobody inhibitors

Présentée le 31 mars 2020

à la Faculté des sciences de la vie
Unité du Prof. Radtke
Programme doctoral en approches moléculaires du vivant

pour l'obtention du grade de Docteur ès Sciences

par

Grégory LA SALA

Acceptée sur proposition du jury

Prof. E. Meylan, président du jury
Prof. F. Radtke, Prof. O. Hantschel, directeurs de thèse
Prof. V. Zoete, rapporteur
Prof. V. Sexl, rapporteuse
Prof. B. Correia, rapporteur

ACKNOWLEDGEMENTS

First and foremost, I would like to thank my thesis advisor, Oliver Hantschel, for the opportunities he has given me over these last four years, for the freedom we had in our research, and for his unconditional support throughout my PhD. I am particularly grateful to you, as even in stressful times, I could always trust that you would do the right thing and that you would assume your responsibilities towards your students. This has been very noble of you and I shall aim to behave similarly.

I also would like to thank Freddy Radtke, my thesis co-director, for agreeing to take me onboard when nothing forced him to do so. I was particularly positively surprised when you immediately agreed to become my co-director, despite the administrative burden, without needing me to extensively plead my case. Thank you as well for your support which, I am sure, proved valuable when I was awarded an EMBO short-term fellowship.

Furthermore, I would like to thank my thesis jury, along with the previous committees who gave me feedbacks throughout my PhD: Prof. Etienne Meylan, Prof. Bruno Correia, Prof. Vincent Zoete and Prof. Veronika Sexl for their scientific inputs, valuable discussions and for the time they invested in the revision of this work.

There is something to learn from everyone, and learning is what I did for these last four years. This thesis marks the end of a journey towards obtaining my PhD. I have not walked the path alone, and I have grown on many levels. I am grateful to the people who walked with me, even for a moment, as they helped me understand what, and who I would like to be.

I would like to thank Sandrine Georgeon, for being a role model both on a personal and on a professional level. I very much appreciated the scientific discussions we had, and thank you for your empathy during the more difficult times, as well as for your continuous support and care. Furthermore, I want to thank the entire Hantschel lab for the lessons I learnt from all of you. Thank you for your inputs and scientific contributions to my work. You helped me become an independent scientist and for that, I will forever be grateful.

Similarly, I would like to thank the entire Gönczy lab for their cheerful attitude, for the good memories and for unofficially “adopting me” when my lab moved to Germany. I am particularly grateful to Georgios Hatzopoulos. I owe you my deepest thanks for the countless times I interrupted you with questions, and for all the solutions or advices you provided with a smile. You have been

Acknowledgements

an outstanding scientific mentor, especially when teaching me the computational aspects of ChimeraX.

I am also grateful to my friends, to those I knew for a long time and to those I met at EPFL. I was really privileged to join the Association of Doctoral students in life sciences (ADSV). I will remember the exiting times we had discussing science and philosophy. Elias, Timo, Alexandra, Lucie, Silvia and Allie, thank you all for the moments we shared together. There are few people I will forever associate with my time at EPFL, but you are all among them. I wish you all the best for your future lives.

I would like to thank my family. Merci à mon père, à ma mère et à ma sœur pour leur soutiens inconditionnel. Merci pour avoir sacrifié tant en ne souhaitant rien en retour. Merci pour votre amour et pour avoir été des modèles dans ma vie.

Last, but foremost to my heart, I want to thank the person who shared my life for these last four years. Laure, I am incredibly lucky to have you in my life, thank you for your everlasting support – I could not have done this PhD without you. Thank you for your ideas and suggestions regarding my work and for the moments we shared together which are worth everything to me. Thank you for teaching me so much and making me a better person. Words cannot express how thankful and glad I am to share my life with you.

ABSTRACT

Many targeted cancer therapies fail to improve the overall survival of patients. Limitations involve low drug selectivity and the rapid development of resistance. Moreover, the majority of oncogenic drivers presently remain considered as “undruggable” as these proteins often lack well-defined binding pockets able to fit small molecular antagonists. The need for novel strategies to expand the number of “druggable” targets thus appears crucial.

STAT3 is a transcription factor that is constitutively active in a majority of solid and hematological tumors. It is considered a central target for cancer therapies, as it induces the transcription of genes essential for tumor proliferation, including anti-apoptotic genes, cell cycle regulators and angiogenic factors. Therefore, the inhibition of STAT3 represents a promising therapeutic strategy. However, the targeting of STAT3 still remains a formidable challenge due to the sparse number of chemical probes able to bind to non-enzymes. The engineering of protein binders could overcome many of the challenges in developing STAT3 antagonists. While most common approaches to preclude STAT3 activation consist in either inhibiting its phosphorylation by upstream tyrosine kinases with clinically-approved drugs, or in preventing the SH2 domain-dependent STAT3 dimerization using pre-clinical small molecule probes, the targeting of other STAT3 domains, such as its Coiled-coil or N-terminal domains, has not been thoroughly investigated.

Our lab uses small engineered antibody mimics derived from a fibronectin type 3 scaffold – termed monobodies – capable of high affinity and selective binding. In addition, their small size (~10 kDa) and lack of disulfide bonds makes them promising candidates for intracellular antagonistic use. In this work, we selected several monobodies using phage and yeast display that bind to previously untargeted domains of STAT3 with low nanomolar affinities. The monobodies MS3-6 and MS3-N3, binding to the Coiled-coil and N-terminal domain of STAT3 respectively, showed high selectivity to STAT3 as compared to other STAT family members and other unrelated proteins. Additionally, the monobodies strongly inhibited the transcriptional activity of STAT3 in luciferase reporter assays, reduced mRNA levels of STAT3 downstream genes in human lung cancer cells, decreased STAT3 phosphorylation levels upon IL-22 stimulation and interfered with STAT3 nuclear translocation. Notably, the precise blockade of these previously untargeted key domains using monobodies provide new insights into the STAT3 signaling and expand the current strategies to preclude its activity. Altogether, we have developed the first selective monobody inhibitors against a transcription factor implicated in cancer and inflammatory diseases, and used them as biochemical tools to further characterize a poorly understood alternative IL-22R signaling axis involved in STAT3-driven human disorders such as colitis and psoriasis.

Abstract

Keywords: Protein engineering, Oncogenic Signaling, Protein-protein interaction, Targeting STAT Transcription Factors, Undruggable proteins.

RESUME

Actuellement, de nombreuses thérapies ciblées contre le cancer n'ont encore qu'un faible impact sur la durée de vie des patients. Les limitations actuelles incluent une mauvaise spécificité des médicaments, ainsi que le développement rapide de résistances. De plus, la majorité des protéines oncogéniques favorisant le développement de la maladie demeurent toujours considérées comme étant « impossible à inhiber », car ces protéines n'ont pas de poches bien définies capables d'accueillir des antagonistes moléculaires. Il est donc crucial de développer de nouvelles stratégies afin d'accroître le nombre de protéines sur lesquelles nous pouvons agir.

STAT3 est un facteur de transcription constitutivement activé dans la majorité des tumeurs solides et hématologiques. Il est considéré comme étant une cible centrale pour les thérapies anticancéreuses, car il induit la transcription de gènes essentiels à la prolifération tumorale, tels que des gènes anti-apoptotiques, des régulateurs du cycle cellulaire et des facteurs angiogéniques. Par conséquent, l'inhibition de STAT3 représente une stratégie thérapeutique prometteuse. Cependant, le ciblage thérapeutique de STAT3 demeure encore un formidable défi dû au manque de sondes chimiques capables d'interagir avec des protéines non-enzymatiques. Néanmoins, l'ingénierie de protéines apparaît comme une solution pour développer des inhibiteurs de STAT3. Alors que les approches communément explorées pour bloquer l'activation de STAT3 consistent en l'inhibition de sa phosphorylation par des protéines kinases grâce à des médicaments cliniquement approuvés ou en tentant d'empêcher la dimérisation de STAT3 médiée par son domaine SH2 grâce à des composés précliniques, le ciblage alternatif de régions supplémentaires, tels que le domaine *Coiled-coil* ou N-terminal n'a pas encore été exploré.

Notre laboratoire utilise des protéines qui reproduisent la liaison des anticorps – appelés *monobodies* – dérivant d'une structure de fibronectine qui sont capables de se lier à une cible spécifique avec une affinité élevée. De plus, leurs petites tailles (~10 kDa) et l'absence de ponts disulfures dans leurs structures en font des candidats prometteurs pour une utilisation en tant qu'antagonistes intracellulaires. Dans cette thèse, nous avons utilisé des techniques d'exposition sur phages et levures afin de sélectionner plusieurs *monobodies* se liant à des domaines auparavant non ciblés de STAT3, et ce, avec de très hautes affinités (nanomolaires). Les monobodies MS3-6 et MS3-N3, se liant respectivement au domaine *Coiled-coil* et N-terminal de STAT3, ont montré une sélectivité élevée pour STAT3 par rapport aux autres membres de la famille STAT ainsi qu'à d'autres protéines non apparentées. De plus, les *monobodies* ont fortement diminué l'activité transcriptionnelle de STAT3 tel que démontré par des reporteurs luciférase, ont réduit les niveaux d'ARNm de gènes cibles de STAT3 dans des cellules cancéreuses de poumon humain, ont diminué

Résumé

les niveaux de phosphorylation de STAT3 lors de stimulations avec de l'IL-22 et ont interféré avec la translocation nucléaire de STAT3. Notamment, le blocage précis de ces domaines clés, qui n'avaient jusque-là jamais été ciblés, en utilisant des *monobodies* nous a fourni de nouvelles informations sur la signalisation de STAT3 et élargit les stratégies actuelles pour empêcher son activité.

En conclusion, nous avons développé les premiers *monobodies* inhibiteurs sélectifs contre un facteur de transcription impliqué dans le cancer et des maladies inflammatoires et les avons utilisés comme outils biochimiques pour davantage caractériser l'axe de signalisation supplémentaire du récepteur IL-22 qui est aussi impliqué dans des maladies humaines provoquées par STAT3 comme la colite et le psoriasis.

Mots-clés: Ingénierie protéique, Signaux oncogéniques, Interaction protéine-protéine, Ciblage de facteur de transcriptions STAT, Protéines impossibles à inhiber.

TABLE OF CONTENT

ACKNOWLEDGEMENTS	III
ABSTRACT	V
RESUME	VII
TABLE OF CONTENT	IX
LIST OF FIGURES.....	XI
LIST OF TABLES.....	XIII
1. INTRODUCTION	1
1.1. ONCOGENIC SIGNALING	1
1.1.1. Genetic alterations leading to cellular transformation	1
1.1.2. Protein functions and oncogenic signal transduction	2
1.1.3. The role and implication of transcription factors.....	3
1.2. TARGETED THERAPIES.....	5
1.2.1. Current approaches and limitations	6
1.2.2. What makes proteins undruggable and how to target them	7
1.3. MONOBODIES	8
1.3.1. Expanding the scope of targeted therapies using monobodies.....	10
1.4. UNDRUGGABLE TRANSCRIPTION FACTORS AS INTRACELLULAR TARGETS.....	12
1.4.1. JAK-STAT signaling pathway.....	14
1.4.2. Lessons from the STAT3 structure.....	17
1.5. STAT3 FUNCTIONS AND IMPLICATIONS IN CELLULAR PROCESSES.....	20
1.5.1. STAT3 canonical and non-canonical signaling pathway	22
1.5.2. STAT3 post translational modifications and cellular activities	24
1.6. STAT3 IMPLICATION IN TUMOR DEVELOPMENT.....	26
1.6.1. Uncontrolled STAT3 signaling during tissue repair drives tumorigenesis	26
1.6.2. Aberrant STAT3 signaling favors cancer stem cells maintenance and the development of metastatic niches	29
1.6.3. STAT3 oncogenic mutants identified in patients	29
1.6.4. STAT3 may act as a conditional oncogene.....	31
1.7. STRATEGIES TOWARDS THE TARGETING OF STAT3	32
1.7.1. Natural feedback loops	33
1.7.2. Indirect STAT3 inhibition	34
1.7.3. Direct STAT3 inhibition.....	35
2. RESULTS	37
2.1. SELECTIVE TARGETING AND INHIBITION OF STAT3 SIGNALING USING COILED-COIL AND N-TERMINAL DOMAIN SPECIFIC MONOBODIES	37
2.1.1. Generation of high affinity monobodies targeting STAT3.....	38
2.1.2. STAT3 monobodies are highly selective in cells.....	39
2.1.3. Monobodies inhibit STAT3-dependent transcription.....	45
2.1.4. The mode of action of MS3-6 differs from common targeting strategies	47
2.1.5. Structural basis of MS3-6/STAT3-CF interaction	49
2.1.6. MS3-6 reduces STAT3 nuclear translocation.....	53
2.1.7. MS3-6 reduces STAT3 Y705 phosphorylation in a IL-22R dependent manner..	57
2.2. MONOBODY EFFECTS ON SOLID AND HEMATOLOGIC CELLULAR CANCER CELL LINES	60
2.2.1. Perturbation of STAT3 signaling using monobodies does not lead to several cancer cell lines apoptosis.....	60

2.2.2. Monobody effects on STAT3 mutants identified in cancer patients	64
3. DISCUSSION.....	67
3.1. TARGETING TRANSCRIPTION FACTORS WITH MONOBODIES: FROM THEORY TO PRACTICE	67
3.2. IMPACT OF INDIVIDUAL STAT3 DOMAIN BLOCKADE USING MONOBODIES	68
3.2.1. MS3-6 mediated STAT3 inhibition relies on cumulative synergistical mechanisms	68
3.2.2. STAT3 NTD blockade by MS3-N3 as an innovative inhibitory strategy.....	70
3.3. CANCER CELL VIABILITY OFTEN DOES NOT RELY ON THE STAT3 CONSTITUTIVE SIGNALING.....	72
3.4. THE USE OF MONOBODIES AS BIOCHEMICAL TOOLS TOWARDS THE DISSECTION AND MODULATION OF STAT3 SIGNALING.....	74
3.4.1. MS3-6 interferes with alternative IL22-R signaling	74
3.4.2. Monobody mediated STAT3 targeted degradation	76
3.5. CONCLUDING REMARK AND FUTURE PERSPECTIVES	77
4. MATERIALS AND METHODS.....	81
4.1. ANTIBODIES, CELL LINES AND REAGENTS.....	81
4.2. CLONING AND PLASMIDS	81
4.2.1. Conventional cloning	81
4.2.2. Gateway cloning.....	82
4.2.3. In-Fusion cloning.....	82
4.2.4. Site directed mutagenesis	83
4.3. MONOBODY SELECTION.....	83
4.4. YEAST BINDING ASSAY	83
4.5. RECOMBINANT PROTEIN EXPRESSION	84
4.6. NI-NTA GRAVITY FLOW PURIFICATION.....	84
4.7. SIZE EXCLUSION CHROMATOGRAPHY.....	85
4.8. SDS-PAGE AND COOMASSIE STAINING.....	85
4.9. X-RAY CRYSTALLOGRAPHY.....	85
4.10. SCRIPT USED FOR STRUCTURE VISUALIZATION ON PYMOL	86
4.11. ITC.....	87
4.12. FLUORESCENCE POLARIZATION.....	88
4.13. CELL CULTURE.....	88
4.14. MAMMALIAN CELL TRANSFECTION	89
4.15. MAMMALIAN CELL LYSATE PREPARATION.....	89
4.16. WESTERN BLOT ANALYSIS.....	90
4.17. MAMMALIAN CELL TRANSDUCTION	90
4.17.1. Retroviral infection	90
4.17.2. Lentiviral infection.....	91
4.18. MONOBODY MAMMALIAN CELL EXPRESSION AND FLOW CYTOMETRY ANALYSIS	91
4.19. LUCIFERASE ASSAY	92
4.20. QUANTITATIVE REVERSE TRANSCRIPTION-POLYMERASE CHAIN REACTION (RT-QPCR)	92
4.21. TANDEM AFFINITY PURIFICATION AND MASS SPECTROMETRY	93
4.22. GST PULL DOWN ASSAY	93
4.23. NUCLEAR/CYTOPLASMIC FRACTIONATION AND IMMUNOFLUORESCENCE (IF)	94
4.24. ANNEXIN V/7AAD FLOW CYTOMETRY ANALYSIS	95
4.25. REALTIME-GLO CELL VIABILITY KIT	95
5. REFERENCES	97
CURRICULUM VITAE.....	109

LIST OF FIGURES

FIGURE 1.1: TARGETING TRANSCRIPTION FACTORS DRIVING TUMORIGENESIS.	5
FIGURE 1.2: THE CHALLENGES OF NON-ENZYMES AS DRUG TARGETS.	8
FIGURE 1.3: MONOBODIES AS ANTIBODY-MIMICS DERIVED FROM A FN3 SCAFFOLD.	9
FIGURE 1.4: PROTAC MEDIATED TARGETED DEGRADATION MECHANISM.	12
FIGURE 1.5: CURRENT STRATEGIES TO INHIBIT TRANSCRIPTION FACTORS. ...	14
FIGURE 1.6: JAK-STAT SIGNALING PATHWAY, FUNCTION AND ASSOCIATED PATHOLOGIES.	16
FIGURE 1.7: LINEAR DEPICTION OF THE DOMAIN OF THE STAT FAMILY MEMBERS.	18
FIGURE 1.8: CRYSTAL STRUCTURE OF THE STAT3 PARALLEL DIMER.	19
FIGURE 1.9: TOP VIEW CARTOON DEPICTION OF A STAT5A ANTI-PARALLEL DIMER.	20
FIGURE 1.10: CANONICAL STAT3 SIGNALING PATHWAY.	21
FIGURE 1.11: SCHEMATIC REPRESENTATION OF STAT3 ISOFORMS A AND B.	22
FIGURE 1.12: STAT3 NUCLEAR AND CYTOSOLIC ACTIVITIES.	23
FIGURE 1.13: INFLAMMATION DURING TISSUE REPAIR LEADS TO CELLULAR TRANSFORMATION UPON EXCESSIVE STAT3 SIGNALING.	28
FIGURE 1.14: GENETIC ALTERATIONS OF STAT3 IDENTIFIED IN PATIENTS.	31
FIGURE 2.1: SELECTION OF HIGH AFFINITY, STAT3 SELECTIVE MONOBODY BINDERS.	40
SUPPLEMENTARY FIGURE 2.1: STAT3 TARGET PROTEIN CONSTRUCTS AND MONOBODIES CHARACTERIZATION.	43
SUPPLEMENTARY FIGURE 2.2: MONOBODIES MS3-6 AND MS3-N3 BINDING TO STAT3 IN CELLULAR CONTEXTS.	44
FIGURE 2.2: MONOBODY INHIBITION OF THE STAT3 TRANSCRIPTIONAL ACTIVITY.	46
SUPPLEMENTARY FIGURE 2.3: RECOMBINANT P-Y705 STAT3 DIMER AND IN VITRO FLUORESCENT POLARIZATION ASSAYS.	48
FIGURE 2.3: MS3-6 INFLUENCES STAT3 DNA BINDING LEVELS.	49
FIGURE 2.4: CO-CRYSTAL STRUCTURE OF MS3-6 BOUND TO THE STAT3 COILED-COIL DOMAIN.	50
SUPPLEMENTARY FIGURE 2.4: STRUCTURAL ALIGNMENT OF THE STAT3/MS3-6 COMPLEX WITH PREVIOUSLY PUBLISHED STATS STRUCTURES.	52

FIGURE 2.5: MS3-6 REDUCES STAT3 NUCLEAR LOCALIZATION.....	55
SUPPLEMENTARY FIGURE 2.5: MS3-6 DECREASES THE NUCLEAR/CYTOSOLIC STAT3 RATIO UPON CYTOKINES STIMULATION.....	56
FIGURE 2.6: MS3-6 REDUCES STAT3 Y705 PHOSPHORYLATION LEVELS UPON IL-22 STIMULATION.....	58
SUPPLEMENTARY FIGURE 2.6: MS3-6 REDUCES STAT3 P-Y705 LEVELS UPON IL-22 STIMULATION.....	59
FIGURE 2.7: CELL LINES SCREENING FOR STAT3 SENSITIVITY.	61
FIGURE 2.8: NPM-ALK CELL PROLIFERATION AND VIABILITY ARE NOT IMPAIRED UPON MONOBODY INDUCTION.....	62
FIGURE 2.9: CONSTITUTIVE MONOBODY EXPRESSION DOES NOT LEAD TO NPM- ALK CELLS APOPTOSIS.	64
FIGURE 2.10: EFFECT OF MONOBODIES ON THE STAT3-Y640F ONCOGENIC MUTANT DRIVEN HPC-7 CELLS PROLIFERATION.	65
FIGURE 3.1: SCHEME DEPICTING THE OVERALL MS3-6 MODE OF ACTION.	69
FIGURE 3.2: BINDING SITES OF PROTEINS PHYSICALLY INTERACTING WITH STAT3.	70
FIGURE 3.3: NTD-MEDIATED STAT3 OLIGOMERIZATION.	71

LIST OF TABLES

TABLE 1.1: DESCRIPTION AND ACCESSION CODES OF THE STAT3 STRUCTURES FOUND IN THE PROTEIN DATA BANK (PDB).	17
TABLE 2.1: ORIGINAL MONOBODY LIBRARIES AND SELECTED STAT3 BINDERS.	39
TABLE 2.2: STAT3/MS3-6 COMPLEX (PDB: 6TLC) CRYSTAL STRUCTURE DATA COLLECTION AND REFINEMENT STATISTICS.	53

1. INTRODUCTION

1.1. Oncogenic signaling

Cancer is a pathological condition resulting from an uncontrolled cellular outgrowth caused by the acquisition of genetic alterations in transformed cells¹. Certain specific signaling pathways, such as those regulating cell-cycle progression, apoptosis and cell growth, are commonly altered. However, the modification of these precise cellular processes may vary among different individual tumors and cancer types. In that sense, cancer is not to be considered as a single disease type, but instead as a multiplicity of diseases given that every tumor is genetically different from another. This has important implications for the development of cancer therapies, as it implies that a profound understanding of the molecular causes driving cancer must be achieved².

1.1.1. Genetic alterations leading to cellular transformation

Over the past decades, the improvement of DNA sequencing approaches allowed for a systematic identification of genetic alterations in cancer cells^{3,4}. Frequently altered pathways were uncovered across many cancers, such as the RAS/MAP-kinase or the PI3K/Akt signaling pathways⁵. Interestingly, the frequency of gene alterations in these key pathways vary, as some are often mutated, while others are only rarely modified⁶.

This led to the understanding that specific mutational events can provide a Darwinian evolutionary advantage in favor of the pathological development of the tumor. Indeed, alterations of specific genes, called driver mutations, lead to a direct promotion of the disease, while others, called passenger events, lack these functional effects⁷. Therefore, tumorigenesis results from a selective pressure for advantageous mutations in transformed cells⁸. It is however common to find a multitude of individual alterations in tumor cells, as additional mutations accumulate over time, leading to a high mutational background in transformed cells^{9,10}. These genetic changes consist for

the most part in two types of alterations: (I) gain-of-function mutations in proto-oncogenes, which lead to increased driving capacities of specific genes such as RAS, BCR-ABL as well as some receptor tyrosine kinases, and (II) loss of function mutations in so called tumor suppressor genes¹¹. These genes normally function as gatekeepers, preventing the propagation of unhealthy cells by activating DNA repair programs and cell division checkpoints. Nonetheless, should the genetic alterations or mis-regulated cell cycle persist, tumor suppressor genes can ultimately trigger apoptosis and cell destruction, thus preventing the continuous growth and pathological development of cells. However, transformed cells suffering from loss-of-function mutations in these key tumor suppressor genes can evade regulatory control programs and therefore are able to persistently grow and proliferate¹². Additional mechanisms, such as epigenetic control of gene expression and loss of heterozygosity are also found to mediate cellular transformation^{13,14}.

These mechanisms highlight the importance of controlling the pathological development of cells in healthy systems. To do so, signaling pathways are tightly controlled in healthy tissues to maintain cellular functions. Indeed, a complex regulatory machinery capable of terminating signal transductions prevents the rising of oncogenic phenotypes. This is due to the reversible termination of signaling by protein phosphatases and other negative regulators of enzymes, as well as the irreversible proteasomal degradation of proteins tagged with polyubiquitylation chains, a post-translational modification carried out by E3 ubiquitin ligases. For example, the Cbl E3-ubiquitin ligase protein family is able to specifically recognize and ubiquitylate target proteins, thus leading to their degradation¹⁵. Therefore, Cbl, among other E3-ubiquitin ligases, plays an essential role in controlling and regulating proteins activity. Conversely, Cbl proteins suffering from loss-of-function mutations are rendered unable to polyubiquitinylate activated target proteins such as kinases. As a consequence, cells harboring non-functional E3-ubiquitin ligases suffer from a loss of signaling pathways termination. Hence, altogether, tumorigenesis results from genetic alterations causing the constitutive activation of oncogenes and loss of tumor suppressor genes.

1.1.2. Protein functions and oncogenic signal transduction

Cancer hallmarks, including enhanced proliferative signaling and resistance to cellular death result from the accumulation of altered cellular mechanisms¹. Therefore, in addition to the three classical approaches to treat cancer using surgery, radiation therapy and chemotherapy, an additional strategy relies on the identification of altered genes of interest. Among the known oncogenes, a number of protein families are commonly found, such as protein and lipid kinases or transcription factors (TFs). Kinases like BCR-ABL or EGFR for example, are often found to become hyperactive in

cancer. Most intracellular signal transduction pathways involve protein kinases, which are responsible for the phosphorylation of their downstream partners. Thus, the resulting exaggerated transmission and amplification of particular responses promotes cellular transformation¹⁶. The specificity of their signaling is mediated by the selectivity of the binding partners¹. Among the best examples for signaling specificity are the Src-homology 2 (SH2) domains. They allow protein interactions with tyrosine phosphorylated sequences and couple phosphorylated receptor tyrosine kinases (RTKs) to their downstream partners¹. SH2 domains have a pivotal role in the transmission of signaling cascades, which results in the activation of TFs able to regulate the expression of target genes. These proteins ultimately control the cellular behavior by precisely regulating genetic responses to stimuli. On the other hand, TFs who suffer from an activating mutation often show higher transcriptional activity levels. Strikingly, many TFs are potent oncogenes and important drivers of tumorigenesis¹⁷. In that sense, the oncogenic activation of several TFs such as Myc¹⁸, STAT3¹⁹ and STAT5²⁰ is an important event for the establishment and progression of the disease.

1.1.3. The role and implication of transcription factors

TFs are a class of proteins capable of influencing gene transcription. These proteins are classically composed of a transactivation domain involved in protein-protein interaction with other TFs and members of the core transcriptional machinery as well as chromatin modifying complexes. They additionally contain a domain allowing binding to specific DNA sequences. TFs can directly induce gene expression or, in some cases, repression. They control the cellular proliferation and regulate cell fate by modulating the apoptotic genes activity. Mechanistically speaking, the expression of target genes is favored by the recruitment of the basal transcription machinery on promoter regions, which leads to gene transcription. Importantly, TFs are also capable of recruiting specific enzymes which trigger processes such as the chromatin remodeling, favoring their physical access to DNA. Notably, TFs are one of the largest classes of proteins, comprising over 2000 genes as demonstrated by analysis of the human genome²¹. While many of them remain to be studied, TFs can be classified according to common structural features. Indeed, various protein motifs are responsible for DNA binding, including the zinc fingers, the helix-turn-helices, the helix-loop-helix motifs as well as the leucine zippers among others^{22,23}. An alternative classification relies on the distinct responses of TFs, as some have specific roles driven by precise internal or surface receptor mediated stimuli²¹. This signal dependent group comprises many proteins, whose therapeutic targeting may prove valuable in the context of various human diseases, including cancer. Among these numerous potential molecular targets, TFs were considered as ideal candidates due to the convergence of multiple signaling pathways to a common downstream TF, which carries out the regulation of the

genes responsible for the cellular outgrowth. For this reason, inhibiting the function of a single transcription factor may in fact prohibit numerous upstream oncogenic signals. This is especially important as the oncogenic activity of some TFs are tightly linked to signaling addictions in transformed cells^{24,25}. Because of their pivotal role in controlling development, cell differentiation and proliferation, transcription factors are spatially, temporally and sequentially regulated in healthy cells. Altering their control often results in the pathological development of cellular processes¹⁷. For example, Myc has been shown to play a critical role in cancer and is among the commonly altered TFs responsible for tumorigenesis²⁶. While Myc is rapidly synthesized following mitotic signaling in healthy cells, cancer cells often bypass the requirements of extracellular stimulation by constitutively expressing higher Myc protein levels. Augmented Myc levels resulting from transcriptional, post-transcriptional or post-translational altered mechanisms cause extended cellular proliferation and genetic instability¹⁸. Furthermore, additional Myc alterations including a chromosomal translocation into an immunoglobulin loci in lymphomas and several point mutations, such as T58A and E39D, were observed in a panel of human cancers including lung, breast, cervical and ovarian carcinomas²⁷. The mutant Myc proteins often bear an altered transactivation domain, resulting in an impaired negative regulation of their activity leading to prolonged half-life. Despite being considered as one of the “most wanted” protein target for cancer therapy, current limitations such as its lack of defined ligand binding site translated into a lack of clinically-suitable inhibitors²⁸.

Many additional TFs such as c-Jun, NF- κ B and various STATs²⁶, are similarly often constitutively activated in cancer and are hypothesized to render transformed cells addicted to these oncogenic TFs signalings^{29,30}. Therefore, their blockade is postulated to decreased transformed cells viability. Conversely, hindering TFs is thought to have little impact in healthy cells due to the redundancies of transcriptional control³¹. Because of this higher tolerance in normal cells, impairing TFs activity appears as a promising targeted strategy that may be more effective and significantly less toxic than current approaches^{32,33}. Figure 1.1 illustrates the potential beneficial impact of transcription factor inhibition on critical features of their regulation, which could be altered in the context on cancer³⁴. These critical features have been associated with the activity of oncogenic transcription factors in various cancer types (reviewed in ³⁴). For example, MLL-AF9 was identified as a master regulator of stem cell-like properties in acute myeloid leukemia (AML), while in glioblastoma, GABP led to increased proliferation and replicative immortality potential by increasing hTERT expression levels. Similarly, the epithelial to mesenchymal transition (EMT) is a known critical step favoring tissue invasion which is initiated in breast and prostate cancer by the transcriptional activity of RUNX2. Additionally, RUNX2 transcriptional activation was found to bypass known upstream oncogenic signaling, rendering melanoma cancer cells resistant to the BRAF vemurafenib inhibitor.

A close family member, RUNX1 was identified in key autoregulatory feedback loops and signaling cascades driving AML, while additionally allowing immune evasion by actively downregulating CD48 expression. As a consequence of this, reduced levels of NK cell-mediated tumor cell recognition and killing were reported. Lastly, cancer cells are often unable to undergo differentiation programs. For instance, the PML-RAR α transcriptional activity was found to prevent cellular differentiation in acute promyelocytic leukemia (APL).

Therefore, the targeting of pathological transcription factors appears as an interesting strategy. Nonetheless, directly precluding a precise transcriptional activity implies its selective inhibition. Such reasoning provided the foundation of the targeted therapies strategy.

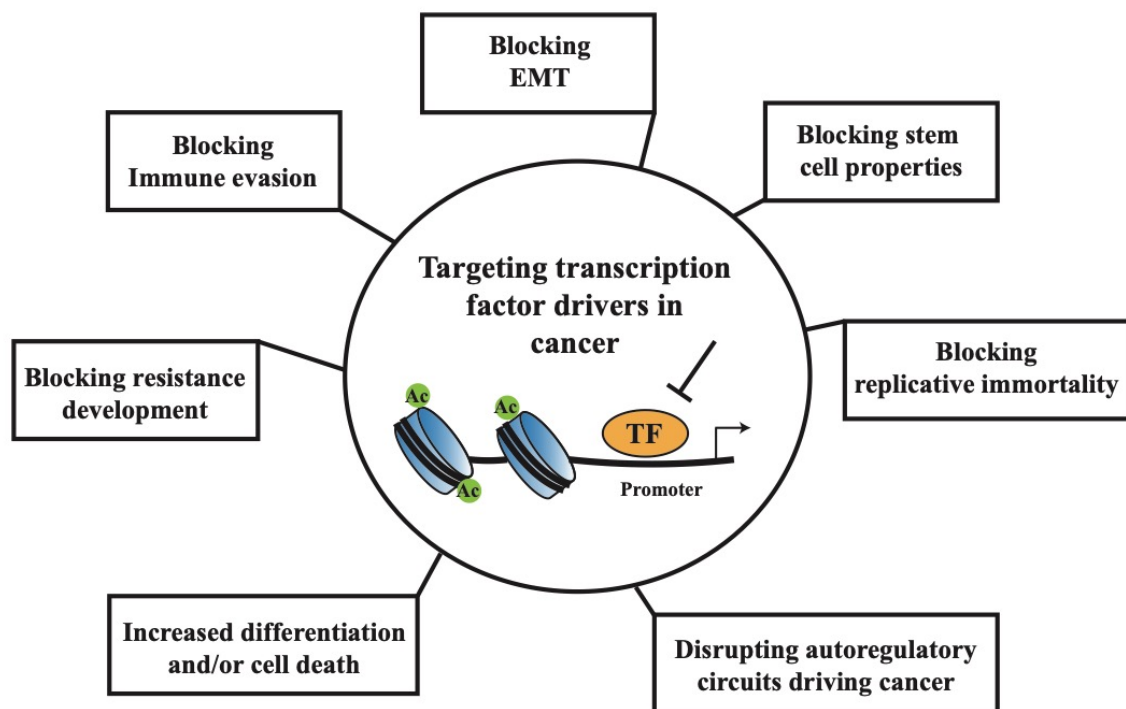


Figure 1.1: Targeting transcription factors driving tumorigenesis.

Beneficial outcomes expected upon precluding the transcriptional activity of key TFs implicated in cancer. EMT: epithelial-to-mesenchymal transition. Figure adapted from³⁴.

1.2. Targeted therapies

Classically, the therapeutic approaches for cancer treatment consist in three main axes: surgery, chemotherapy and irradiation³⁵. While these approaches have proven effective in many cases, they

suffer from the major drawback that is the lack of selectivity for cancer cells. Because of that, side effects are observed and result in systemic toxicity. In addition, because of their lack of specificity, the chemotherapeutic agent concentrations in tumors often are insufficient and lead to the development of drug-resistant tumors cells able to escape treatments, thus causing relapses in patients³⁶. In contrast, targeted therapies aim at specifically targeting genetic drivers in cancer cells or in their local microenvironment by inhibiting precise proteins responsible for the tumor growth and proliferation. Of note, it is nonetheless worth mentioning that currently, in an effort to reach maximum treatment efficacy in the clinic, targeted therapies are still often used in conjunction with chemotherapy or alternative approaches.

In the past two decades, the discovery of additional key oncoproteins has been achieved using techniques such as cDNA microarrays and tumor sequencing^{37–39}. These oncoproteins, including Cyclin D, CDK-4 and PTEN, have a functional role as tumor drivers, as evidenced by their over expression, mutational and knock-out studies in model organisms⁴⁰. Thus, impairing the function of such altered proteins is expected to lead to a significant decrease of the tumor burden. This rationale explains the interest in developing cancer therapies against specific key targets. Generally speaking, targeted therapies lead to the blockade of cancer cell proliferation, trigger cell death by apoptosis or autophagy, and lead to the promotion of cell cycle checkpoint regulatory mechanisms⁴¹.

1.2.1. Current approaches and limitations

Two main approaches are commonly exploited in targeted therapies: the first one is mediated by therapeutic monoclonal antibodies (mAb), which bind to extracellular targets such as the surface receptors EGFR or VEGFR⁴². The second approach relies on the use of small-molecule drugs whose molecular weights are under 1KDa in order to inhibit enzymes such as kinases⁴³.

Antibodies proved particularly useful as protein therapeutics. These proteins typically show high affinities for their respective targets due to an important surface area available to form contacts. Therefore, the region of the target recognized, called the epitope, often covers large areas and is not required to be particularly hydrophobic. However, antibody therapies are restricted to the cellular surface targets due to the antibodies large size, their amphiphilic nature and due to the lack of adapted transmembrane carriers, highlighting their use for extracellular target inhibition^{44,45}. On the other hand, because of their small sizes, small-molecule compounds are capable of rapidly diffusing across the cellular membrane of mammalian cells, which enables their use against

intracellular targets. These drugs however only possess a small surface area capable of interacting with the protein target. This implies that, in order to amplify the inhibitory effect, small-molecule probes must form a stable complex by creating hydrophobic contacts in key pockets crucial for the overall enzymatic activity of the target. In other words, such small-molecules probes importantly rely on the presence of a solvent exposed deep hydrophobic pocket^{46–48}. Currently, approximately a dozen of mAB and 34 kinase inhibitors entered clinical practice in oncology⁴⁹. Nonetheless, despite the significant number of approved targeted therapeutics that became available over the past 20 years, only a few led to significant long-term clinical improvements. This is perhaps best exemplified by imatinib (commercialized as Gleevec), a BCR-ABL kinase inhibitor, which led to a tremendous improvement in overall survival of Chronic Myeloid Leukemia (CML) patients. Nevertheless, the limited long-term efficacy of many targeted therapeutics can be explained by the often rapid development of drug resistance and low specificity leading to toxicity caused by off-targets interferences⁵⁰. Moreover, an additional limitation of current targeted therapies is the narrow number of pathways that are currently antagonized: many therapeutics are directed towards the same pathways or specific kinases despite essential oncoproteins remaining unharmed.

Indeed, despite the latest advances in the research field, there still are unmet medical needs illustrated by the mixed results of targeted therapies in the clinics³⁵. Due to the numerous accumulated mutations in most human tumors, single agents targeting unique signaling pathways often translate into limited efficacy. This can be explained by the rapid rewiring of cellular processes, which bypass the inhibited upstream target protein⁵¹. Therefore, a combination of drugs, hitting simultaneously different signaling pathways is desirable and could result in a beneficial reduction of feedback compensatory signaling networks rewiring. Similarly, inhibiting transcription factors, acting on a downstream level, where many oncogenic pathways converge, may result in an increased efficiency. Nonetheless, many proteins currently remain undruggable using the existing targeted therapeutic approaches described above. Therefore, the need for novel strategies to expand the number of “druggable” targets appears crucial.

1.2.2. What makes proteins undruggable and how to target them

Given the current technologies, a protein is considered druggable if it fulfils a number of criteria such as having an extracellular surface exposition, which allows a specific antibody recognition or possessing a hydrophobic pocket able to accommodate a small-molecular probe. Among the current

intracellular drug targets are receptors (such as nuclear receptors), ions channels and enzymes (i.e. kinases and proteases) which contain deep grooves able to fit an antagonistic low-molecular weight small molecule⁵². Due to their well-defined active and allosteric/orthosteric sites, these enzymatic targets naturally have interesting regions for an antagonistic interaction. However, non-enzymes (which represent the majority of the human proteome and known oncogenes) lack these obvious binding pockets, maintain a certain structural disorder and use Protein-Protein Interactions (PPIs) over large areas to carry out their functions⁵² (Figure 1.2). As a consequence, the vast majority of proteins remain unreachable by the two commonly used drug categories presented above⁴⁴. This suggests that future inhibitors of such non-enzymatic proteins should typically either prevent their interaction with binding partners or otherwise modify and alter their structure, function or cellular localization.

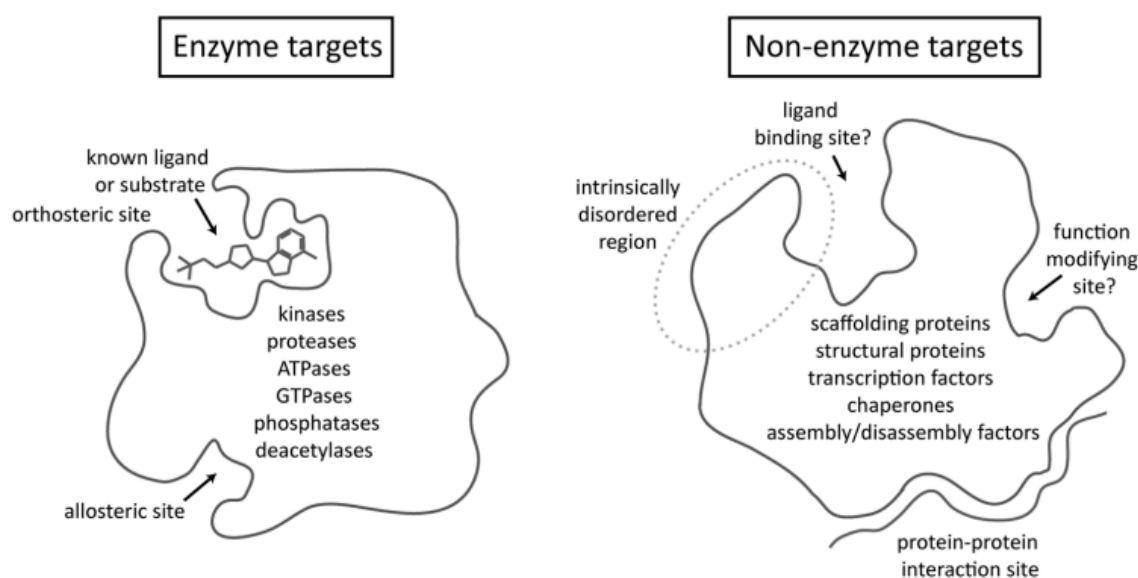


Figure 1.2: The challenges of non-enzymes as drug targets.

While enzymes have strictly defined binding pockets or functionally relevant sites, non-enzymes PPI region spreads out over a diffuse area and often have structurally uncharacterized domains, preventing the use of structure-mediated drug design⁵².

1.3. Monobodies

Monobodies are small antibody-mimics of approximately ~10 kDa. Their scaffold was initially proposed in 1998 by Shohei Koide⁵³ and is derived from a fibronectin type III domain (FN3) endogenously expressed in nearly 2% of animal proteins. These are all naturally capable of binding specific ligands because of the surface loops of their FN3 domains acting as binding sites. The FN3 scaffold was thus an interesting framework to work with: upon engraftment of specific loops, the

Koide lab was able to engineer FN3 mutants with an affinity towards ubiquitin⁵³. Structurally speaking, the FN3 domain resembles the immunoglobulin domain⁵⁴. As shown in Figure 1.3A, both the antibody variable heavy chain domain (V_HH) and the FN3 scaffold globally have a β -sandwich fold. Such similarities have originally inspired the design of FN3 loops with different sequences and length, thus resembling the natural variability of an antibody's complementarity determining regions (CDRs)⁵⁴. These original loop-based libraries have in turn evolved into alternative “side-and-loop” designs (Figure 1.3B) where in addition to the loop, a surface of the β -sheet and a loop on the opposite side of the FN3 scaffold (CD-loop) are modified as well. This further increased the range of variability achievable and led to a concave variable region which favors the binding to a target protein by geometrically matching the functional cleft⁵⁵.

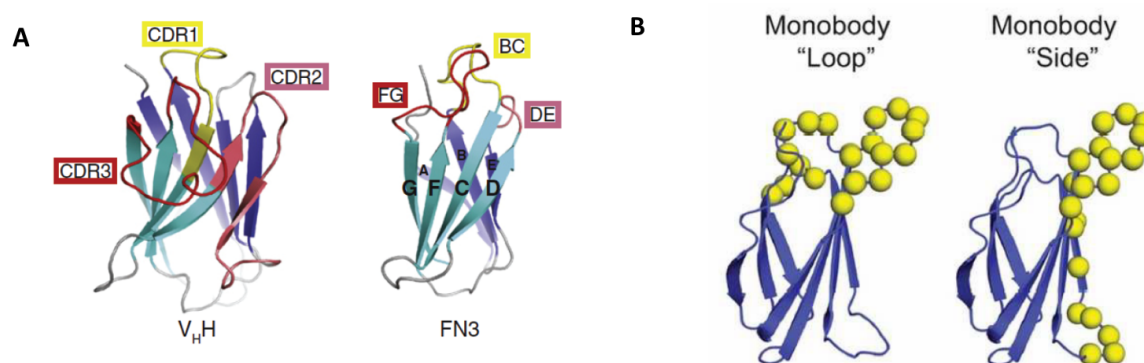


Figure 1.3: Monobodies as antibody-mimics derived from a FN3 scaffold.

(A) Similarities between antibody V_HH domain (Left) and a FN3 scaffold (right). The CDR regions on the V_HH domain and their homologues in the FN3 scaffold are color coded and labeled. The β -sandwich structure is colored in blue and purple and the FN3 β -strands are labeled A to G. The “loop” and “side-and-loop” libraries of monobodies are shown in (B). The CDRs-like variability of the “loop” monobody and the concave variable region of “side” one are depicted in yellow. Figure adapted from⁵⁵.

Monobody libraries are generated by PCR using randomized oligoes to diversify residues on the loop and side of the monobodies. The best affinity binders against a given recombinant target protein are then selected using phage and yeast surface-display strategies. However, these clones are selected without knowing exactly where the epitope on the target protein resides. Interestingly, despite the overall approach being unbiased in terms of epitope selection, monobodies are often found to bind important functional regions on the molecule of interest⁵⁵. This can be intrinsically explained by the nature of functional domains which are naturally enriched in amino acids favoring interactions (i.e. Tyr, Trp and Arg), while nonfunctional surfaces are enriched in “interaction-breaking” amino acids (i.e. Glu and Lys)⁵⁵. Conversely to the immunoglobulin domain, the folding of these non-antibody scaffolds does not rely on disulfide bonds as they lack cysteines. This makes

monobodies convenient for both recombinant protein production in *E. coli* and use in intracellular applications upon transfection or viral transduction.

Interference with intracellular signaling has already been achieved using a monobody called HA4, which prevented Abl-mediated phosphorylation of its downstream partners, resulting in the inhibition of STAT5 activation⁵⁶. Moreover, by coupling HA4 to another monobody termed 7c12, Grebien et al. were able to reduce BCR-ABL activity and trigger apoptosis in CML cell lines and primary cells from patient suffering from CML⁵⁷. Moreover, a study where the high affinity monobody AS25 could target the SH2/kinase interface with single digit nanomolar K_D value provided further evidences for the allosteric inhibition of BCR-ABL⁵⁸. Similarly, monobodies against the N- and C-terminal SH2 domains of the Src-Homology 2 domain-containing Phosphatase 2 -SHP2 (which is a known complex partner of BCR-ABL favoring cell transformation) prevented the downstream ERK signaling activation⁵⁹. More recently, the precise SH2 domains targeting of the SRC family kinases using monobodies demonstrated the exceptional specificity and intracellular activity modulation of proteins implicated in cancer⁶⁰. Altogether these studies demonstrate the potential of monobodies as highly specific intracellular antagonists.

In these examples, the inhibition of PPIs via the blockade of the SH2 domain could impair leukemogenesis. A similar approach directed towards inhibiting essential oncoproteins would have a similarly positive outcome on tumor development. The monobody protein delivery to cancer cells would enable their use as intracellular inhibitors. Our lab demonstrated that the delivery of stoichiometric amounts of protein could be achieved using a Shiga toxin derived construct in cells expressing the Gb3 receptor (also called CD77)⁶¹. Similarly, the engineering of the monobody surface by mutating residues to positively charged lysines led to the development of a polycationic scaffold which was capable of cell penetration (Hantschel lab, unpublished observations).

In this work, I aimed at targeting previously un-drugged key oncogenic transcription factors using intracellular monobodies.

1.3.1. Expanding the scope of targeted therapies using monobodies

The intracellular use of monobodies provides an opportunity to combine the advantages of the two main approaches in the field of today's targeted therapies. Indeed, while therapeutic antibodies are restricted to the extracellular surface, small molecules inhibitors on the other hand remain an

approach limited to certain categories of protein targets. However, by combining the affinity and specificity of an antibody, while being applicable to the inhibition of virtually any intracellular target, monobodies open the door to the development of biologics capable of binding and modulating intracellular protein functions.

Many of the “most wanted” oncogenes exist as a variety of protein isoforms. However, monobodies are capable of selectively binding to precise oncoproteins as demonstrated in 2016 by Spencer-Smith et al. with the development of a monobody (NS1) capable of binding to H and K-Ras in both their GTP and GDP bound conformations but not to N-Ras⁶². The subsequent oncogenic signaling mediated by H- and K-Ras was impaired due to the binding of the monobody which, in turn, prevented an efficient Ras dimerization. This example perfectly illustrates the potential of monobodies as drugs, together with their critical use as molecular tools to dissect intracellular signaling pathways and help isolate and define protein regions responsible for previously undescribed interactions. Indeed, the role of individual protein domains or given specific regions remains to be explored and better understood in many cases. This is particularly true for TFs, as their interaction with the transcriptional machinery in the nucleus relies on various domains⁶³. In a pathological context such as cancer, the oncogenic activity of TFs may rely on specific regions, which favor their nuclear translocation and transcriptional activity for example. Hence, a beneficial outcome is expected upon the precise blockade of defined key domains. Furthermore, the targeting of a precise domain might prevent the exaggerated transcriptional activity of oncogenic TFs, while sparing the scaffolding or non-canonical activities carried out by their additional domains. Thus, by precisely perturbing a single protein function by specifically blocking a defined domain, the overall non-transcriptional functions of TFs may remain unaltered, which may prove important to reduce toxicity in healthy cells.

In the past decade, additional strategies were explored to expand the range of targeted therapies such as the repurposing of the proteasomal degradation machinery. Among those, the PROteolysis-Targeting Chimeras (PROTACs) technology consist in a bifunctional compound allowing binding to a target protein on one hand, and to a subunit of an E3 ubiquitin ligase complex on the other as depicted in Figure 1.4. As a consequence, the target protein is brought in close proximity to the ubiquitin ligase and forms a ternary complex with E2 ubiquitin-conjugating enzymes. This leads to the polyubiquitination of the target protein hence marking it for proteasomal degradation. The PROTAC compound itself is then recycled in the cytosol and mediates the targeted degradation of another target proteins. This concept was first proposed by Crews et al. in 2001⁶⁴. Since then, four E3 ligases (MDM2, IAP, cereblon and VHL) have been used in this context⁶⁵. Among those, the Von Hippel-Lindau (VHL) ubiquitin ligase was found to be particularly effective^{66,67}. Currently,

the targeting moieties of these PROTACs consist mainly in small molecules or peptides with affinities towards the key protein target. Nonetheless, an important limitation remains the development of probes capable of binding to challenging target protein in order to trigger their degradation. In that sense, the development of monoclonal binders to key undruggable oncoproteins may serve as exceptional warheads to facilitate the target polyubiquitination by E3 ubiquitin ligases. Our lab previously has explored this approach using a monoclonal directed against LCK fused to the VHL ubiquitin ligase. Upon expression of the construct, LCK degradation could be observed in cells⁶¹. In this context, a major advantage of monoclonal antibodies is their high affinity binding to the protein target, regardless of whether they have an inhibitory activity on their own or not. Hence, this work highlights the use of high affinity monoclonal binders capable of specifically binding to previously undruggable proteins and to mediate their targeted degradation when coupled to VHL proteins. Such an approach applied to STAT3 was undertaken during this thesis to develop a monoclonal-mediated targeted degradation system (see results section - chapter 2.1.2).

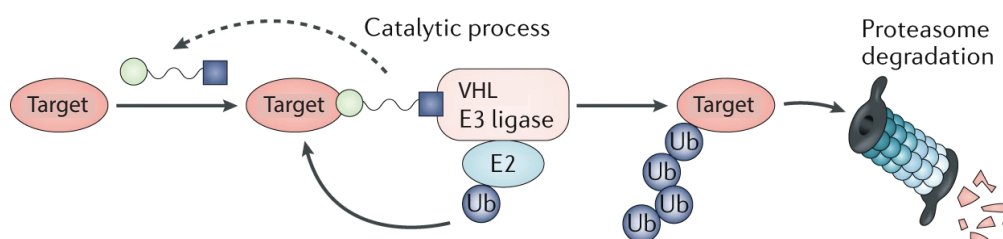


Figure 1.4: PROTAC mediated targeted degradation mechanism.

The PROTAC compound (green circle and blue square) links the target protein to the VHL ubiquitin ligase, which recruits the poly-ubiquitination machinery responsible for the tagging and proteasomal degradation of the target. Figure adapted from³⁴.

1.4. Undruggable transcription factors as intracellular targets

Over the last years, many deregulated transcription factors were validated as critical players implicated in the development of cancer as well as various other diseases⁶⁸. Nonetheless, despite being considered as key protein targets for drug intervention, TFs still remain largely undruggable. However, this paradox is slowly evolving as novel approaches are being developed in order to modulate their transcriptional activity. The intrinsic challenges in targeting TFs rely on their lack of deep pockets in the regions required for protein-protein interaction together with their convex DNA binding interfaces often enriched in positively charged residues, which makes it difficult for small chemical probes to provide drug-like properties.

Nonetheless, recent efforts undertaken by pharmaceutical companies revealed the feasibility of inhibiting the activity of TFs in the context of solid and hematological cancers as demonstrated by a number of currently ongoing clinical trials^{34,69}. However, the successful inhibition of these proteins has been limited to a narrow number of cases and often relied on the targeting of the sex hormones receptors, the retinoic acid receptors and the vitamin D receptors³⁴. These exceptions can be explained by the capacity of the targets to directly bind a ligand, thus allowing a direct molecular manipulation using therapeutics. Nonetheless, many challenges in directly targeting TFs remain, such as (I) their nuclear localization, making them inaccessible to antibodies, (II) their overlapping roles over various cellular processes, underlying the issue of specificity and obstruction of unwanted cellular processes and (III) the nature of their DNA binding domain, which relies on key residues separated by various oligonucleotides irrelevant for DNA binding⁷⁰. Hence, preventing transcription factors from binding to DNA implies an important three-dimensional obstruction covering distant critical residues. In comparison, a kinase inhibition can be carried out, for example, using simple ATP derivatives⁷⁰.

Nevertheless, various strategies were undertaken to target and inhibit transcriptional activities. Some indirect approaches rely on targeting the upstream receptors and kinases, or by regulating the histone modifications. On the other hand, direct strategies targeting TFs have been developed and consist in three main approaches: (I) inhibition of the TFs dimerization using small peptides or chemical compounds, (II) blockade of specific DNA binding sequences and (III) usage of decoy oligonucleotides (Figure 1.5)⁷¹. These approaches could lead to an inefficient protein-protein interaction, protein/DNA complex formation and impaired target gene regulation. Similarly, additional inhibitory mechanisms which currently remain to be further explored consist in the inappropriate nuclear localization, interfering with binding to cofactors and preventing physical binding to DNA by actively remodeling chromatin (Figure 1.5)^{17,71,72}.

Among the transcription factors, STATs are considered as particularly relevant in the context of cancer. Unfortunately, the specific inhibition of STATs remains currently challenging as illustrated by the present lack of available FDA approved drugs.

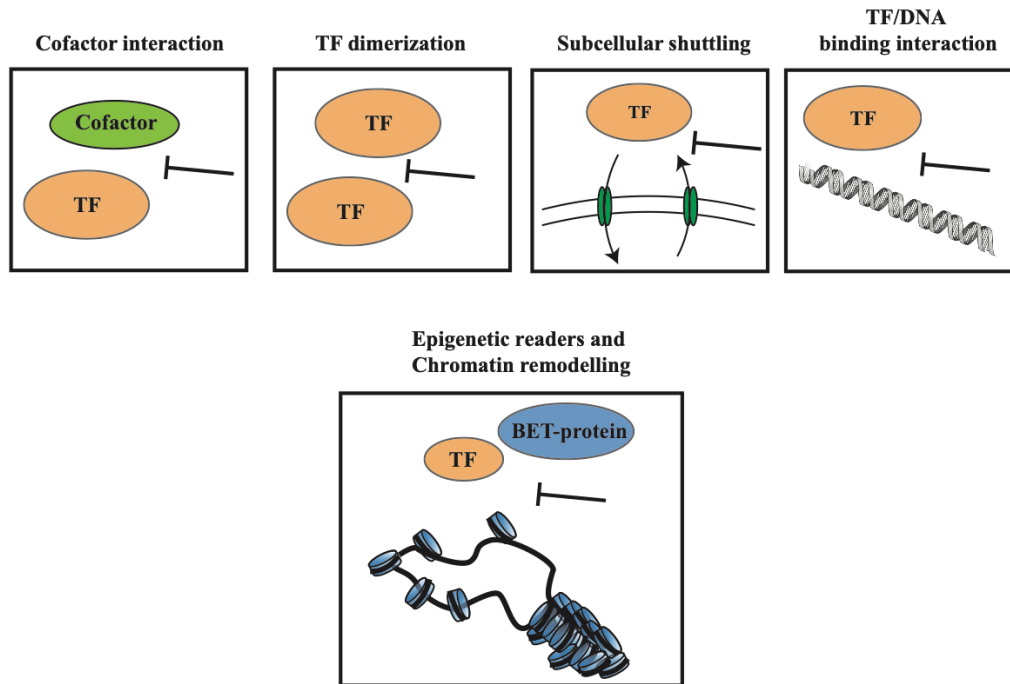


Figure 1.5: Current strategies to inhibit transcription factors.

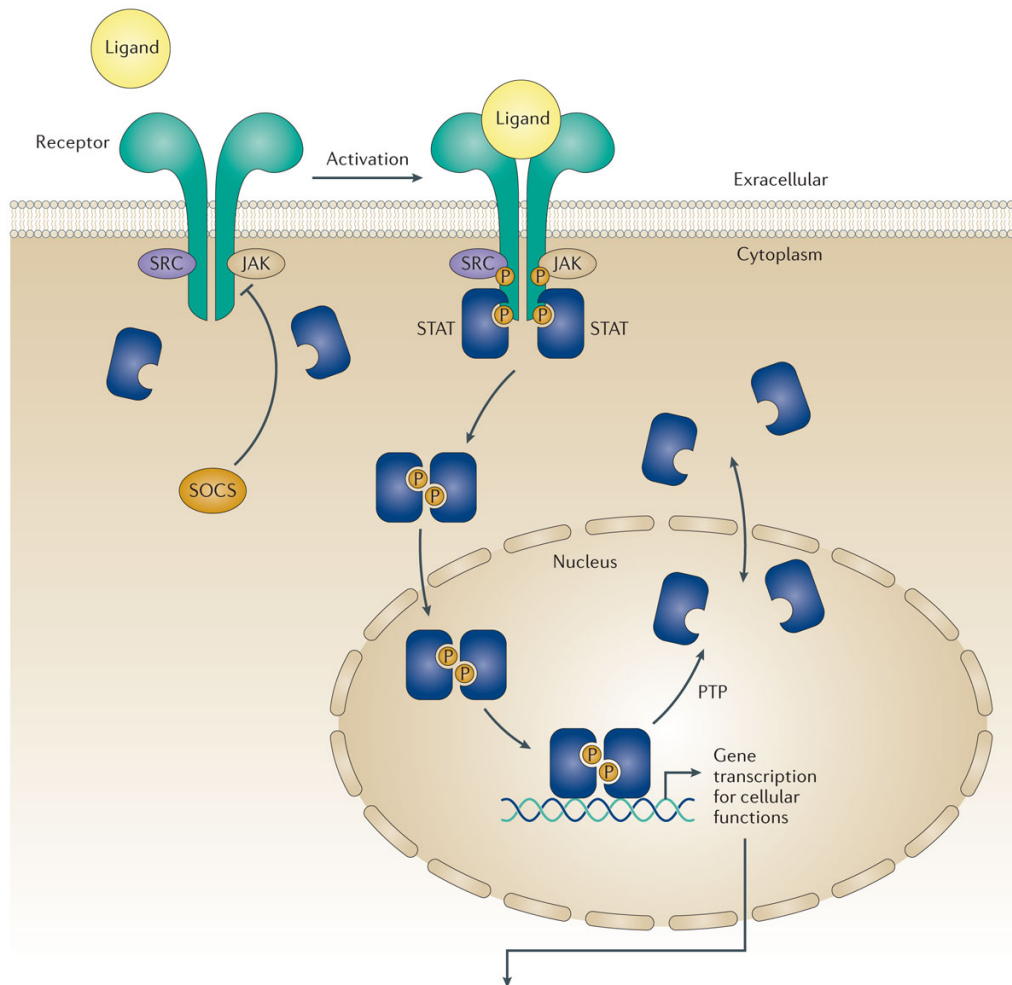
Schematic TF is shown in orange depicted as a monomer or dimer. Five main approaches are depicted. Figure adapted from⁷¹.

1.4.1. JAK-STAT signaling pathway

The signal transducer and activator of transcription factors (STATs) are responsible for the cellular responses upon stimulation by cytokines and growth factors. STATs activation is mediated by a panel of upstream tyrosine kinases receptors^{72,73}. The receptor-associated Janus kinases (JAKs) are mainly implicated in the phosphorylation of a critical tyrosine residue resulting in the activation of the STAT signaling cascade⁷⁴. The STAT family (composed of STAT1-4, STAT5a, STAT5b and STAT6) is normally implicated in inflammation, proliferation, differentiation, cell survival and immune responses⁷⁵. These responses are driven by cytokines, including interleukin-6 (IL-6) stimulating receptors upstream of JAKs⁷². Activation of the upstream receptor causes the phosphorylation of STATs which triggers their dimerization mediated by the reciprocal interaction between their SH2 domains and phospho-tyrosines. STAT dimers then migrate into the nucleus and bind DNA to regulate specific target genes expression^{76,77}. The overall JAK-STAT signaling pathway (illustrated in Figure 1.6) is strictly controlled and regulated in healthy cells by negative regulators, such as protein tyrosine phosphatases (PTP) and the suppressors of cytokines signaling (SOCS) proteins. However, dysfunction or mis-regulation of STAT signaling has been often associated with the development of various diseases (Figure 1.6)⁷⁸.

For instance, STAT1 mediates the cellular responses to interferon (IFN) stimulation which controls the activity of various T cell subsets, such as T helper type 1 cells (T_H1), T_H2 and T_H17 cells. Loss of STAT1 function results in immune pathologies and increased sensitivity to infections⁷⁹. STAT2 is similarly implicated in the IFN α and β signaling cascades driving antiviral responses and may also promote cancer progression by triggering STAT3 signaling via the release of IL-6⁸⁰. Furthermore, STAT4 equally regulates T_H1 cell differentiation and acts as a pivotal messenger protein in the IL-22 signaling implicated in the regulation of inflammation⁸¹. Hence, perturbation of STAT4 signaling is associated with various autoimmune pathologies⁸². Additionally, STAT6 is triggered by IL-4 and IL-13 stimulation in order to regulate allergic and inflammatory responses and is thus involved in asthma and allergies upon dysfunction²¹⁸.

Most interestingly, pathological activities of STAT3 and STAT5 have been associated with tumorigenesis. Indeed, STAT3 and STAT5, which can be found as two isoforms (STAT5A and STAT5B), are constitutively active in many tumors and induce the transcription of essential genes for tumor growth, such as anti-apoptotic regulators (i.e. Bcl-xL, Mcl-1 and survivin), cell cycle regulators (i.e. cyclin D1, cyclin D2) and angiogenic factors (i.e. VEGF)⁷⁸. Additionally, both STAT3 and STAT5 are often mutated in tumor cells. For instance, a STAT5 double mutant (termed STAT5 1*6) frequently observed in various types of leukemias, consists in the substitution of two residues (H299R and S711F) located in the DNA-binding domain and transactivation domain respectively. The exact mechanisms of oncogenic transformation mediated by STAT5 1*6 remain currently poorly understood. However, it is possible that a conformational change is responsible for an increased oligomerization and interaction with activated kinases, causing the double STAT5 mutant to be constitutively phosphorylated on key tyrosine residues. This in turn leads to an increased DNA-binding activity which renders cells independent from extracellular signaling and is associated with the disease onset⁸³. The inhibition of STAT3 and STAT5 thus represents an interesting therapeutic strategy expected to confer pro-apoptotic phenotypes to cancer cells^{20,75,83}. In this work, we focused our attention on novel way to therapeutically target a specific STAT family member importantly implicated in cancer: STAT3.



STAT	Cellular functions	Major diseases
1	<ul style="list-style-type: none"> Cell growth and apoptosis T_H1 cell-specific cytokine production Antimicrobial defence 	<ul style="list-style-type: none"> Atherosclerosis Infection Immune disorders
2	<ul style="list-style-type: none"> Mediation of $IFN\alpha/IFN\beta$ signalling 	<ul style="list-style-type: none"> Cancer Infection Immune disorders
3	<ul style="list-style-type: none"> Cell proliferation and survival Inflammation Immune response Embryonic development Cell motility 	<ul style="list-style-type: none"> Cancer
4	<ul style="list-style-type: none"> T_H1 cell differentiation Inflammatory responses Cell proliferation 	<ul style="list-style-type: none"> Experimental autoimmune encephalomyelitis (multiple sclerosis) Systemic lupus erythematosus
5A	<ul style="list-style-type: none"> Cell proliferation and survival IL-2Rα expression in T lymphocytes Mammary gland development Lactogenic signalling 	<ul style="list-style-type: none"> Cancer Chronic myelogenous leukaemia
5B	<ul style="list-style-type: none"> Cell proliferation and survival IL-2Rα expression in T lymphocytes Sexual dimorphism of body growth rate NK cell cytolytic activity 	<ul style="list-style-type: none"> Cancer Chronic myelogenous leukaemia
6	<ul style="list-style-type: none"> Inflammatory and allergic immune response B cell and T cell proliferation T_H2 cell differentiation 	<ul style="list-style-type: none"> Asthma Allergy

Figure 1.6: JAK-STAT signaling pathway, function and associated pathologies.

Upon stimulation and phosphorylation by upstream receptors, STAT dimers migrate into the nucleus to carry out their transcriptional activity. STAT-dependent gene induction is often implicated in the development of pathologies. Activation of STAT proteins is controlled by negative protein modulators such as Suppressor Of Cytokine Signaling (SOCS) and Proteins Tyrosine Phosphatases (PTPs)⁷⁸.

1.4.2. Lessons from the STAT3 structure

In the past 20 years, significant efforts were invested in the determination of the structure of STAT3. Currently, the X-ray crystallographic structures of several STAT3 recombinant fragments have been solved in either a monomeric or dimeric form (Table 1.1)⁸⁴. STAT3 shares high sequence and structural homology levels with other STAT family members and is composed of six main structural motifs corresponding to the N-Terminal Domain (NTD, also sometimes called the oligomerization domain), the Coiled-Coil domain (CC), the DNA-Binding Domain (DBD), the Linker Domain (LD), the Src Homology 2 domain (SH2) and the Transactivation Domain (TAD) as illustrated in Figure 1.7.

Table 1.1: Description and accession codes of the STAT3 structures found in the Protein Data Bank (PDB).

Description	PDB Accession codes	Reference
p-Y705/AcK685 STAT3 core fragment / DNA complex	6QHD	85
Mouse U-STAT3 core fragment	3CWG	86
STAT3 β /DNA complex	1BG1	87
U-STAT3 β core fragment bound to DNA	4E68	88
STAT3 NTD	4ZIA	89
STAT3 in complex with compound SD36	6NJS	90
STAT3 in complex with compound SI109	6NUQ	90

The TAD is an intrinsically disordered region which comprises key residues for STAT3 function. For example, S727 phosphorylation importantly mediates non-transcriptional STAT3 activities. Similarly, the STAT3 structures highlighted the role of a specific tyrosine residue located in the TAD, Y705, whose phosphorylation by upstream kinases is critical for the activation of STAT3. Indeed, Y705 phosphorylation allows the reciprocal recognition of two SH2 domains and the formation of a “parallel” dimer (Figure 1.8). Therefore, the role of the TAD in stabilizing STAT3 parallel dimers relies on the recognition of the phosphorylated Y705 by an arginine residue (R609) located in the SH2 domain of the other monomer⁹¹. Hence, the p-Y705 STAT3 parallel dimers are stabilized due to the electrostatic interaction between the Y705 phosphate (negatively charged) and the positively charged amino group of R609. Similarly, the acetylation of an additional lysine

residue, K685, has been reported to mediate the p-Y705 parallel dimer formation. However, Belo et al. recently solved the X-ray structure of an AcK685, p-Y705 STAT3 dimer and highlighted that acetylated K685 had no effect on dimer stabilization or DNA binding affinity⁸⁵ (Figure 1.8).

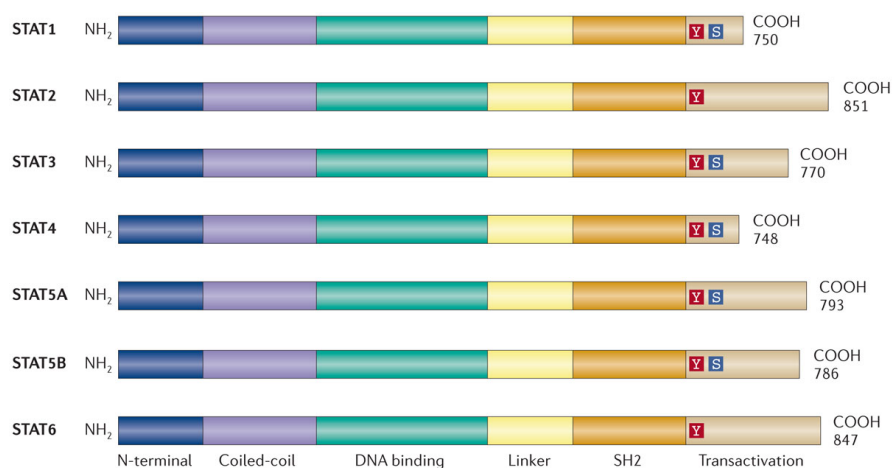


Figure 1.7: Linear depiction of the domain of the STAT family members.

Key Tyrosine (Y) and Serine (S) residues for protein functions are highlighted in the transactivation domain⁷⁸.

Importantly, the parallel p-Y705 STAT3 dimer is imported in the nucleus and drives the transcriptional activity upon binding to target DNA motifs mediated by residues located in the DBD of STAT3. Conversely, the NTD of STAT3 is not directly implicated in the formation of STAT3 parallel dimers, nor in the binding to DNA. Therefore, the role of the NTD remained elusive for a long time and it often was considered as dispensable for the overall activity of STAT3. Nonetheless, recent studies have identified the NTD as critical for the recognition of weak DNA binding sites and the formation of DNA bound STAT3 tetramers composed by pairs of pY705 dimers⁸⁹.

Similarly, the implication of the NTD in the formation of un-phosphorylated STAT (U-STAT) dimers was discovered. Indeed, various STAT family members have been additionally shown to form “anti-parallel” dimers. These antiparallel dimers rely on a binding interface between the DBD and the CC domains of two U-STAT monomers as illustrated in Figure 1.9 by the STAT5a anti-parallel dimer crystal structure⁹². The formation of a similar STAT1 dimer was found to be encouraged by the initial dimerization of two NTD, which in turn, favors the antiparallel dimer formation⁹³. Due to the high structural conservation among STAT family members, a similar unphosphorylated STAT3 anti-parallel dimer is likely relying on the implication of its NTD, CC and DBD, despite the lack of crystallographic evidence so far. Thus, for a long time, U-STAT3 was

thought to exist only as a monomer in the cytoplasm. However, the complexity of the STAT3 signaling emerged as low amount of U-STAT3 anti-parallel dimer were equally found in the nucleus, and to be capable of binding to DNA, remodeling chromatin and controlling specific gene expression^{88,94–96}.

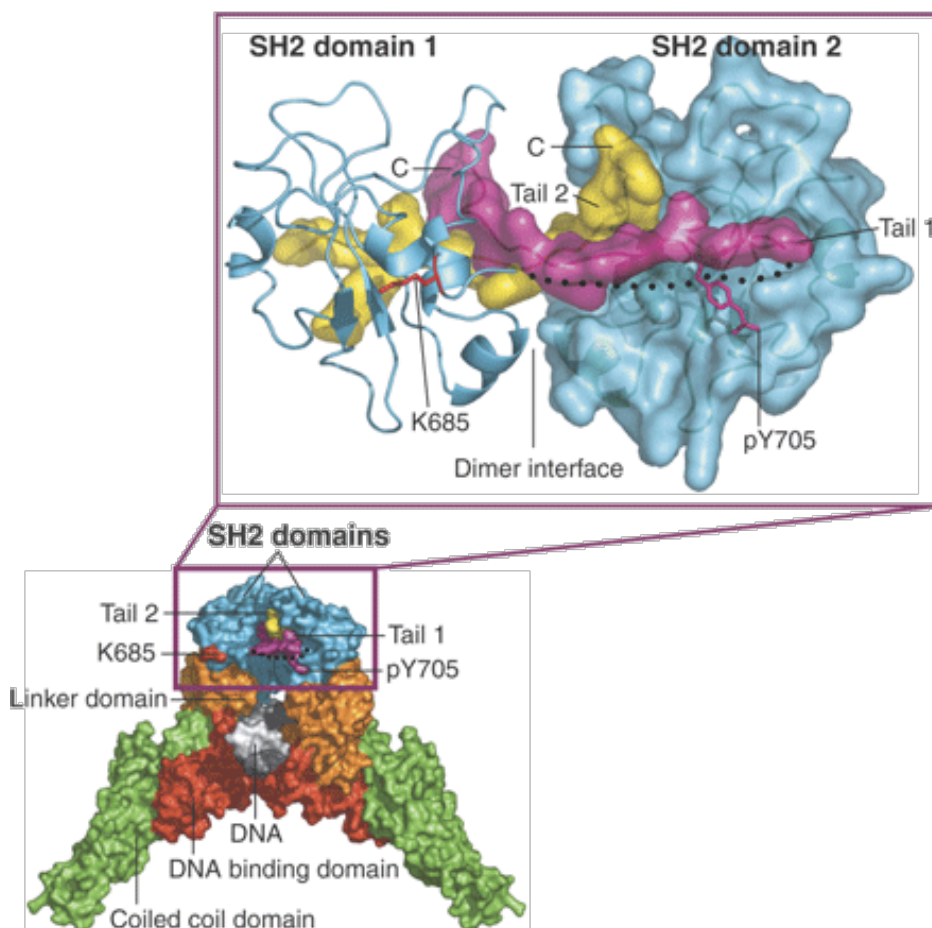


Figure 1.8: Crystal structure of the STAT3 parallel dimer.

Protein domains are color-coded as indicated in the figure. The SH2 dimerization interface is detailed. Two C terminal tails are color-coded in magenta and yellow respectively and contain the p-Y705 residues mediating dimer formation. Similarly, the K685 whose acetylation could stabilize the dimer is depicted in red. An unstructured peptide is represented by a dotted line⁹⁷.

Altogether, these crystallographic studies led to a better understanding of the molecular mechanisms responsible for the cellular activities of STAT3. Structural investigation revealed that, in addition to the DBD and SH2 domain playing important roles in the transcription factor activity, the NTD and coiled-coil domains of STAT3 are similarly implicated in critical processes such as the nuclear translocation, the recognition of weaker DNA binding sites, and the dimerization of unphosphorylated STAT3 in the cytosol⁸⁹. Therefore, selecting a monoclonal antibody against the coiled-coil

domain or NTD of STAT3 might have critical influence on the overall protein activity. Taken together, these evidences suggest that currently untargeted protein domains are key regions of interest for the development of novel inhibitory strategies.

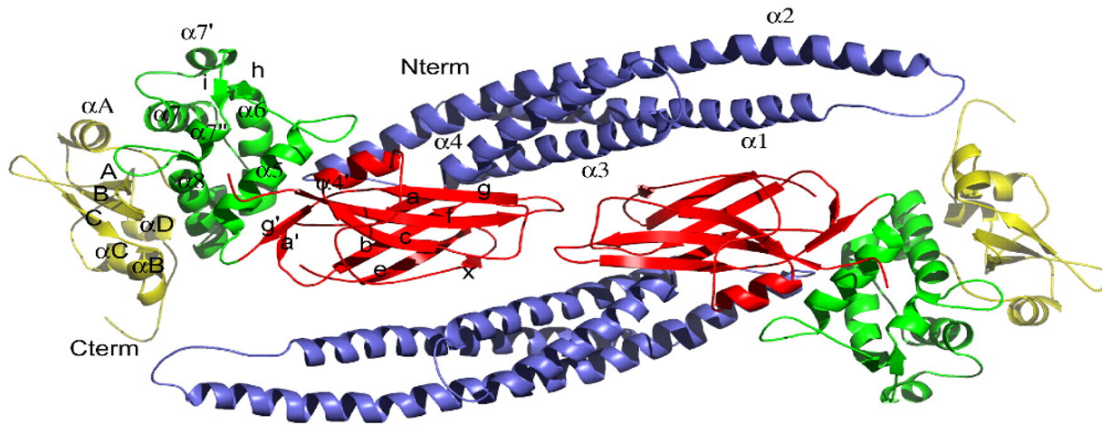


Figure 1.9: Top view cartoon depiction of a STAT5a anti-parallel dimer.

Protein domains are color coded as SH2 domain (part of it) in yellow, Linker domain in green, DBD in red and coiled-coil domain in blue. The dimerization interface responsible for the formation of an unphosphorylated STAT anti-parallel dimer relies on the reciprocal interaction between the CC domain and the DBD. Figure adapted from ⁹².

1.5. STAT3 functions and implications in cellular processes

STAT3 is ubiquitously expressed and canonically activated by a variety of upstream cytokines described here non exhaustively, but including IL-6, leptin, IL-12, IL-17, IL-10, IL-22 and interferons together with growth factors (G-CSF, EGF, PDGF) as well as by its direct oncogenes-mediated Y-phosphorylation by Src, Abl, Sis, Fps, Ros, Met, ErbB2 and others^{98–101} (Figure 1.10). Cytokines responsible for STAT3 activity are classified into subfamilies consisting in either classical or receptor-beta associated receptors according to whether or not they form dimers/oligomers with gp130 receptor- β subunits. This in turns, allows the recruitment of JAKs and the tyrosine phosphorylation of STAT3¹⁰². Similarly, cytoplasmic kinases such as SRC and BCR-ABL can lead to direct STAT3 phosphorylation¹⁰³.

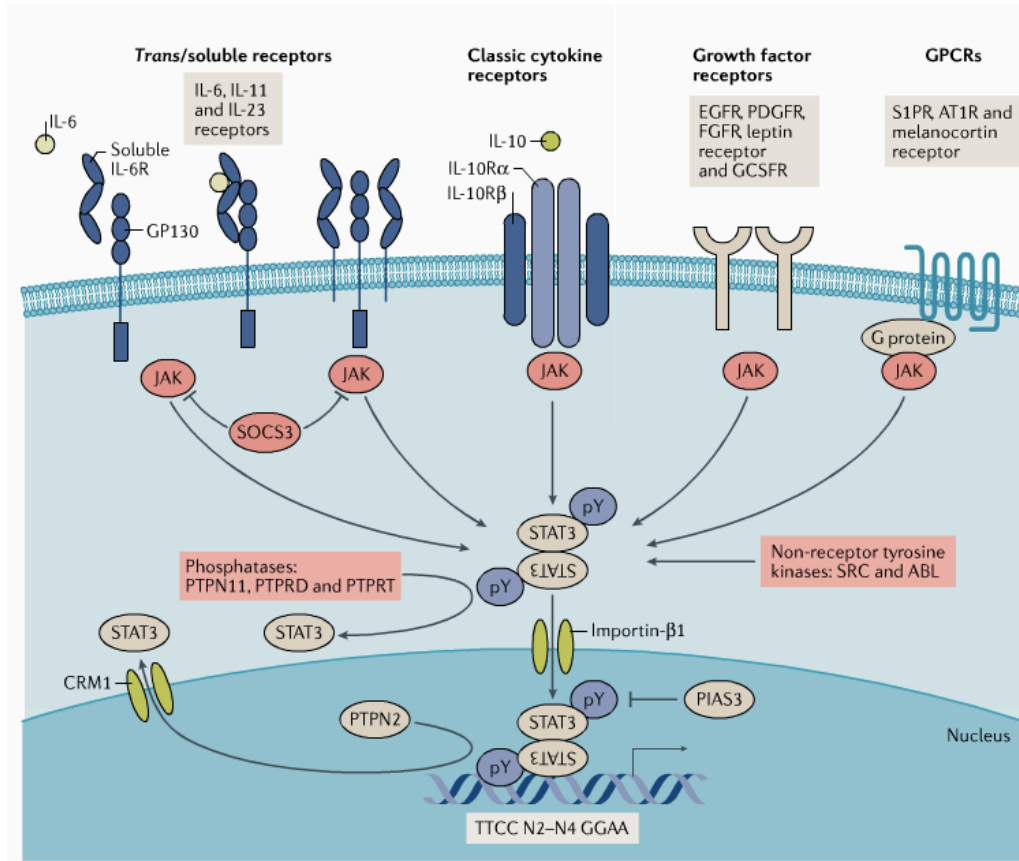


Figure 1.10: Canonical STAT3 signaling pathway.

The panel of upstream receptors responsible for STAT3 activation are depicted. The subsequent nuclear translocation mediated by importins lead to target gene transcription upon binding to palindromic DNA sequences. Negative regulation of STAT3 by SOCS3 and phosphatases are shown¹⁰⁴.

Such a variety of possible stimulatory signals are translated accordingly into a multitude of distinct functions dependent on the cell type and on the stimulatory context. Nonetheless, such a complex regulation of STAT3 illustrates its pivotal and sometimes contradictory role in many cellular mechanisms. It is hence perhaps not surprising that a STAT3 gene inactivation has been reported to be embryonically lethal in mice^{105,106}. STAT3 has indeed a crucial regulatory role in cell growth and survival. A few examples of its many functions include the stimulation of differentiation in B lymphocytes¹⁰⁷, the embryonic stem cells pluripotency maintenance²⁰ and the control of many hematopoietic cell subsets activity^{100,108–113}.

Importantly, STAT3 also exists in two isoforms corresponding to an alternative splicing event of exon 23. As shown in Figure 1.11, STAT3 exists as the full-length protein, (sometimes noted as STAT3 α) as well as a C-terminally truncated STAT3 β which lacks 55 residues, replaced instead by a tail of seven amino acid (FIDAVWK)¹¹⁴. These two isoforms have both unique and overlapping

transcriptional functions^{115–117}. Because the isoform β lost the transcriptional activation domain (TAD) including the S727, but retains the Y705, this isoform can still become phosphorylated on its tyrosine and form dimers. For this reason, this isoform was believed to be a dominant negative form¹¹⁸. However, it has now been shown that STAT3 β also has unique roles in the activation of specific downstream genes. Importantly, one of the key functions of STAT3 β specifically is to suppress systemic inflammation, as demonstrated in mice lacking STAT3 β , which underwent LPS-induced endotoxic shock and developed atherosclerosis^{116,117,119}.

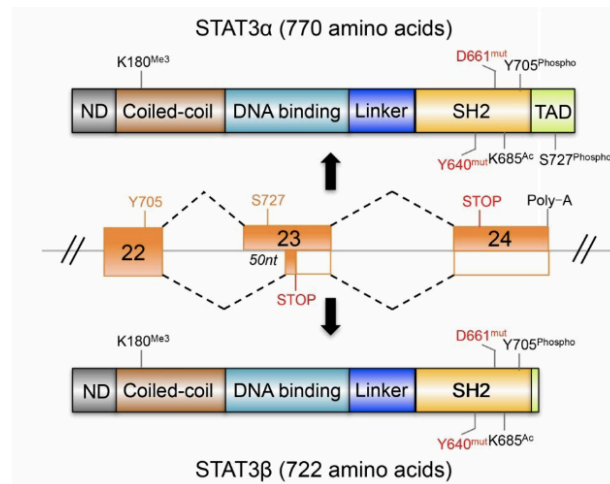


Figure 1.11: Schematic representation of STAT3 isoforms α and β .

The alternative splicing resulting from the frame shift in exon 23 leads to an early STOP codon in isoform β . Individual protein domains and key modifications or mutations of critical residues are indicated¹¹⁴.

1.5.1. STAT3 canonical and non-canonical signaling pathway

As illustrated above, STAT3 activities are complex. But how could one explain such a vast panel of canonical cellular functions? A first answer consists in the ability of STAT3 to precisely activate different target genes in specific cell types according to the local stimulatory environment^{120,121}. Indeed, the availability of STAT3 binding sites in the nucleus, together with its ability to form an active transcriptional complex with other proteins and TFs play a critical role in guiding STAT3 downstream effects. Likewise, the multiplicity of upstream signalings that converge to STAT3 provide a context specific information which determines the overall function of the protein^{103,122,123}.

Interestingly, STAT3 also exists in the cytosol as large protein complexes¹²⁴ that were found to interact with the endoplasmic reticulum (ER)¹²⁵, endosomes¹²⁶ and autophagosomes¹²⁷ together

with modifying the cytoskeleton organization¹²⁸ and modulating mitochondrial activity¹²⁹ (Figure 1.12). The complex roles of STAT3 are thus defined through both the pY-mediated gene transcription (canonical signaling) and pY independent non-transcriptional functions (non-canonical signaling).

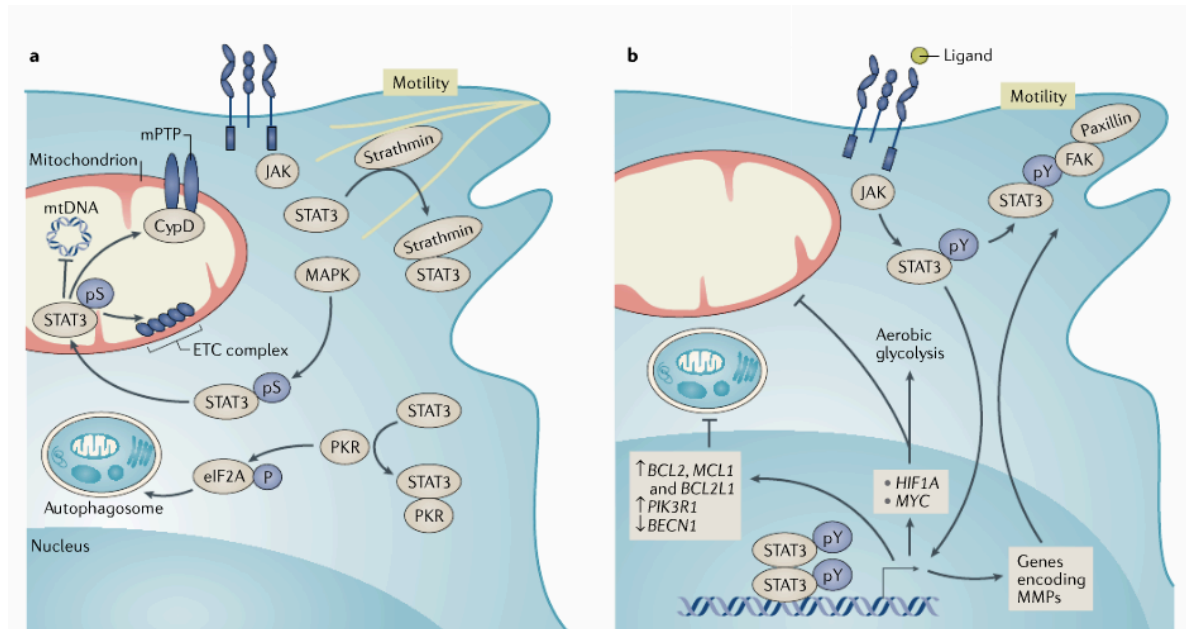


Figure 1.12: STAT3 nuclear and cytosolic activities.

STAT3 exists in the cytosol both as monomers and dimers in association with various cellular structures like the mitochondrion (upon Serine 727 phosphorylation), similarly STAT3 rearranges the cytoskeleton by sequestering paxillin and prevents the formation of autophagosomes (A). Upon tyrosine 705 phosphorylation, the transcriptional activity of STAT3 leads to regulatory control over many cellular mechanisms such as motility, metabolism and extracellular matrix remodeling via matrix metalloproteinases (MMPs) expression (B)¹⁰⁴.

For instance, due to the transcription of essential genes including Bcl2, Bcl211 and Mc11, STAT3 negatively regulates autophagy by preventing the formation of auto-phagosome structures¹³⁰. An additional p-Y705 canonical transcriptional control of STAT3 consists in the promotion of cell motility. This is caused by the expression of key genes such as SLC39A6 and various matrix metallo-proteinases (MMPs)¹³¹. Interestingly however, STAT3 is also capable of controlling cell motility independently of gene transcription by binding to stathmin, a factor responsible for microtubules de-polymerization¹³². As a consequence, the excessive activity of STAT3 in transformed cells favors cellular invasion and metastasis¹³³.

1.5.2. STAT3 post translational modifications and cellular activities

Importantly, besides the Y705 phosphorylation, STAT3 is prone to a number of post-transcriptional modifications on specific residues, which influence its overall cellular localization and activity. The non-Y phosphorylated dependent activities, or so called non-canonical STAT3 signaling functions, raised a lot of interest in regard to their roles in cancer development and progression. These post-transcriptional modifications detailed below include the (I) serine phosphorylation (II) oxidation and glutathionylation (III) acetylation and (IV) methylation.

Indeed, an important regulation consists in the Serine 727 phosphorylation. This phosphorylation is required for certain downstream genes to be optimally transcribed in the nucleus¹³⁴. Intriguingly, a p-S727 dependent role of STAT3 was reported in the endoplasmic reticulum (ER). The co-localization of STAT3 with the ER membrane in breast cancer cell lines influences the calcium release and regulates apoptosis in a transcription-independent manner¹²⁵. Similarly, S727 phosphorylation of STAT3 also favors its mitochondrial localization where it drives critical functions linked to energy metabolism¹³⁵. Indeed, a small portion of cytosolic STAT3 is capable of entering the mitochondria and represses the transcription of mitochondrially encoded genes. The direct association of STAT3 with TFAM, a mitochondrial transcription factor, as well as with mitochondrial DNA could be demonstrated in specific cell types¹³⁶. Moreover, mitochondria are critical sites for the production and reduction of ROS. Animal models showed that various tumors underwent a STAT3-mediated increase in glycolysis rate, while conversely having a reduced Electron Transport Chain (ETC) activity caused by the increased transcription of key metabolic genes¹³⁷. A hallmark of cancer consists in the metabolic shift leading to an increased glycolysis rate together with a reduced mitochondrial activity¹³⁸. This can seem counterintuitive at first as glycolysis has a lower rate of ATP production than the Krebs cycle and the mitochondrial respiration. However, provided that there is a limitless supply of glucose, glycolysis is overall much faster than aerobic respiration which gives an advantage to cancer cells over other cell types, including immune cells.

Interestingly, both p-Tyrosine and p-Serine STAT3 activities are importantly implicated in the regulation of the metabolic switch. Pathologically active STAT3 promotes the aerobic glycolysis by transcriptional induction of the Hypoxia-Inducible Factor 1 (HIF1) but also by actively down regulating the mitochondrial respiratory activity due to the diminished transcriptional control of genes encoding for the Electron Transport Chain (ETC)¹³⁹. In addition to the nuclear transcriptional

control of essential genes, the Serine phosphorylated form of STAT3 directly localizes in the mitochondria where it interacts with specific proteins from the complex 1 of the ETC as demonstrated by immunoprecipitation assays¹²⁹. Taken together, these evidences could account for a STAT3-mediated regulation of mitochondrial activity, but the exact mechanism remains poorly understood and still has to be further studied¹⁴⁰. However, as a consequence of this metabolic shift, cancer cells have increased lactate production as well as decreased levels of reactive oxygen species (ROS). This protects cancer cells from apoptosis and senescence while favoring transformation¹⁴¹. Linked to that, recent work suggested that STAT3 oxidation might help achieve ROS detoxification, highlighting a potential implication of STAT3 in the redox homeostasis control^{142,143}. Indeed, upon oxidative stress conditions or specific stimulations, the oxidation and glutathionylation of multiple cysteines of STAT3 was shown to modify its canonical transcriptional activities^{143–145}.

The third and fourth post-translational modification of STAT3 rely on lysines (K). Lysines are key residues prone to acetylation (Ac) and methylation (Me). Indeed, in response to upstream stimulation, the CBP/p300 histone acetyltransferase carries out the acetylation of various lysines with important consequences on STAT3 downstream activity favoring the canonical or non-canonical functions. For instance, the Ac of K685 was shown to favor gene transcription by STAT3 due to an increased tyrosine phosphorylation level leading to STAT3 dimer formation¹⁴⁶. Additionally, by locally recruiting the DNA methyltransferase 1 to their promoter regions, K685-acetylated STAT3 is capable of silencing tumor suppressor genes¹⁴⁷. In contrast, the Ac of K87 upon insulin stimulation drives the mitochondrial translocation of STAT3 and its non-canonical activity¹⁴⁸. Nonetheless, the Ac of lysines is reversible due to the activity of the Silent Information Regulator Protein 1 (SIRT1), which mediates STAT3 deacetylation in an NAD-dependent process¹⁴⁹. As a consequence of deacetylation, both the canonical nuclear transcriptional activity and the non-canonical mitochondrial function and localization of STAT3 were impaired¹⁵⁰. Additionally, K140 and K180 are prone to methylation, which has precise consequences on downstream signaling. While the histone methyltransferase SET9 methylates K140 on STAT3 bound to promoters, causing an impaired transcriptional function¹⁵¹, the K180 tri-methylation, carried out by EZH2 (a member of the polycomb histone methyltransferase complex 2), is required for the maintenance of the transcriptional activity in certain malignancies such as glioblastoma and prostate cancer¹⁵².

Altogether, accumulating evidence suggest that STAT3 is capable of regulating gene expression via epigenetic mechanisms including DNA methylation and chromatin regulation¹⁵³. While p-

STAT3 dimers are capable of DNA binding, unphosphorylated STAT3 (U-STAT3) was found to bind specific DNA structures as well, either as monomers or dimers, which impacts the three-dimensional organization of the human genome⁹⁵. Accordingly, upon stimulation by IL-6 or LIF, STAT3 triggers topological modifications of the chromatin. The exact roles of U-STAT3 in the context of cancer still have to be elucidated as they currently remain poorly characterized. Nonetheless, acetylation, together with phosphorylation of STAT3 similarly impacts epigenetic modifications on the DNA. Indeed, while P-Y705 STAT3 leads to the DNA methyltransferase 1 expression (DNMT1)^{154,155}, STAT3 acetylation however regulates DNMT1 activity by allowing it to bind promoter regions of known Tumor Suppressor Genes (TSG). The methylation of the promoters that follows thus reduce the expression of these TSG, including DIRAS3, CDKN2A and PTPN6 as observed in human cancer cell lines^{147,156}.

Overall, the wide variety of cellular functions mediated by STAT3 highlight how crucial a deep understanding of this signaling pathway is. Dissecting STAT3 signaling pathways using novel tools specifically achieving precise domain blockade may help reveal more of its secrets. Additionally, the multiplicity of local modifications on STAT3 favoring, or in contrast, preventing a given function perfectly illustrate how precisely blocking a defined domain of STAT3 may have a great impact on the downstream activity of the protein as opposed to a general knock-down/knock-out approach.

1.6. STAT3 implication in tumor development

Among the STAT family, STAT3 and STAT5 are of particular interest due to their role in cancer progression¹⁵⁷. Both STAT3 and STAT5 are considered relevant therapeutic targets. However, STAT3 further qualifies as a target for cancer therapy, as it possesses additional unique features. Indeed, while both STAT3 and STAT5 directly participate in tumor progression, STAT3 also uniquely contributes to cancer cell proliferation and survival due to its pivotal role in regulating the stroma^{158–160}. For example, STAT3 activity in immune cells recruited at the tumor site was found to act as an immune checkpoint, perturbing the local antitumor immune responses and thus, favoring the tumor development^{103,159}.

1.6.1. Uncontrolled STAT3 signaling during tissue repair drives tumorigenesis

In addition to the intricacies of STAT3 functions, another layer of complexity needs to be taken into account and consists in its activity under either physiological or pathological conditions. Indeed, STAT3 itself is often constitutively activated in a variety of malignancies. Among the numerous upstream stimulatory receptors that result in STAT3 activity, some have been importantly implicated in tumor development, such as the epidermal growth factor receptor (EGFR) and ALK receptor tyrosine kinases, or some intracellular tyrosine kinases. Therefore, the constitutive activation of STAT3 may result from an increased upstream stimulation due to higher levels of cytokines in the local microenvironment. Importantly, IL-6 signaling is considered to be the most important driver of STAT3 activity in tumors. Indeed, among the panel of potential upstream stimulation of STAT3, IL-6 stimulation of epithelial and immune cells is most notably implicated in various processes promoting inflammation, which, if uncontrolled, can drive oncogenesis^{102,111,161}. For that reason, cancer is often presented as a “wound that never heals”. Indeed, in addition to the cell intrinsic characteristics required for tumorigenesis, the interplay between cancer cells and the microenvironment is key for the establishment of a long-lasting pathology¹ (Figure 1.13). While spatially and temporally controlled STAT3 activity is critical for restoration of tissue integrity upon damage¹⁶², a persistent activation of STAT3 in neoplastic cells as well as in the surrounding healthy cells favors the development of epithelial tumors. Typically, an efficient wound healing process must be carefully coordinated by a dynamic interaction of epithelial, stromal and immune cells¹⁶³. This collaboration leads to the local recruitment of anti-inflammatory immune cells and to the triggering of proliferative processes in epithelial cells in order to repair the tissue damage. Nonetheless, these highly proliferative cells under sustained STAT3 activation also are often responsible for the stimulation of local tissue stem cells and favor the local vascularization and promotion of migration and invasion¹⁰⁴. During this procedure, the local immune system remains tolerant and does not intervene. However, a critical function of macrophages and monocytic cells also consists in the precisely and temporally controlled secretion of cytokines and chemokines to ensure an effective wound healing process¹⁶⁴. Strikingly, the IL-6 family cytokines especially, and therefore STAT3 by extension, are implicated in assisting in tissue remodeling and in promoting angiogenesis¹⁶⁴. Thus, these mediators must be carefully released and remain only transiently available in a healthy process. In a pathological context however, the uncontrolled presence of STAT3 stimulating signals trigger a transcriptional regulation of genes responsible for promoting survival and proliferation together with a facilitation of invasion and migration¹⁶⁵. This process is supported by experimental evidence in mice where uncontrolled epithelial STAT3 activity led to intestinal tumor growth in presence of oncogenic driver mutations¹⁶⁶. In addition, chronic local inflammation driven by IL-6 and IL-11 were found to cause a persistent activation of STAT3 observed in the intestine in animal models, with as a consequence

an increased epithelial turnover favoring tumorigenesis^{167,168}. Additionally, notorious oncogenes such as BCR-ABL and RAS lead to increased IL-6 expression/secretion in leukemia and skin cancer^{169,170}. These findings emphasize the implication of the IL-6/STAT3 signaling axis in tumor development. Because of its activation due to the upregulation of IL-6, STAT3 may indeed serve as an interesting protein to prevent oncogenes-mediated tumor progression.

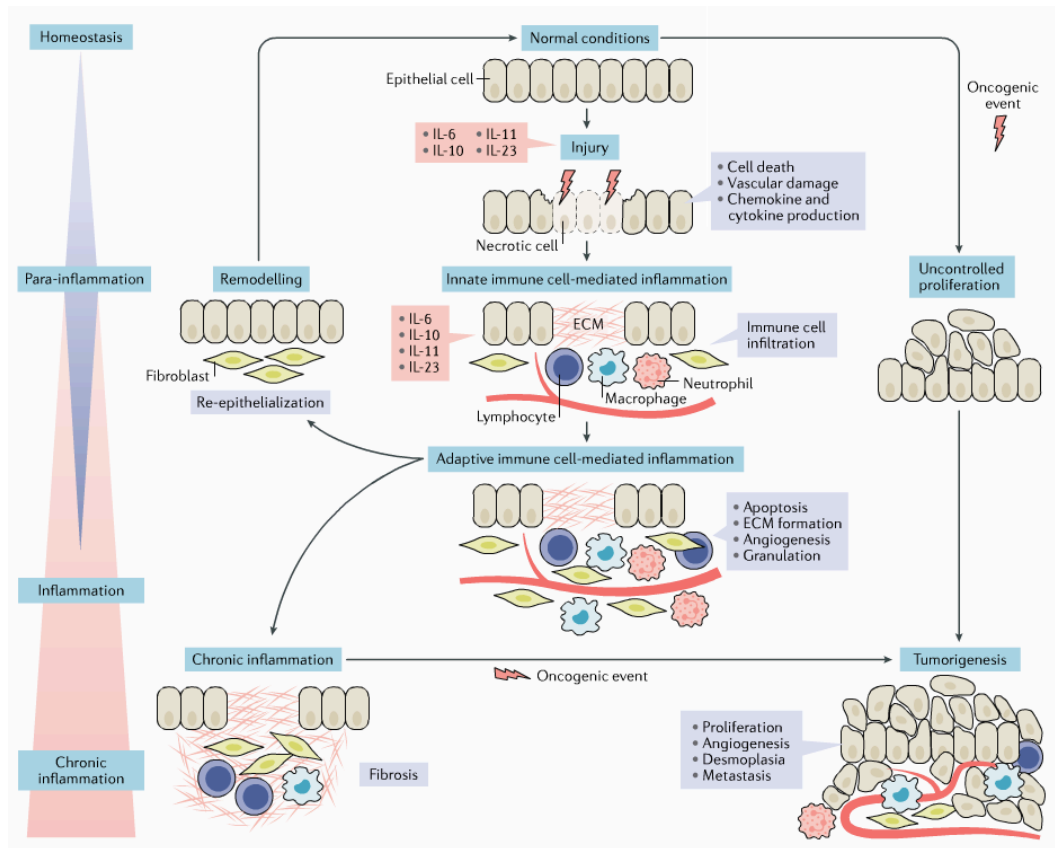


Figure 1.13: Inflammation during tissue repair leads to cellular transformation upon excessive STAT3 signaling.

The highly orchestrated mechanisms driving tissue repair are tightly regulated under homeostasis. However, overactive STAT3 signaling resulting from constitutive cytokine or oncogenic stimulation leads to a stem cell-like states which favors the development of fibrosis and is associated with mutational events. Sustained inflammatory signals lead to neoplasm and tumor progression¹⁰⁴.

Similarly, other members of the IL-6 family have been identified to promote tumorigenesis via STAT3 signaling. Strikingly, among them, Leukemia Inhibitory Factor (LIF) was established as an essential player for the activation of STAT3 in various cancer types, including glioblastoma, pancreas adenocarcinoma and nasopharyngeal carcinoma¹⁷¹. In the latter for example, higher LIF blood levels were observed and correlated with reduced sensitivity to radiotherapy together with

increased local recurrence¹⁷². Of interest, LIF (in synergy with TGF β) was demonstrated to activate JAK-STAT3 signaling leading to glioma tumor growth¹⁷³.

1.6.2. Aberrant STAT3 signaling favors cancer stem cells maintenance and the development of metastatic niches

In addition to the IL6-JAK/STAT3 signaling axis being pivotal for the development of inflammation-mediated cancers, STAT3 is importantly implicated in the de-differentiation of Cancer Stem Cells (CSCs) and the formation of pre-metastatic niches^{174,175}. Indeed, in addition to the direct role of STAT3 in tumor cell growth and proliferation, the JAK-STAT3 signaling pathway favors the formation of local niches that allow the establishment of metastatic cells¹⁷⁶. These so called pre-metastatic niches consist in a local population of immune cells, which permit the establishment of disseminating tumor cells. This is caused by the aberrantly augmented STAT3 signaling in myeloid cells (a subset of immune cells including macrophages, neutrophils and granulocytes), which as a consequence, favors the cancer cells proliferation and resistance to apoptosis. As metastatic cells colonize these niches, myeloid cells in the local micro-environment favor the development of metastases due to their increased production of cytokines and various growth factors, which in turn, promote tumor cell growth¹⁷⁶. In this regard, a correlation between increased STAT3 activity and elevated number of premetastatic niches was found in lymph nodes of patients suffering from non-small cell lung cancer¹⁷⁷. For this reason, it was stipulated that targeting STAT3 may represent an effective therapeutic strategy to prevent the formation of metastatic niches. Moreover, in addition to the critical roles of STAT3 in tumor cells and in tumor-associated immune cells, it was also shown that STAT3 has important implications for CSCs. CSCs represent a subgroup of tumor cells capable of self-renewal and which have a phenotype and gene expression pattern resembling healthy stem cells. These cells are critical for disease progression and were shown to be responsible for therapy resistance in both solid and hematologic cancers¹⁷⁸. In this context, STAT3 is a driver of the expression of genes implicated in the stem-like phenotype¹⁷⁹, but also acts as repressor of the transcription of genes critical for cell differentiation¹⁵². Thus, the complex network of gene under STAT3 transcriptional control is responsible for the CSC population maintenance¹⁸⁰.

1.6.3. STAT3 oncogenic mutants identified in patients

The activity of STAT3 was for a long time considered to be mainly carried out by the direct transcription of downstream genes. Nevertheless, accumulating evidence suggest that additional mechanisms also drive tumorigenesis. While the phospho-tyrosine mediated transcriptional functions of STAT3 are required for cellular transformation¹⁸¹, STAT3 is also required in a transcriptionally independent fashion for Ras-mediated cellular transformation¹³⁵. Additionally, cellular transformation caused by the v-Src oncogene was prevented in the presence of a transcriptionally dead STAT3 mutant: STAT3-Y705F. Strikingly, this was not the case in cells transformed with v-Ras further suggesting that the implication of STAT3 in cellular transformation is not only limited to its transcriptional activity¹⁸¹. As an additional example, the control of mitochondrial functions appears to be an important mechanism for cancer progression, as illustrated by several recent studies^{129,135}.

Activating mutations identified on STAT3 promote both its transcriptional and non-transcriptional functions leading to tumorigenesis^{100,103,182}. Indeed, genetic alterations of STAT3 identified in both solid and hematological malignancies are schematized in Figure 1.14¹⁸³. For instance, an active STAT3 double mutant referred to as STAT3-C where residues A661 and N663 located in the SH2 domain are mutated to cysteines was identified in lymphoid neoplasms¹⁸⁴. The resulting extensive disulphide bonding causes a stabilization of the STAT3 dimers and an increased transcription factor activity resulting in cell transformation¹⁸⁴. Additional mutants in the SH2 domain were identified in patients and found to actively drive cellular proliferation, but their mode of action remains poorly understood. Importantly, two major somatic mutations of the STAT3 SH2 domain, Y604F and D661Y, were found in over 70% of patients suffering from large granular lymphocytic leukemias^{185–187}. Although the exact molecular mechanisms remain poorly understood, these mutations were shown to increase the STAT3-mediated transcription of downstream genes such as JAK2 and BCL2L1¹⁸⁷. Additionally, recent evidence from the Sexl lab confirmed that the stable expression of several oncogenic STAT3 mutants (Y640F, D661Y and S614R) in hematopoietic progenitor (HPC-7) cells led to a significant advantage in cellular proliferation and colony formation (personal communication). Altogether, STAT3 mutations were found in patients suffering from a number of different lymphomas and leukemias (summarized in Figure 1.14) with a final count of up to 250 identified cases overall¹⁸⁸.

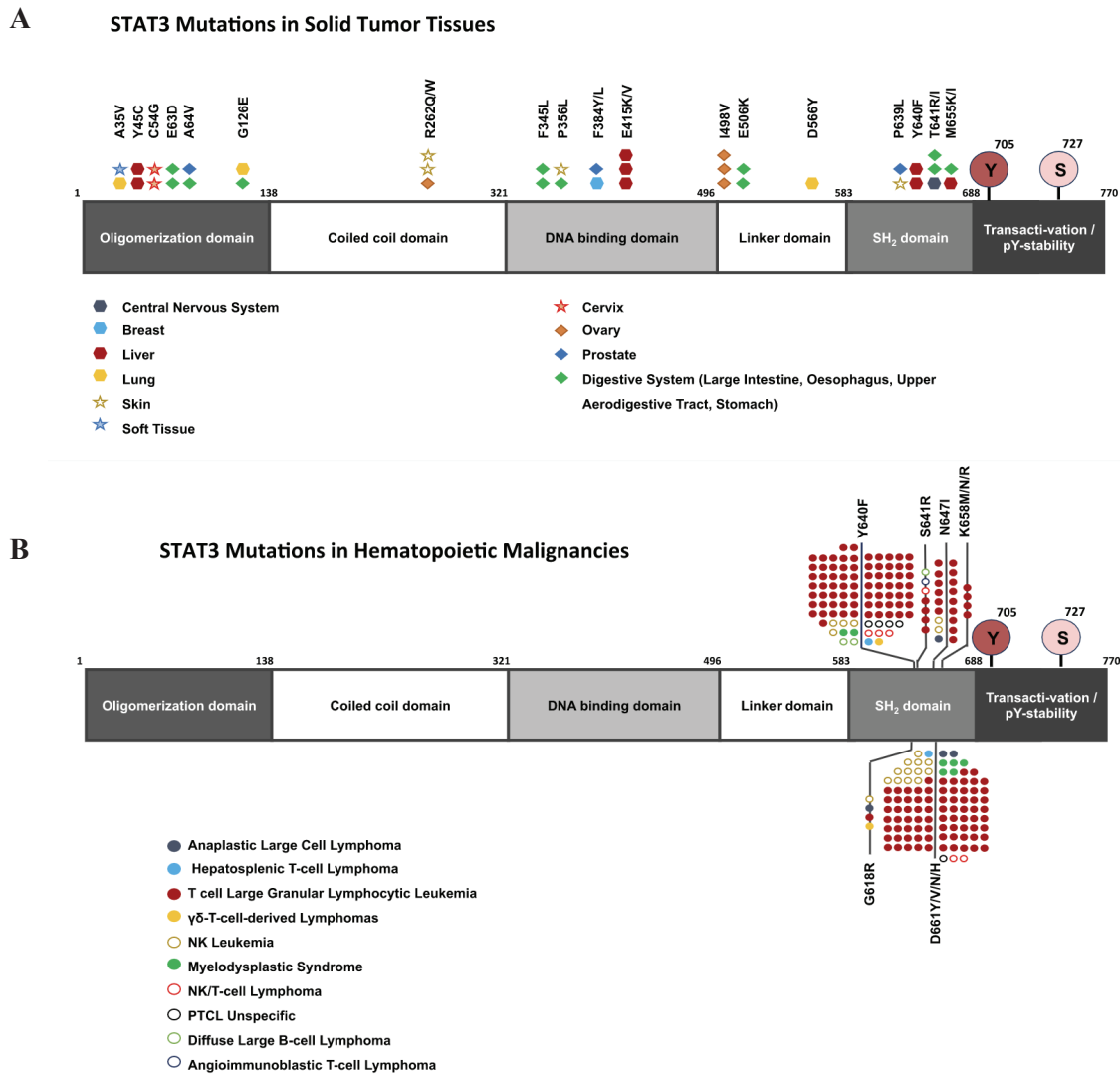


Figure 1.14: Genetic alterations of STAT3 identified in patients.

A schematic structure of STAT3 with the oncogenic mutations identified in patients are indicated for solid (A) and hematopoietic malignancies (B)¹⁸³.

1.6.4. STAT3 may act as a conditional oncogene

However, due to the complexity of its activities, STAT3 may also function as a tumor suppressor in certain contexts. In 2008, STAT3 was shown to inhibit the cellular growth of PTEN-mutated glial tumors. Indeed, the simultaneous deletion of STAT3 and PTEN led to a strong increase in cell proliferation and tumor formation in SCID mice, whereas the isolated siRNA knockdown of PTEN alone showed less dramatic effects. In addition, no tumor suppressor function of STAT3 was observed in presence of PTEN, but could only be observed in absence of PTEN¹⁸⁹. Furthermore,

the tumor suppressing activities of STAT3 were observed upon transfection of either STAT3-WT or STAT3C (A661C and N663C, dominant active mutations) in Ras-transformed hepatocytes, which prevented tumor development in mouse xenografts¹⁹⁰. In contrast, a similar experiment using a double negative STAT3 mutant (Y705 and S727) which lack phosphorylation on these key residues, led to tumor development, suggesting that the transcriptional or non-canonical activities of STAT3 are implicated in its tumor suppressive phenotype. The exact mechanisms mediating these effects remain poorly understood. However, it is hypothesized that the presence of a strong oncogene, such as Ras or EGFR leads to a STAT3-mediated tumor suppressing function. In accordance with this hypothesis, the cancer progression and invasiveness were importantly increased upon STAT3 knockout in mice where the oncogenic force was provided by treatments with carcinogenic chemicals (carbon tetrachloride), or overexpression of the multiple intestinal neoplasia (Min) gene^{191,192}. It is speculated that the specific mechanisms driving tumorigenesis may be responsible for STAT3 activity as either an oncogene or as a tumor suppressor. Hence the pathogenesis of specific cancers might influence the role of STAT3 in the local precise context.

Taken together, the role of STAT3 in cancer development or prevention varies depending on the local context, genetic background and advancement of the disease. STAT3 may act as a conditional oncogene depending on the overall context. However, the unregulated activity of constitutively activated STAT3 was found to induce cellular proliferation and resistance to apoptosis together with promoting the invasion and metastasis due to the Epithelial to Mesenchymal Transition (EMT) promotion. Additionally, STAT3 increases energy metabolism caused by an augmented glycolytic activity and confers cancer stem cells-like features to both solid and hematologic malignancies. Finally, constitutively activated STAT3 was found to fundamentally impact the relationship of transformed cells with their local microenvironment due to the alteration of the extracellular matrix by matrix metalloproteinase (MMP) induction, the local down-regulation of immune responses and the promotion of angiogenesis^{193,194}. Altogether, the implications of STAT3 in tumor development were demonstrated under many axes. By directly influencing tumor progression, favoring a microenvironment which sustains tumor metastasis or endorsing CSC phenotypes, STAT3 has become an evident “hot” target for cancer therapies. Yet up to date, inhibiting STAT3 has appeared to be very complex.

1.7. Strategies towards the targeting of STAT3

Despite STAT3 being an attractive target for cancer therapy, there still is a critical need to investigate ways to effectively generate strong antitumor effects by potently inhibiting STAT3. For

that matter, therapeutic interventions that are clinically applicable remain to be further investigated and developed. To date, the lack of FDA-approved drugs targeting STAT3 can be explained by the challenges of a direct and specific inhibition of a non-enzymatic protein. Additionally, the complex STAT3 biology in cancer, with its multiple upstream activators and various biological functions makes it a puzzling protein to target. Consequently, in order to develop effective ways to inhibit STAT3, a deep understanding of the biology and processes governing the signaling pathway is required. In the chapters below, I will cover the natural mechanisms to terminate STAT3 signaling cascades together with past approaches that were undertaken to develop inhibitors of the JAK/STAT3 signaling pathway.

1.7.1. Natural feedback loops

Importantly, the overall process guiding STAT3 activation or inactivation is determinant for the control of its biological activities. Precluding such control often leads to defective and dysregulated STAT3 functions, which in turn usually contributes to the development of pathological conditions. For that matter, STAT3 activation is tightly controlled by several negative regulators such as (I) phosphatases including SHP-1 and SHP-2, which antagonize upstream STAT3 activators, whilst nuclear phosphatases (like T-cell PTP) lead to inhibition of transcription factor activity and signal termination¹⁹⁵. Notably, among the tyrosine phosphatases implicated in the dephosphorylation of active STAT3, many become inactivated in tumor cells due to genetic mutations of epigenetic control, which results in an excessive STAT3 signaling^{196,197}. Secondly (II), a major and crucial negative regulation of STAT3 is the control of receptor-mediated activation of STAT3, which is regulated by the suppressor of cytokine signaling proteins, in particular SOCS3. These proteins are capable of binding an activated receptor via their SH2 domain and subsequently recruit components of an E3 ubiquitin ligase complex resulting in the degradation of the upstream receptors¹⁹⁸. Of note, SOCS protein themselves are among the major STAT3 target genes and are upregulated upon long lasting STAT3 activity providing a classical negative feedback control mechanism¹⁹⁸. SOCS3 thus terminate STAT3 signaling by inducing JAK proteasomal degradation¹⁹⁹. Lastly (III), the Protein Inhibitors of Activated STAT (PIAS) directly targets STAT3 and prevents its binding to downstream DNA sequences²⁰⁰. Indeed, as STAT3 migrates into the nucleus, its transcriptional activity can be antagonized by PIAS3 which acts as an E3 SUMO protein ligase²⁰⁰. These natural inhibitory mechanisms would however be difficult to exploit for therapy as it implies the development of protein agonists (i.e. activators), which would enhance the activity PIAS3 or

SOCS3. This approach would thus prove pharmacologically difficult and has thus remained currently unexplored.

Alongside the upstream cytokines signaling control and de-phosphorylation of STAT3, an additional level of regulation consists in the inhibition of nuclear translocation, which prevents STAT3 from entering in the nucleus and thus binding to DNA²⁰¹. Such mechanism is mediated by binding to importins- α 5 and 7 and importin- β 1^{201,202}. However, to date, direct alteration of this mechanism has not been thoroughly investigated and remains to be associated to a beneficial effect on overall STAT3-mediated tumorigenesis.

1.7.2. Indirect STAT3 inhibition

In order to control and modulate STAT3 activity, several indirect approaches have been investigated such as (I) the receptor/ligand antagonists, (II) the upstream kinases inhibitors and (III) the phosphatases/ubiquitin ligases mediated targeted protein modulation.

The first approach consists in the inhibition of the upstream receptor activation by developing molecules that have higher affinities for the receptor than the natural ligand while being unable to activate its downstream signaling. For example, the IL-6 antagonist Sant7 was demonstrated to block the constitutive activity of STAT3 in U266 cells, which further resulted in a reduction of cell growth²⁰³. Similarly, the development of monoclonal antibodies against various receptors (such as EGFR and HER2) was found to reduce downstream STAT3 activation. This can be explained by the interaction of the neutralizing antibody to the receptor, which in turns prevent the binding of the ligand and therefore, prevent the receptor activation²⁰⁴.

Moreover, the second approach consists in the intracellular inhibition of kinases responsible for the phosphorylation and activation of STAT3. This approach currently remains the most exploited strategy due to the development of many chemical probes and drugs able to inhibit the catalytical activity of kinases such as JAK1 and JAK2. These molecules were investigated in clinical trials and demonstrated efficacy, which led to their approval by the FDA. For example, the JAK1/JAK2 inhibitor Ruxolitinib was found to bind at nanomolar affinities towards its targets and lead to significant inhibitory effects²⁰⁵. Furthermore, the inhibition of additional kinases responsible for STAT3 activation such as SRC or BCR-ABL using similar approaches led to strong clinical benefits. Nonetheless, these upstream tyrosine kinase inhibitors suffer from a broad spectrum of effects, which could result in undesirable off target effects.

Finally, the last category of indirect STAT3 inhibition relies on the modulation of physiological protein modulators. This strategy aims at taking advantage of the knowledge derived from natural protein inhibitors responsible for the downregulation of STAT3. For example, the understanding that PIAS directly binds to STAT3 and leads to decreased DNA binding levels²⁰⁶ provided insights towards the development of molecules able to replicate this effect. Nonetheless, and despite significant efforts, this approach remains mostly unsuccessful as the development of high affinity and specificity inhibitors of STAT3 remains challenging. An alternative strategy is the modulation of STAT3 cellular functions by hijacking phosphatases. While this strategy is raising more and more attention, this strategy applied to specific STAT family members still remains conceptual up to date⁷². However, the development of strong intracellular binders such as monobodies might open the door for strategies towards the targeted modulation of STAT3 activity.

1.7.3. Direct STAT3 inhibition

Among the direct inhibitory strategies, current approaches comprise the targeting of STAT3 SH2 domain with peptide/peptidomimetics and small molecular compounds to prevent its homodimerization. Indeed, the understanding of the dimerization mechanism of STAT3 prompted the development of peptides and small molecule compounds to prevent the reciprocal interaction between the two SH2 domain and their recognition of the pY-705 residue. Yet, this approach has only resulted in inhibitors with modest activity in cells and has not resulted in clinically available therapeutics so far. For example, a study demonstrated that the phospho-peptide P_pYLKTK inhibited the activity of STAT3²⁰⁷. Similarly, several small molecules have been developed to impair STAT3 dimerization including STA-21²⁰⁸, Stattic²⁰⁹, S31-201⁷³ and BP-1-102²¹⁰. These probes are described to bind to the SH2 domain where the pY705 interacts with the other STAT3 monomer. However, they suffer from low specificity and in most cases, lack experimental data showing direct interaction with STAT3. As a consequence, it remains unclear whether the mode of action truly consist in the mechanism described above, as the probes might instead interfere with the receptor binding instead. Another limitation was demonstrated by the compound sensitivity to the biological environment. For example, Stattic showed varying levels of inhibition depending on the temperature and on the presence of dithiothreitol, which suggests an interaction with a cysteine (possibly Cysteine 687)²¹¹. Altogether however, this strategy did not yield compounds that reached the clinic despite extensive efforts and progress.

Another alternative to directly target STAT3 consists in G-rich oligodeoxynucleotides termed G-quartets^{212,213}. This approach consists in a strain of nucleotides able to form potassium dependent intramolecular structures. They were found to be effective at micromolar concentrations but were nonetheless effective in tumor xenograft mouse models^{212,214}. However, their large size and dependence on potassium make them a suboptimal approach for translational application²¹⁵. Alternatively, decoy oligodeoxynucleotides (dODNs) were developed to prevent STAT3 binding to cellular DNA. These short pieces of double-stranded DNA composed of a STAT3 consensus binding sequence and work by recruiting STAT3 away from the nucleus and thus prevent its transcriptional activity²¹⁶.

More recently, a STAT3 selective small molecule-degrader termed SD-36 was developed, which acts as a PROTAC warhead to mediate the polyubiquitination and proteasomal degradation of STAT3⁹⁰. In this approach, a chemical probe binding to the SH2 domain of STAT3 is covalently linked to a binder of the endogenous CRBN E3 ligase and leads to the growth inhibition of MOLM-16 acute myeloid cells and of the anaplastic large cell lymphoma SU-DHL-1 cell line. Similarly, this approach led to a robust anti-tumor activity in murine xenograft mice models, illustrating the benefits of targeting STAT3⁹⁰.

Nonetheless, while most strategies described above rely on the targeting of either the SH2 or DBD of STAT3, alternative targeting strategies have not been currently thoroughly investigated. The coiled-coil domain and NTD of STAT3 have central roles in the activity of the protein. These domains are thus targets of choice for the overall inhibition of STAT3, but remain presently untouched. This paradox is in part due to current technological limitations as small molecules fail to cover the large area responsible for these domains functions.

In this work, I aimed at developing novel targeting approaches of STAT3 using the monobody scaffold as inhibitor. Similarly, by taking advantage of the monobody binding to STAT3, we aimed at selectively degrading STAT3 by high-jacking the poly-ubiquitination machinery.

2. RESULTS

2.1. Selective targeting and inhibition of STAT3 signaling using Coiled-coil and N-terminal domain specific monobodies

This chapter is based on the result section of a pre-print version of a paper which will be submitted in early 2020.

Authors and affiliations

Grégory La Sala¹, Camille Michiels², Tim Kukenshöner¹, Kelvin Lau³, Florence Pojer³, Veronika Sexl⁴, Laure Dumoutier², Oliver Hantschel¹.

- 1- **Swiss Institute for Experimental Cancer Research (ISREC)**, School of Life Sciences, École polytechnique fédérale de Lausanne (EPFL), Station 19, 1015 Lausanne, Switzerland.
- 2- **Experimental Medicine unit, de Duve Institute**, Université catholique de Louvain, Brussels, 1200, Belgium.
- 3- **Protein Crystallography Core Facility**, School of Life Sciences, École polytechnique fédérale de Lausanne, Station 19, 1015 Lausanne, Switzerland.
- 4- **Institute of Pharmacology and Toxicology**, University of Veterinary Medicine, Vienna, Austria.

Authors contributions

G.L.S and O.H. conceived the work. Intellectual input on the alternative IL-22R work was provided by C.M. and L.D. V.S provided intellectual input, expertise on STAT3 signaling and hosted G.L.S. for experiments to be performed in her lab. T.K. and G.L.S. performed the monobody selection and ITC experiments. G.L.S designed and performed experiments, including the cloning of the constructs used in this paper, the purifications of recombinant proteins, the initial luciferase assay screening, the tandem affinity purifications, the in-vitro assays and microscopy experiments. C.M. designed and performed luciferase reporter assays, Flow cytometry experiments and GST-pull downs in regards to the alternative IL-22R signaling. G.L.S. together with K.L. and F.P. solved the crystal structure of the STAT3/MS3-6 complex. G.L.S. and O.H. wrote the paper, with inputs from C.M. and L.D. All authors commented on the manuscript.

2.1.1. Generation of high affinity monobodies targeting STAT3

In order to generate monobody binders against STAT3, we first recombinantly expressed the biotinylated core fragment (CF) of STAT3, encompassing the coiled-coil, DNA binding and SH2 domains (STAT3-CF, a.a. 127-722), as well as the N-terminal domain (NTD, a.a. 3-129; Figure 2.1A). Size exclusion chromatography analysis following affinity purification of the constructs revealed that both proteins were monomeric in solution (Supplementary Figure 2.1A). Coomassie staining of the concentrated recombinant proteins confirmed their high purity levels (Supplementary Figure 2.1B). We generated monobodies from the combinatorial “side-and-loop” library using an established phage and yeast display selection strategy^{54,58,217}. Overall, seven monobody clones with unique sequences binding to STAT3-CF and five clones binding to STAT3-NTD were isolated and further characterized (Table 2.1). In order to measure the binding affinities to their respective targets, increasing concentrations of recombinant STAT3 proteins were titrated to yeast cells displaying the monobodies, revealing low nM K_D affinities for each clone (Supplementary Figure 2.1C; Table 2.1). The highest affinity towards STAT3-CF was obtained with monobody MS3-6 (31 ± 6 nM), while several clones showed comparable affinities towards STAT3-NTD, among which monobody MS3-N3 (40 ± 4 nM) additionally had higher solubility levels (Table 2.1; Figure 2.1B). Interestingly, despite their different sequences, all monobodies generated against the core fragment of STAT3 were found to share a common epitope as revealed by their competition for STAT3 binding in presence of MS3-6 (Supplementary Figure 2.1D). Efforts were thus concentrated on the characterization of the MS3-6 monobody, which had the highest affinity. In the past decade, a number of STAT3 oncogenic mutants were identified in patients suffering from both solid and hematological malignancies. We wondered whether MS3-6 bound to oncogenic STAT3 mutants. We measured high affinity binding to the STAT3-S614R and STAT3-D661V oncogenic mutants, as well as to the STAT3-Y705F dominant negative mutant with K_D values of 94.7 ± 15.9 nM, 18.5 ± 6.1 nM and 17.6 ± 7.4 nM respectively (Supplementary Figure 2.1E) indicating that MS3-6 is capable of binding to STAT3 exhibiting point mutations in its SH2 domain. The binding of MS3-6 to STAT3-CF (WT) was further investigated using isothermal titration calorimetry (ITC) experiments, revealing an enthalpically-driven binding (ΔH values = -22.5 ± 0.5 kcal/mol) with a stoichiometry of 1:1 and with high affinity (K_D of 7.6 ± 4.5 nM) (Figure 2.1C). The recombinant monobodies expressed in *E. coli* showed high solubility and a monodisperse MS3-6/STAT3-CF 1:1 complex formation was observed by Size Exclusion Chromatography coupled to Multi-Angle Light Scattering (SEC-MALS) analysis (Supplementary Figure 2.1F; 2.1G).

Table 2.1: Original monobody libraries and selected STAT3 binders.

Amino acid sequences of two different libraries are shown on top, where “X” corresponds to a blend of 30% Tyr, 15% Ser, 10% Gly, 5% Phe, 5% Trp and 2.5% each of all remaining amino acids with the exception of Cys. “B” denotes a mixture of Gly, Ser and Tyr. “J” corresponds to a mixture of Ser and Tyr; “O”, a mixture of Asn, Asp, His, Ile, Leu, Phe, Tyr and Val. “U”, a mixture of His, Phe and Tyr. “Z”, Ala, Glu, Lys and Thr. Monobodies selected against STAT3-CF are indicated in the upper panel (MS3-1 to MS3-8), while monobodies selected against STAT3-NTD are shown in the lower panel (MS3-N1 to MS3-N7). Dissociation constants (K_D) are indicated according to yeast binding assays. Binding curves can be found in supplementary Figure 2.1C.

Library/Clone	K_D (nM)	Amino acid sequence
		10 20 β C 40 CD β D 50 60 70 FG 90
side-and-loop		VSSVPTKLEVVAATPTSLISWDAPAVT-VOUYQITYGETG(X ₅₋₆)-QZFZVPGSKSTATISGLSPGVDTITVYA(X ₇₋₁₃)-----SPISINVRT
loop-only		VSSVPTKLEVVAATPTSLISWDA(X ₅₋₆)VXYRITYGETGGNSPV-QEFTVPBJJJTATISGLSPGVDTITVYA(X ₇₋₁₃)-----SPISINVRT
MS3-1	127 ± 6	VSSVPTKLEVVAATPTSLISWDAPAVT-VDFYHITYGETGGNSPV-QEFTVPGSKSTATISGLKPGVDYITITVYANTGVPSQIKA-----SPISINVRT
MS3-2	104 ± 10	VSSVPTKLEVVAATPTSLISWDAPAVT-VDFYHITYGETGGNSPV-QEFTVPGSKSTATISGLKPGVDYITITVYAVSVPEYVFP-----SPISINVRT
MS3-4	64 ± 8	VSSVPTKLEVVAATPTSLISWDAPAVT-VDFYHITYGETGGNSPV-QEFTVPGSKSTATISGLKPGVDYITITVYAWSDYIPLWEGSSSPISINVRT
MS3-5	88 ± 14	VSSVPTKLEVVAATPTSLISWDAPAVT-VDFYHITYGETGYGPP-QEFTVPGSKSTATISGLKPGVDYITITVYAWAYERL-----SPISINVRT
MS3-6	31 ± 6	VSSVPTKLEVVAATPTSLISWDAPAVT-VDFYHITYGETGGNSPV-QEFTVPGSKSTATISGLKPGVDYITITVYAVSYPEYVFP-----SPISINVRT
MS3-7	135 ± 23	VSSVPTKLEVVAATPTSLISWDAPAVT-VDFYHITYGETGGNSPV-QEFTVPGSKSTATISGLKPGVDYITITVYANQSVGEYYSK-----SPISINVRT
MS3-8	235 ± 48	VSSVPTKLEVVAATPTSLISWDAPAVT-VDFYHITYGETGGNSPV-QEFTVPGSKSTATISGLKPGVDYITITVYANGGYSQY-----SPISINVRT
MS3-N1	65 ± 10	VSSVPTKLEVVAATPTSLISWDAPAVT-VDFYHITYGETGWYSGY-QEFTVPGSKSTATISGLKPGVDYITITVYAAYMYYSQYEWSS-----SPISINVRT
MS3-N3	40 ± 4	VSSVPTKLEVVAATPTSLISWDAPAVT-VLYYHITYGETGSYGGV-QEFTVPGSKSTATISGLKPGVDYITITVYAYFGYQPSERYSSPISINVRT
MS3-N5	39 ± 6	VSSVPTKLEVVAATPTSLISWDAPAVT-VVYHITYGETGSYGGV-QEFTVPGSKSTATISGLKPGVDYITITVYAYYGFYVSWAKRYS-----SPISINVRT
MS3-N7	38 ± 5	VSSVPTKLEVVAATPTSLISWDAPAVT-VDFYHITYGETGWYSGY-QEFTVPGSKSTATISGLKPGVDYITITVYAYYGFYVSWAKRYS-----SPISINVRT

2.1.2. STAT3 monobodies are highly selective in cells

Due to the high sequence and structural conservation among the STAT family members, the development of probes discriminating between STAT family members remains challenging. Strikingly, no binding of MS3-6 to the recombinant core fragment of STAT5B (a.a. 129-712, Supplementary Figure 2.1E) was detected *in vitro*. In order to comprehensively evaluate, if MS3-6 and MS3-N3 are able to bind to STAT3 in a complex cellular environment, we stably transfected HEK293 cells with 6xMyc tagged monobodies and tested for binding to endogenous STAT3. Enrichment of STAT3 in the Myc-tag pull down fraction was observed by immunoblot suggesting an effective binding between STAT3 and MS3-6 or STAT3 and MS3-N3 in the complex and reducing environment of mammalian cells (Supplementary Figure 2.2A). In order to assess functional engagement of STAT3 by the selected monobodies in a cellular context, we engineered a targeted degradation system by fusing the monobodies to the Von Hippel–Lindau (VHL) protein, which is the substrate receptor of the Cullin2/RBX1 E3 ubiquitin ligase complex. Inducible expression of MS3-6-VHL fusions in NPM-ALK expressing mouse thymoma cells resulted in the degradation of STAT3 as assessed by immunoblot analysis (Figure 2.1D; 2.1E). MS3-N3-VHL similarly leads to the degradation of STAT3 over time, whereas the non-binding HA4-Y87A-VHL control had no effect on STAT3 protein levels. Hence, the monobodies mediated targeted degradation of STAT3 showed functionality of the expressed monobody in cells and highlighted the successful target engagement.

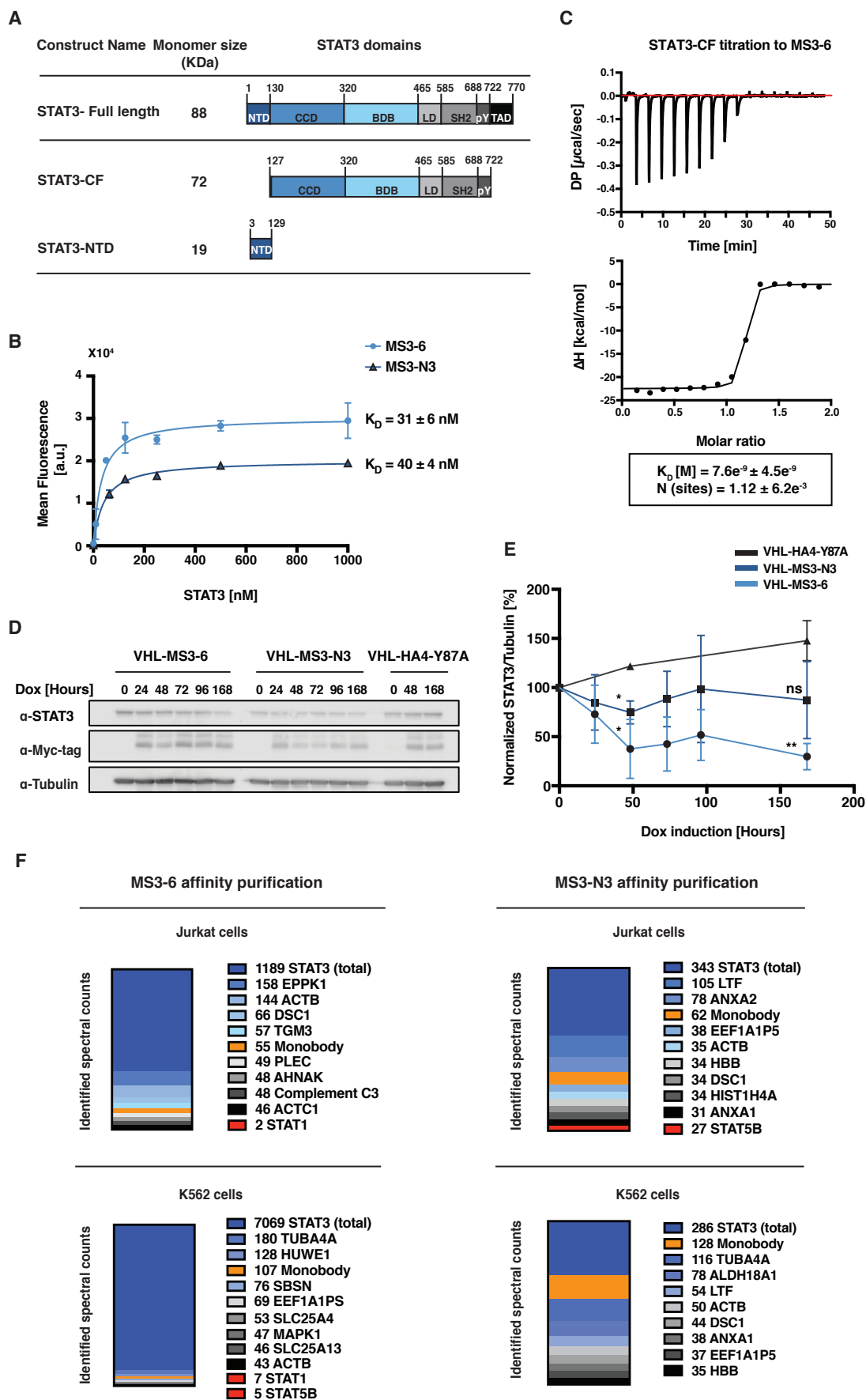


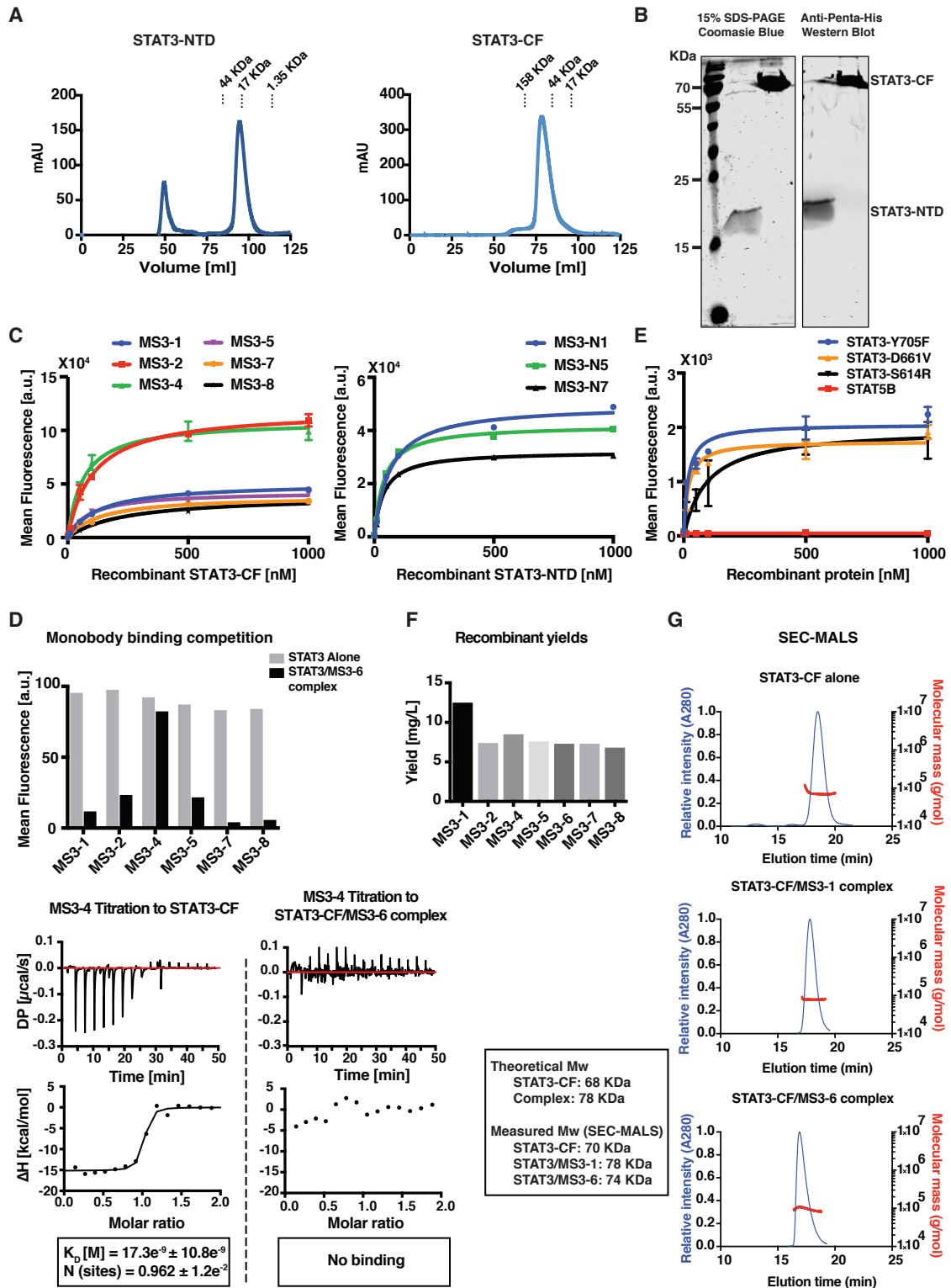
Figure 2.1: see next page for caption.

Figure 2.1: Selection of high affinity, STAT3 selective monoclonal binders.

(A) Schematic representation of the recombinant STAT3 constructs used for monoclonal selection. (B) Titration of yeast cells displaying monoclonal antibodies at their surface to recombinant STAT3 proteins, the mean fluorescence intensity of yeast cells bound to the target are plotted as a function of the protein concentration. Data from three individual experiments, mean \pm SD are shown and a curve fitting 1:1 binding model was used. (C) Isothermal calorimetric titration (ITC) of STAT3 (100 μ M) to a MS3-6 solution (10 μ M) performed at 25°C. The upper panel shows raw heat signal, while the lower panel shows the integrated calorimetric data of the area for each peak. A best fit 1:1 binding model was used and is illustrated by a black line (Microcal software). K_D and stoichiometry values (N) are indicated in the figure. ΔH (Kcal/mol) = -22.5 ± 0.5 ; ΔG (Kcal/mol) = -11.1 . (D) Representative immunoblot analysis of monoclonal-VHL fusion expression overtime upon doxycycline treatment (1 μ g/ml) leading to STAT3 degradation. (E) STAT3 degradation levels were quantified and plotted from three independent experiments. Mean \pm SD are shown and significance is indicated according to an unpaired t-test against HA4-Y87A control * $P \leq 0.05$, ** $P \leq 0.01$. (F) Most enriched proteins and STAT family members identified from the mass spectrometry analysis of the monoclonal interactomes. Total spectrum counts are indicated next to the protein acronyms: EPPK1, Epiplakin; ACTB, Actin; DSC1, Desmocollin-1; TGM3, Protein-glutamine gamma-glutamyltransferase E; PLEC, Plectin; ACTC1, Actin, alpha cardiac muscle 1; TUBA4A, Tubulin alpha-4A chain; HUWE1, E3 ubiquitin-protein ligase HUWE1; SBSN, Suprabasin; EEF1A1P5, Eukaryotic translation elongation factor 1 alpha 1; SLC25A4, ADP/ATP translocase 1; MAPK1, Mitogen-activated protein kinase 1; SLC25A13, Calcium-binding mitochondrial carrier protein Aralar2; LTF, Lactotransferrin; ANXA2, Annexin A2; EEF1A1P5, Putative elongation factor 1-alpha-like 3; HBB, Hemoglobin subunit beta; HIST1H4A, Histone H4; ALDH18A1, Delta-1-pyrroline-5-carboxylate synthase.

Yet, the selectivity of MS3-6 and MS3-N3 remained to be comprehensively assessed in an unbiased assay on a proteome-wide scale. To do so, we performed a tandem affinity purification (TAP) in two cell lines that endogenously express STAT3, the chronic myeloid leukemia cell line K562 and Jurkat acute lymphoblastic leukemia T cells. TAP-tagged monoclonal antibodies were constitutively expressed by retroviral transduction. K562 cells were found to express higher monoclonal levels than Jurkat cells (Supplementary Figure 2.2B). 10^9 cells were used for two sequential affinity purification steps followed by extensive washing steps. Immunoblot analysis of the fractions retrieved after the second affinity purification step showed that both the monoclonal and its “on-target” STAT3 were efficiently recovered (Supplementary Figure 2.2B). The composition of the recovered fractions was assessed by SDS-PAGE analysis (Supplementary Figure 2.2C). Two main bands were found at ~20kDa and ~80kDa corresponding to the molecular weight of the monoclonal antibodies and STAT3 respectively. The subsequent unbiased analysis of all the proteins in the samples by liquid chromatography coupled to tandem mass spectrometry (LC-MS/MS) showed that full length STAT3 and its β isoform were highly enriched among the most abundant proteins recovered, whereas only very low levels of STAT5 and STAT1 were detected (Figure 2.1F). MS3-6 led to a difference of >500-fold identification of STAT3 as compared to STAT1 in Jurkat cells as well as a ~1000-fold identification difference in K562 cells. Similarly, STAT3 was retrieved >1000-fold more abundant than STAT5B in K562 cells. MS3-N3 led to a 12-fold difference in STAT3 detection as compared to STAT5B in Jurkat cells, while no other STAT family members than STAT3 were identified upon MS3-N3 affinity purification in K562 cells. The spectral counts assigned to the 10 most enriched specific protein interactors as well as to other STAT family members identified in Jurkat and K562 cells following MS3-6 or MS3-N3 affinity purification are shown in Figure 2.1F. Most of the proteins identified by LC-MS/MS included STAT3 isoforms,

the monobody itself and additional ubiquitous proteins highly expressed in the cytosol such as tubulin and actin, which are likely contaminants. Therefore, these results demonstrate the exquisite selectivity of MS3-6 and MS3-N3 for STAT3 as compared to other STAT family members and did not consistently bind to other unrelated proteins off-targets. Taken together, these evidences show that the selected monobodies bind with high affinity and selectivity to the core fragment and to the previously untargeted NTD of STAT3.

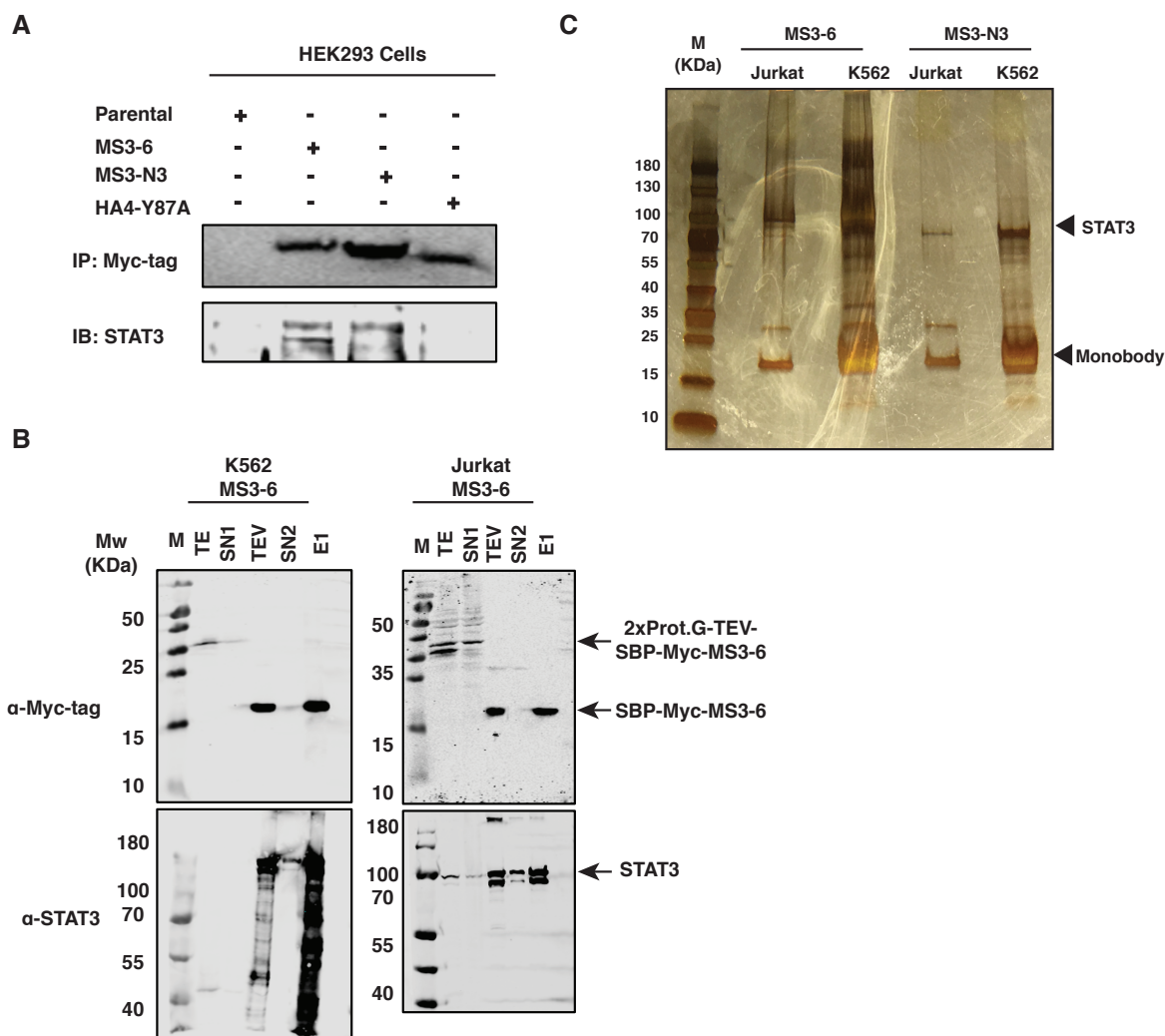


Supplementary Figure 2.1: STAT3 target protein constructs and monobodies characterization.

(A) Size exclusion chromatography traces of the purified STAT3 proteins. Protein purity and identity was assessed by Coomassie staining and western blot analysis shown in (B). (C) Yeast binding assay of all additional monobody clones against the STAT3-CF (left panel) and STAT3-NTD (right panel). Affinities are reported in Table 2.1. (D) Pre-complex formation of STAT3-CF/MS3-6 prevents other monobodies to bind to STAT3 as measured by yeast binding assay (upper panel) with the exception of MS3-4. This can be explained as the affinities of MS3-6 and MS3-4 are in a comparable range. Hence, to determine whether MS3-6 and MS3-4 shared a similar epitope, a higher sensitivity

Chapter 2. Results

technique (ITC) was used to demonstrate that MS3-4 does not bind to the pre-formed MS3-6 complex as well (D - lower panel). MS3-4 binding to STAT3-CF alone: ΔH (Kcal/mol) = -15.2 ± 0.5 ; ΔG (Kcal/mol) = -10.6 . (E) Binding of MS3-6 to STAT3 point mutants located in its SH2 domain identifies in patients suffering from various hematological malignancies. (F) Monobodies recombinant yields expressed in *E. coli* reported in mg of protein per liter of lysogeny broth (LB) expression medium.



Supplementary Figure 2.2: Monobodies MS3-6 and MS3-N3 binding to STAT3 in cellular contexts.

(A) Myc-tagged monobody pull down upon transient transfections in HEK293 cells was performed to assess STAT3 binding in the complex reducing cellular environment. STAT3 Co-immunoprecipitation is detected with MS3-6 and MS3-N3, but not with HA4-Y87A control monobody. (B) Immunoblot analysis of Tandem-affinity purification (TAP) experiments from MS3-6 expression in Jurkat and K562 cells. Legends: M, Marker; TE, total extract; SN1 supernatant after protein G affinity capture; TEV, eluate after TEV cleavage; SN2, supernatant after streptavidin beads pull down; E1, eluate from streptavidin beads. Both the monobody (bait) and STAT3 (target protein) were identified by immunoblotting by anti-Myc tag and anti-STAT3 antibody detection. (C) 10% of the eluate (E1) fraction were resolved by SDS-PAGE and visualized by silver staining to assess the overall sample purity for MS3-6 and MS3-N3 in Jurkat and K562 cells. Major bands corresponding to the monobodies and STAT3 were identified in all fractions.

2.1.3. Monobodies inhibit STAT3-dependent transcription

To test whether the high-affinity and selective binding of MS3-6 and MS3-N3 interfered with STAT3 cellular functions, we first employed an established U3A stable reporter cell line expressing luciferase under the transcriptional control of STAT3 response elements²¹⁸. MS3-6, MS3-N3 and a non-binding monobody control (HA4-Y87A)⁵⁶ were expressed as eGFP fusion proteins, along with an eGFP negative control in a doxycycline inducible expression system. After transient monobody expression for 48 hours, GFP⁺ cells were FACS-sorted and upon oncostatin M (OSM) stimulation, luciferase activity was measured to infer STAT3 activation (Figure 2.2A). MS3-6 strongly reduced the transcriptional activity of STAT3 as compared to eGFP alone and to the HA4-Y87A monobody control (Figure 2.2B). Strikingly, the perturbation of STAT3 activity by MS3-6 was stronger than that caused by a transcriptionally inactive dominant negative mutant (STAT3-Y705F), by the siRNA knock-down of the STAT3's upstream kinase JAK1 or by the treatment of cells with the potent JAK1/JAK2 kinase inhibitor Ruxolitinib (Figure 2.2B). Expression of MS3-N3 led to a less pronounced inhibition of the transcriptional activity (Figure 2.2B). As these results demonstrated potent STAT3 inhibition, we investigated the mechanism-of-action and activity of MS3-6 in different cellular and stimulatory contexts. To do so, we took advantage of BW5147 and Ba/F3 cells, which we engineered to express a panel of cytokine receptors including the IFN λ R, the IL-22R and the IL-20Ra/b. Cells were electroporated with plasmids containing either MS3-6 or the negative control HA4-Y87A monobody together with a dual Firefly/Renilla luciferases system under the transcriptional control of STAT3. Stimulation of cells with the mIL-9, hIL-22, hIL24 and hIFN λ 3 cytokines led to strong inductions of the Firefly/Renilla luciferase signals in the presence of the non-binding monobody control (Figure 2.2C). In contrast, expression of MS3-6 resulted in the strong reduction of STAT3 activity upon stimulation by all four cytokines (Figure 2.2C). We next investigated if MS3-6 would inhibit STAT3 transcriptional activity in a physiological context in non-engineered cells. To test this hypothesis, we used the A549 lung cancer cell line, which endogenously expresses the hIL-6 and hIL-22 receptors. We stably expressed the monobodies under a doxycycline inducible system. Cells were transiently transfected with a STAT3 responsive Firefly/Renilla luciferase reporters. Expression of MS3-6 strongly decreased STAT3 activity as compared to the HA4-Y87A control following IL-6 and IL-22 stimulation (Figure 2.2D). We next investigated whether the observed inhibition of STAT3 results in endogenous gene expression changes. To do so, the effect of monobodies on mRNA expression of five different STAT3 downstream genes was assessed by RT-qPCR in A549 cells. Upon IL-22 stimulation, gene expression of SOCS3, MMP9, IL-6 and BCL-3 showed strongly reduced mRNA induction levels in the presence of MS3-6 as compared to HA4-Y87A monobody control, while MS3-N3 led to more modest effects (Figure 2.2E). Interestingly, expression of CLND2 was increased in presence

Chapter 2. Results

of MS3-6, but remained unaffected by MS3-N3. Altogether, these data indicated that MS3-6 and, to a lower extend, MS3-N3, potentially perturb STAT3 transcriptional activity.

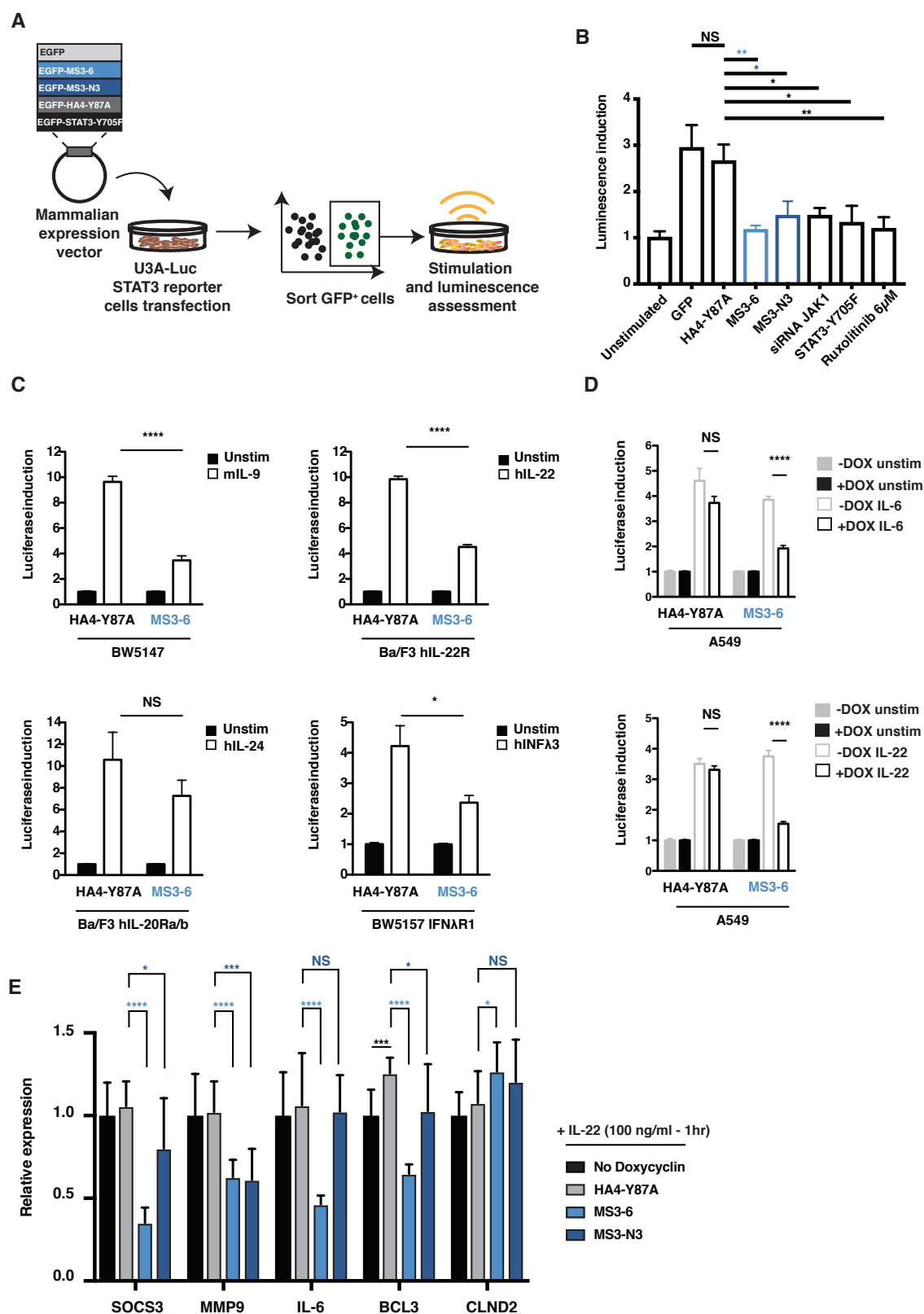


Figure 2.2: see next page for caption.

Figure 2.2: Monobody inhibition of the STAT3 transcriptional activity.

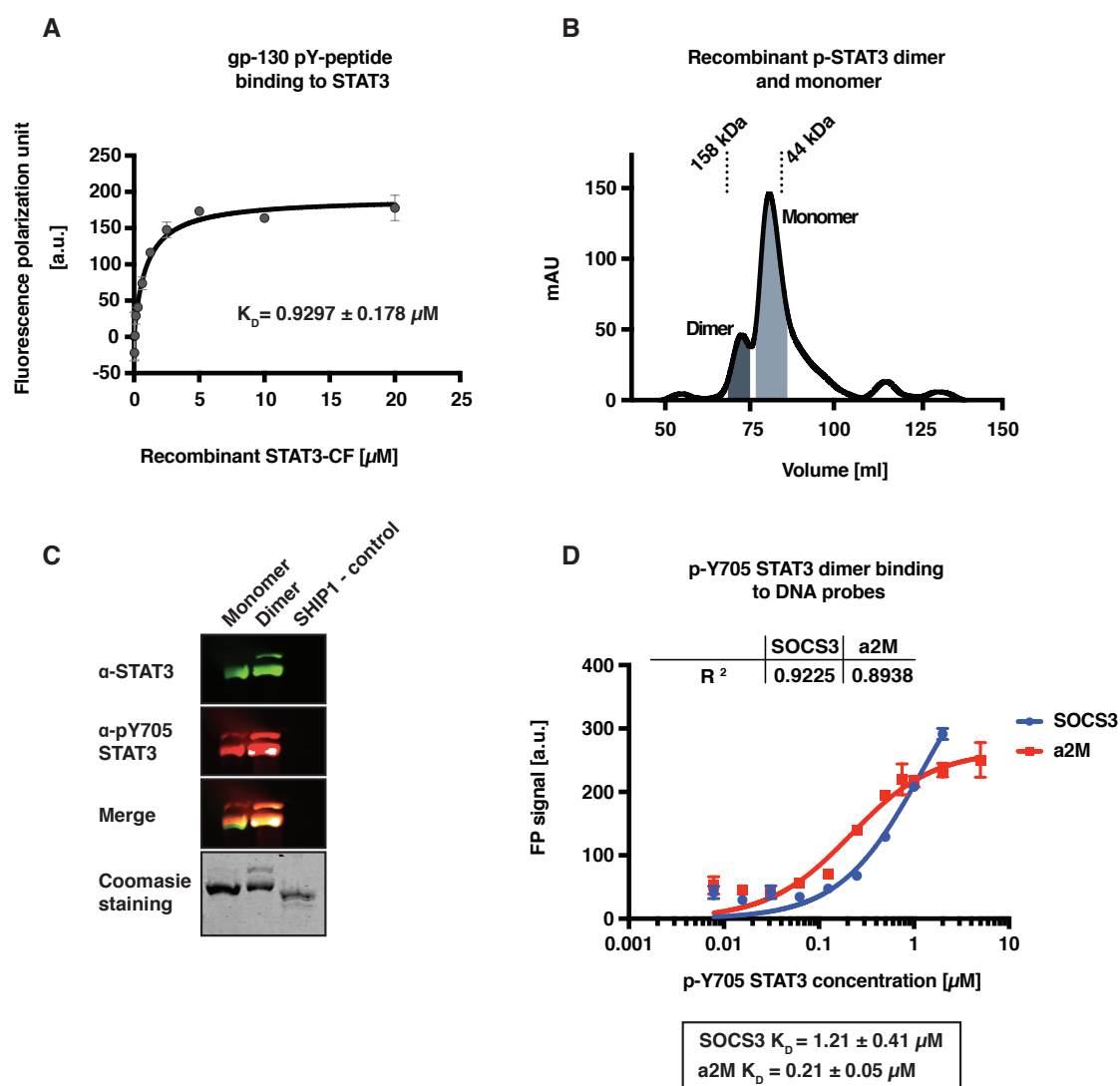
(A) Scheme depicting the initial screening strategy to validate the monobodies inhibitory activity. U3A cells stably expressing a luciferase reporter gene under transcriptional control of STAT3 were transfected with eGFP-monobody fusion plasmids or eGFP-STAT3-Y705F dominant negative mutant as control. 48 hours after transfection, GFP⁺ cells were sorted into 96 well plates and stimulated with OSM. Luciferase activity inductions normalized to that of unstimulated cells, which was arbitrarily set to 1, are reported. Results from two individual experiments performed in triplicates are shown in (B) (data presented as mean \pm SEM). Unpaired t-test analysis was performed against the HA4-Y87A monobody control: * $P \leq 0.05$, ** $P \leq 0.01$. (C) BW5147 or Ba/F3 cells (10^7) were electroporated with the monobody, the pGL3-Pap1 luciferase reporter plasmid as a specific promoter for STAT3 activation and the pRL-TK plasmid and stimulated with control medium or murine IL-9 (100 U/ml, left upper panel), human IL-22 (500 ng/ml, right upper panel), human IL-24 (HEK293 supernatant 2%, left lower panel) or human IFN λ 3 (HEK293 supernatant 2%, right lower panel) for 4 hours. Data are presented as mean \pm SEM of two or three independent experiments performed in triplicates. (D) Luciferase assay on A549 with inducible monobody (HA4-Y87A or MS3-6) expression. A549 (5×10^3) were plated in 96-well plate and treated for 24 hours with control medium or doxycycline (1 μ g/ml). Cells were transiently transfected with the pGL3-Pap1 luciferase reporter plasmid and the pRL-TK plasmid as internal control of transfection. 4 hours after transfection, cells were stimulated with control medium or human IL-6 (100 ng/ml, upper panel) or human IL-22 (500 ng/ml, lower panel) for 20 hours. Data are presented as mean \pm SEM of three independent experiments performed in triplicates. Panels (C) and (D) were obtained from experiments performed by Camille Michiels in the lab of Laure Dumoutier. Significance in (C) and (D) is shown according to Mann-Whitney test analysis: * $P \leq 0.05$, ** $P \leq 0.01$, *** $P \leq 0.001$, **** $P \leq 0.0001$. (E) RT-qPCR for expression of STAT3 downstream genes in A549 cells expressing monobodies upon IL-22 stimulation (100 ng/ml, 1hr at 37°C). Gene expression was normalized against actin and is presented as fold change against that of untreated A549 cells (no monobody expression), which was arbitrarily set to 1. Data from three independent experiments performed in triplicates are presented as mean \pm SD. Significance was calculated against mRNA levels in the HA4-Y87A monobody control condition. Significance is shown according to unpaired t-test analysis: * $P \leq 0.05$, ** $P \leq 0.01$, *** $P \leq 0.001$, **** $P \leq 0.0001$.

2.1.4. The mode of action of MS3-6 differs from common targeting strategies

To elucidate the molecular mechanism of action of the developed monobodies, we focused on MS3-6, which showed the strongest inhibitory effects. An obvious way to inhibit STAT3 relies on the perturbation of its dimerization and of its interaction with upstream cytokines receptors as a result of the blockade of its SH2 domain, which is employed by several small molecule chemical probes^{73,75,209,219,220}. We thus initially investigated whether MS3-6 targets the SH2 domain. We used a fluorescent pY-peptide encompassing the pY905 docking site of gp130 (GMPKSpYLPQTVR), which bound to the recombinant core fragment of STAT3 with a K_D value of 930 nM in a fluorescence polarization binding assay (Supplementary Figure 2.3A). Addition of increasing concentrations of recombinant MS3-6 did not compete with binding of the gp130 pY-peptide to STAT3 (Figure 2.3A). This result suggests that MS3-6 does not prevent the SH2 mediated STAT3 binding to the gp130 co-receptor of the IL-6 cytokine receptor family and thus, its inhibitory mechanism relies on an alternative mode of action. An additional common strategy to target STAT3 relies on the perturbation of its binding to DNA. To assess whether MS3-6 interferes with DNA binding, a recombinant tyrosine phosphorylated STAT3 dimer was prepared by co-expression of STAT3-CF and the ABL1 tyrosine kinase domain in *E. coli*. Size exclusion chromatography and immunoblot analysis showed dimer formation and strong phosphorylation on Y705 (Supplementary Figure 2.3B; 2.3C). The purified recombinant STAT3 dimer was assessed

Chapter 2. Results

for binding to a fluorescently-labeled double-stranded oligonucleotide corresponding to the STAT3 binding sites in the SOCS3 promoter region and to a higher affinity STAT3 site (a2M)⁸⁹. In fluorescence polarization binding experiments, binding affinities of 1.21 μM and 0.21 μM to the SOCS3 and a2M probes were respectively measured, in line with previously reported values (⁸⁹; Supplementary Figure 2.3D). Addition of recombinant MS3-6, but not of the HA4-Y87A negative control monobody, decreased binding to both the SOCS3 and a2M oligos in a dose-dependent manner (Figure 2.3B). However, complete DNA binding inhibition was not achieved even at high monobody concentration (10 μM). Therefore, this result may argue for an indirect (allosteric) inhibition of DNA binding by MS3-6. Hence, taken together, these data suggest that the mode of action for the MS3-6 driven STAT3 inhibition must rely on an unconventional additional mechanism.



Supplementary Figure 2.3: see next page for caption.

Supplementary Figure 2.3: Recombinant p-Y705 STAT3 dimer and In vitro Fluorescent polarization assays.

(A) Fluorescence polarization experiments were performed to monitor the p-Gp-130 peptide binding to STAT3 SH2 domain. Increasing concentrations of recombinant STAT3-CF was added to a 250nM peptide solution at 25°C. Data from three technical replicates. (B) Size exclusion chromatography trace of a phospho-Y705 STAT3 expressed in *E. coli*. Monomeric and dimeric peaks are highlighted in light and dark blue respectively. STAT3 Y705 phosphorylation was observed by immunostaining (C). Recombinant SHIP1 was used as a negative control. (D) Fluorescence polarization experiments were performed to assess p-Y705 STAT3 dimer binding to two double stranded DNA probes (full sequences in material and methods). Binding affinities are reported as K_D values.

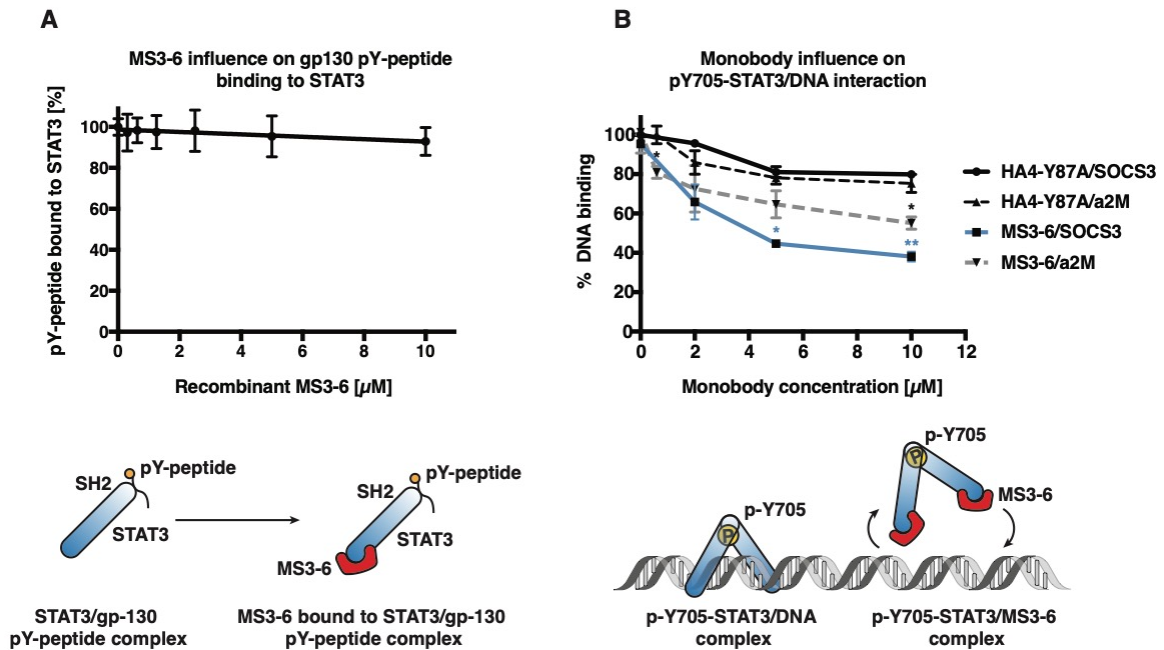


Figure 2.3: MS3-6 influences STAT3 DNA binding levels.

(A) Addition of increasing recombinant MS3-6 concentrations to a solution of STAT3/p-gp130 peptide complex did not lead to the out-competition of the peptide (full sequence in material and methods) for STAT3 SH2 binding as measured by fluorescence polarization. (B) Addition of increasing concentrations of recombinant MS3-6 to a solution of p-Y705 STAT3 dimer bound to DNA probes corresponding to downstream promoter sequences (detailed in material and methods). MS3-6 decreased STAT3 DNA binding levels as compared to HA4-Y87A monobody control. All fluorescence polarization experiments were performed at 25°C. All data are presented from three independent experiments (mean \pm SD). Significance according to an unpaired t-test analysis: * $P \leq 0.05$, ** $P \leq 0.01$.

2.1.5. Structural basis of MS3-6/STAT3-CF interaction

To shed light on the molecular mode of action of MS3-6, we solved the crystal structure of MS3-6 in complex with STAT3-CF at a resolution of 2.9 Å (Figure 2.4A; Table 2.2; PDB 6TLC). The asymmetric unit contains an anti-parallel (unphosphorylated) STAT3 dimer, as previously observed in STAT5a and STAT1 structures (PDB: 1Y1U and 1YVL respectively). Two monobodies are bound to one STAT3 dimer, in line with the 1:1 binding stoichiometry observed by ITC (see Figure 2.1C). MS3-6 binds to the helices $\alpha 1$, $\alpha 2$, $\alpha 3$ and $\alpha 4$ of the STAT3 coiled-coil domain. Interactions

of the monobody with STAT3 is mediated by several residues located in its diversified FG loop (a.a. 75-85), together with a diversified histidine (H33) located in beta strand C of the monobody. The overall buried surface area of the STAT3-MS3-6 interface recognized by the monobody is 834 Å² (Figure 2.4B).

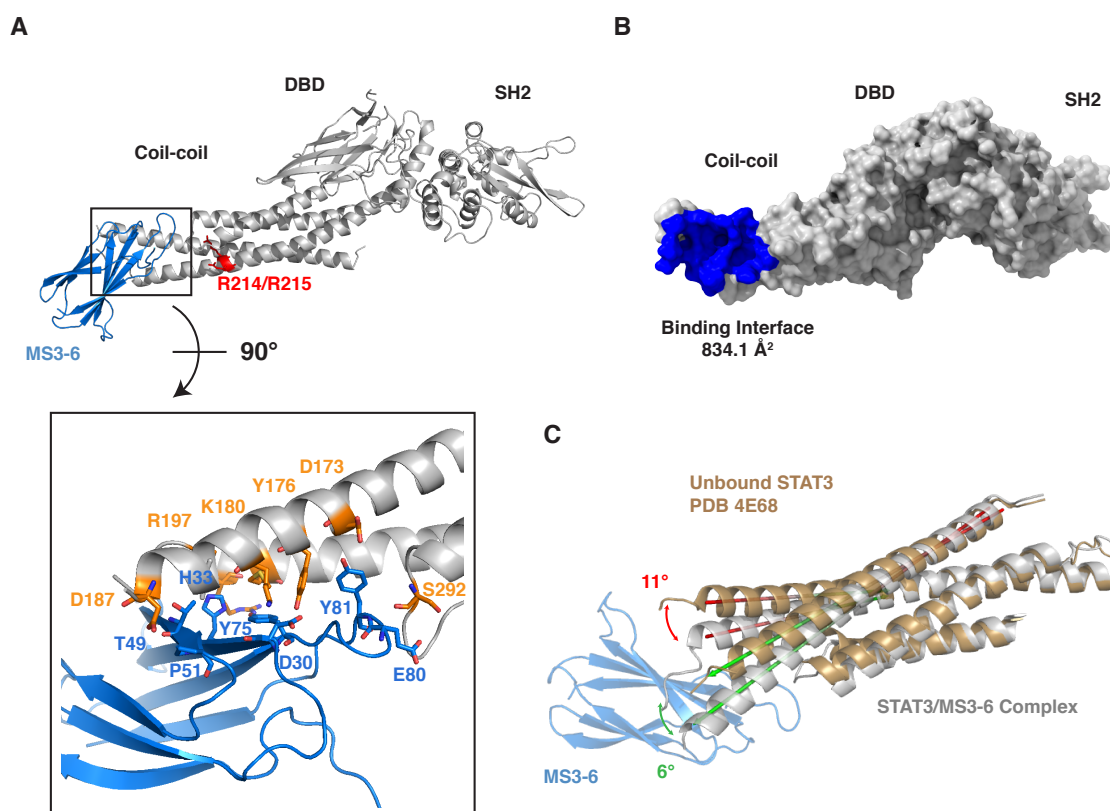
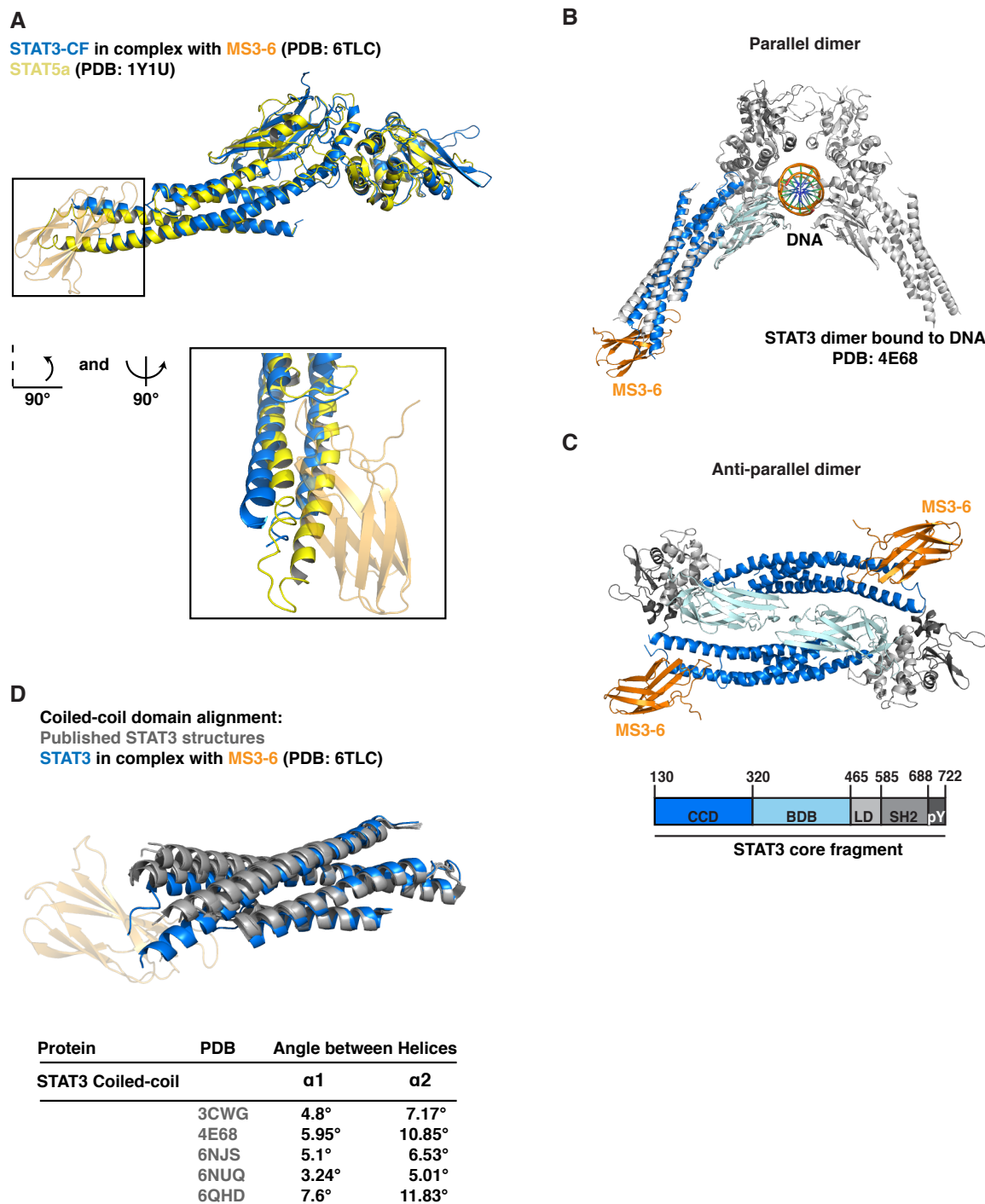


Figure 2.4: Co-crystal structure of MS3-6 bound to the STAT3 coiled-coil domain.

(A) Structure of STAT3 is color coded in light grey and MS3-6 in blue. The upper panel shows an overall view of MS3-6 binding to the coiled-coil domain of STAT3, with key residues of the nuclear localization sequence (NLS) in close proximity to the monobody binding site highlighted in red. The lower panel shows a magnification of the binding interface with epitope residues (threshold set at 4 Å) depicted as sticks. (B) Surface representation of STAT3 (light gray), with the area covered by the monobody colored in blue (according to the Protein Interfaces, Surfaces and Assemblies PISA service). (C) Structural alignment of the coiled-coil domains of STAT3 in complex with MS3-6 together with an unbound STAT3 structure previously published (PDB: 4E68). Monobody binding leads to a conformational distortion of the helices $\alpha 1$ and $\alpha 2$. The angles formed between helices are indicated in green and red respectively (Pymol software).

The structure also explains the exquisite selectivity of MS3-6 for STAT3 over STAT5. In STAT5, helix $\alpha 2$ is more than two turns longer and superimposition of the structures indicates clashing with the monobody (Supplementary Figure 2.4A). Modeling of MS3-6 binding to an active STAT3-CF parallel dimer bound to DNA shows that monobody binding does not sterically interfere with DNA binding or pY705-dependent dimerization of the SH2 domains (Supplementary Figure 2.4B) in line

with the epitope mapping results described above (Figure 2.3). Similarly, binding of MS3-6 is compatible with the formation of an anti-parallel unphosphorylated STAT3 dimer (Supplementary Figure 2.4C). Structural alignment of the MS3-6-STAT3 complex and several previously published structures of STAT3 and other STAT family members (STAT3 PBD: 3CWG, 4E68, 6NJS, 6NUQ, 6QHD and STAT5a PDB: 1Y1U) showed that binding of MS3-6 results in the torsion of the 4-helix bundle (helices α 1-4) of the STAT3 coiled-coil domain and bending of the α 1 and α 2 helices by 4-12 degrees (Figure 2.4C; Supplementary Figure 2.4D). Hence, MS3-6 binding leads to a defined conformational change of the coiled-coil domain orientation, which may allosterically perturb DNA binding. In addition, the nuclear localization signal (NLS) of STAT3 was proposed to include residues R214/215²²¹, which are located in helix α 2 of the coiled-coil domain of STAT3. These residues were previously shown to be responsible for the efficient nuclear import of active phosphorylated STAT3 parallel dimers through recognition by importins²²¹. While these key residues of the NLS are not directly contacted by the MS3-6 monobody, they lie in close proximity to the monobody binding site (Figure 2.4A). Therefore, MS3-6 binding may perturb efficient nuclear import of pY705 phosphorylated STAT3 dimers and hence may indirectly inhibit STAT3 transcriptional activity in the nucleus. As a whole, these structural data indicate that MS3-6 allosterically affects the conformation of STAT3 upon binding by altering the coiled-coil domain orientation which may perturb STAT3 nuclear import.



Supplementary Figure 2.4: Structural alignment of the STAT3/MS3-6 complex with previously published STATs structures.

The alignment of STAT3/MS3-6 complex (PDB: 6TLC) with a STAT5a structure (PDB: 1Y1U) is shown in (A). The magnification of the monobody binding interface highlights the torsion of the STAT3 coiled-coil domain (blue), as compared to the STAT5a coiled-coil domain (yellow). The longer helix 2 of STAT5a clashes with monobody binding (shown in transparency). (B) Structural alignment of the STAT3/MS3-6 complex with a STAT3 dimer bound to DNA (PDB: 4E68) highlight the compatibility of the monobody binding with an efficient p-Y705 STAT3 parallel dimer formation. Similarly, the formation of an anti-parallel STAT3 dimer, as observed in the crystal symmetry unit, is compatible with monobody binding (C). Individual domains are color coded. (D) MS3-6 binding to STAT3 (blue) leads to the torsion of the helices 1 and 2 of the coiled-coil domain as evidenced by the structural alignment with previously published STAT3 structures (in grey). Orientation vectors (Pymol) for each helices were used to measure the angle formed between the respective structures and are reported as a table.

Table 2.2: STAT3/MS3-6 complex (PDB: 6TLC) crystal structure data collection and refinement statistics.

PDB ID	6TLC: MS3-6/STAT3-CF
Data collection	
Space group	P 41 21 2
Cell constants	
a, b, c (Å)	111.31, 111.31, 483.47
α, β, γ (°)	90.00, 90.00, 90.00
Resolution (Å)	49.78 - 2.90 (2.90)
<i>R</i> _{meas}	34.4 (447.9)
CC1/2	99.8 (25.2)
< I/ σ (I) >	8.5 (0.61)
Completeness (%)	99.9 (99.8)
Redundancy	14.27 (14.55)
Refinement	
Resolution (Å)	2.9
No. of reflections	68566
Rwork / Rfree	0.234 / 0.285
No. of atoms	
Protein	10063
Ligand/ion	12
Water	3
<i>B</i> -factor	
Protein	87.9
Ligand/ion	81.5
Water	43.9
Rmsd	
Bond lengths (Å)	0.018
Bond angles (°)	2.00

2.1.6. MS3-6 reduces STAT3 nuclear translocation

Due the close proximity between the monobody binding site and the NLS, we hypothesized that the specific blockade of the coiled-coil domain by MS3-6 could impair STAT3 nuclear translocation. To test this hypothesis, we assessed the nuclear translocation of STAT3 by subcellular fractionation and immunofluorescence experiments. Levels of nuclear and cytoplasmic STAT3 were determined by immunoblot in A549 cells stimulated with IL-6 or IL-22 in presence of MS3-6, MS3-N3 or the negative control HA4-Y87A monobody. MS3-6 led to overall reduced

STAT3 levels in the nuclear fractions upon stimulation with both IL-6 and IL-22 (Figure 2.5A). Similarly, MS3-6 decreased the ratio of nuclear/cytosolic STAT3 and pY705-STAT3 (Figure 2.5B; Supplementary Figure 2.5A). In contrast, MS3-N3 or HA4-Y87A did not interfere with STAT3 nuclear translocation. As a second independent line of experimentation, we monitored the influence of MS3-6 on STAT3 nuclear localization using confocal immunofluorescence microscopy with HEK293 cells that were transiently transfected with GFP-monobody fusions and stimulated with IL-6. We observed decreased STAT3 levels in the nucleus of cells that expressed MS3-6, and MS3-N3 to a lower extent, but not in cells expressing HA4-Y87A (Figure 2.5C; Supplementary Figure 2.5B). Quantitative image analysis corroborated these qualitative results (Figure 2.5D). Hence, these data provide a rationale for the inhibition of STAT3 transcriptional activity by MS3-6 through reduced STAT3 nuclear translocation. Together with the reduction in DNA binding affinity by MS3-6, these two distinct mechanisms may cumulatively/synergistically cause the observed strong inhibition of STAT3 transcriptional activity.

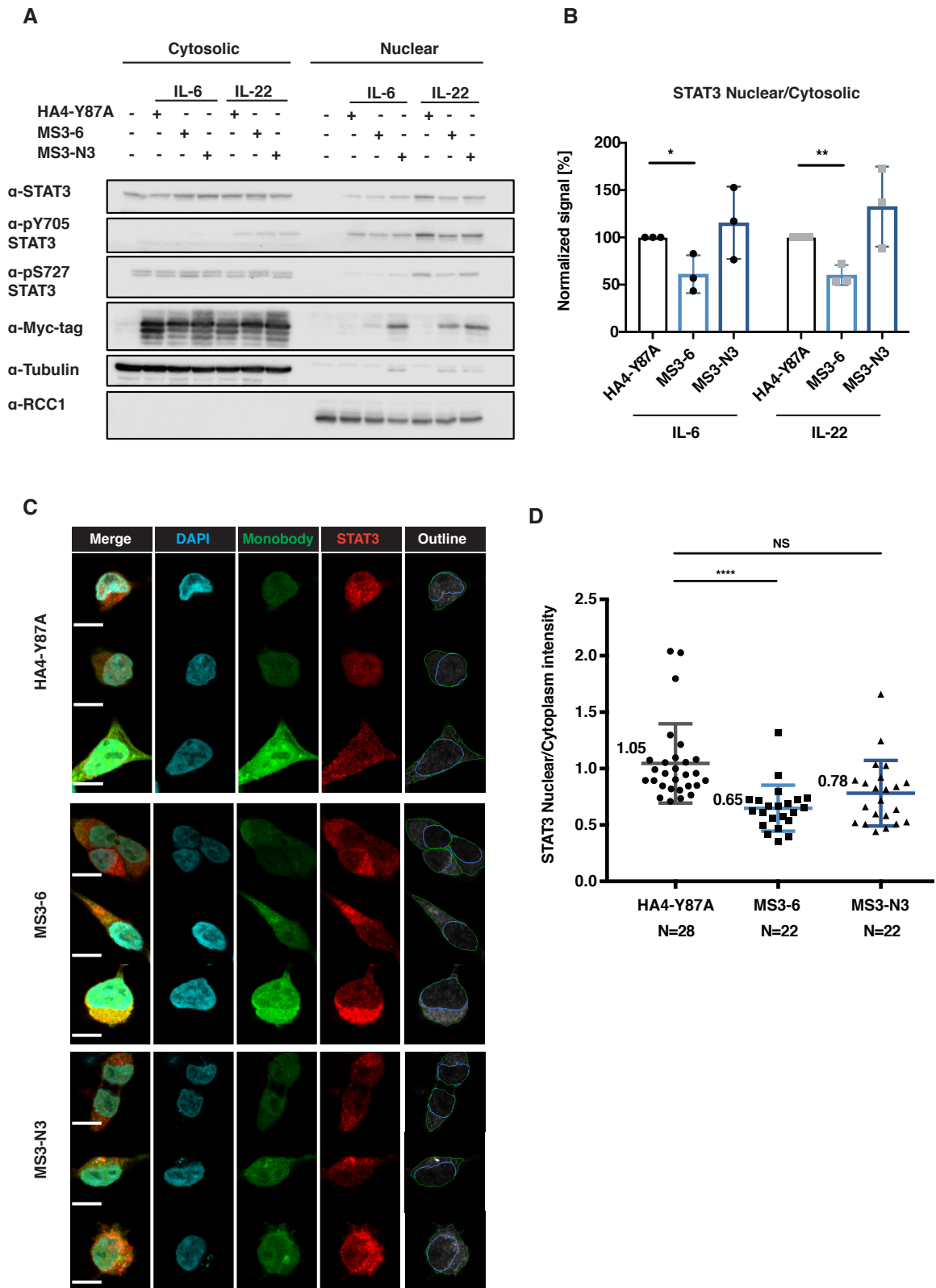
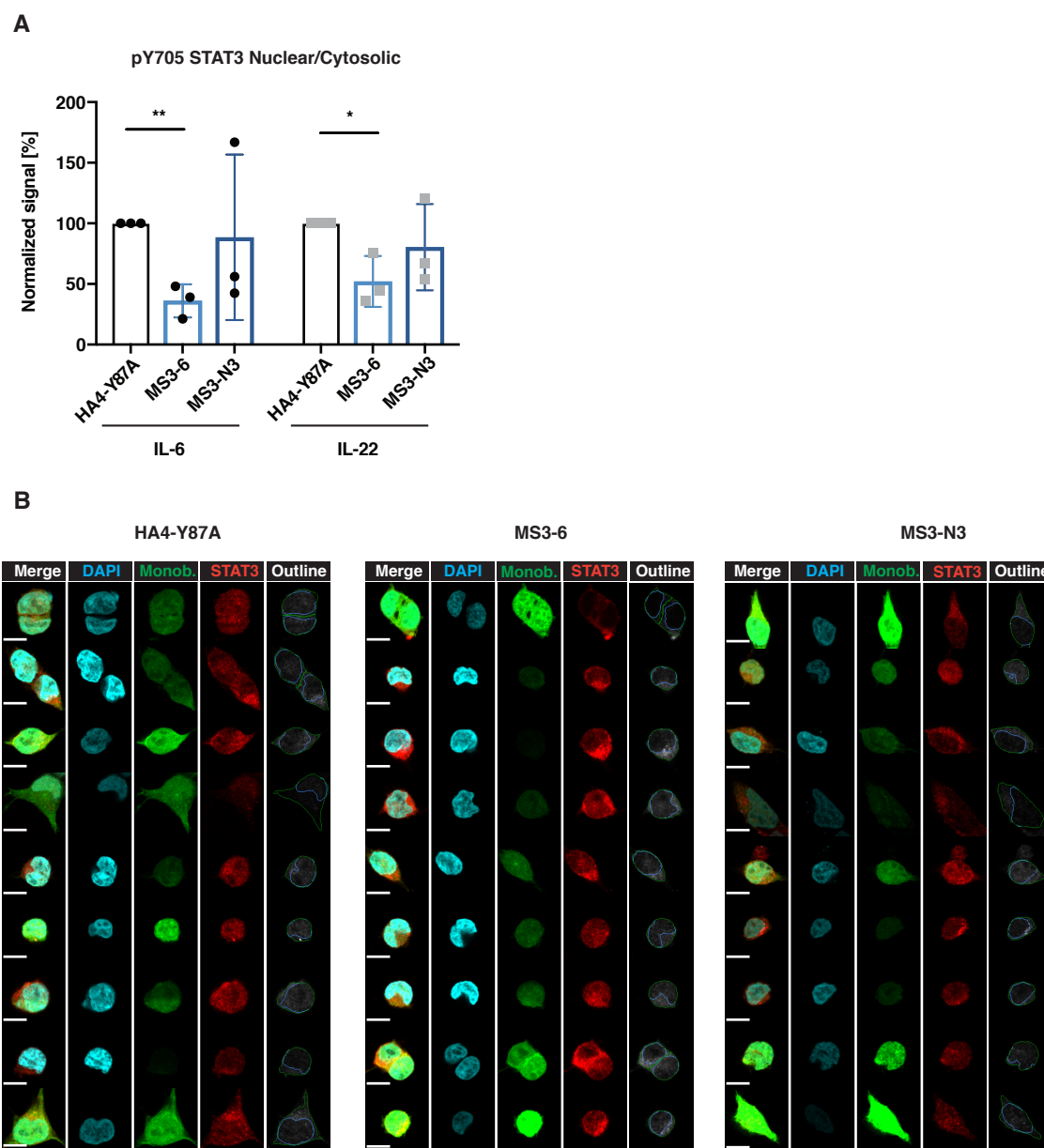


Figure 2.5: MS3-6 reduces STAT3 nuclear localization.

(A) Representative immunoblot analysis of cellular fractionation experiments. A549 expressing monobodies upon 48 hours of 1 μ g/ml doxycycline treatment were stimulated with either IL-6 or IL-22 for 15 minutes. Nuclear (RCC1) and cytosolic (Tubulin) fractions were recovered and probed for total, p-Y705 and p-S727 STAT3. Quantification of three independent experiments normalized to the HA4-Y87A monobody control are shown in (B) and are plotted as mean \pm SD. (C) Confocal microscopy images of HEK293 cells expressing a monobody-GFP fusion and treated with IL-6 to

Chapter 2. Results

assess nuclear translocation. Scale bar represents 10 μ m. The last panel shows the outlines used to determine nuclear and cellular compartments are shown in blue and green lines respectively (CellProfiler). Quantification of STAT3 nuclear/cytoplasmic levels from two independent experiments is shown in (D). Significance according to an unpaired *t*-test analysis: * $P \leq 0.05$, ** $P \leq 0.01$, *** $P \leq 0.001$, **** $P \leq 0.0001$.



Supplementary Figure 2.5: MS3-6 decreases the nuclear/cytoplasmic STAT3 ratio upon cytokines stimulation.

(A) Quantification of three individual immunoblot analysis of cellular fractionation experiments. A549 cells were treated with doxycycline to induce monobody expression for 48h, followed by IL-6 or IL-22 stimulation. (B) Additional representative images from confocal microscopy experiments performed in HEK293 cells transiently transfected with a doxycycline inducible eGFP-monobody fusion and stimulated with IL-6 for 20 minutes at 37°C. The outline panel illustrates the threshold defined (CellProfiler) to determine the nucleus (blue line) and cytosolic compartments (green line).

2.1.7. MS3-6 reduces STAT3 Y705 phosphorylation in a IL-22R dependent manner

Additionally, we investigated the effects of our monobodies on endogenous STAT3 signaling in cancer cells. Using doxycycline induced monobody expression in A549 lung cancer cells, the phosphorylation status on STAT3 Tyrosine 705 and Serine 727, as well as on STAT1 and STAT5 were investigated. The monobodies did not impact STAT1 phosphorylation, nor STAT3 serine 727 phosphorylation (Fig. 2.6A). Interestingly however, MS3-6 led to an increased STAT5 phosphorylation upon IL-22 stimulation, which could be explained by a rapid rewiring of the signaling pathway, with STAT5 compensating for STAT3 inhibition. Surprisingly, while MS3-6 had no significant effect on pY705 STAT3 upon IL-6 stimulation, a strong reduction of Y705 phosphorylation was observed following IL-22 stimulation (Figure 2.6A; 2.6B). Similar results were independently obtained using flow cytometry analysis (Supplementary figure 2.6A-D). We hypothesized that this observation might be due to different molecular mechanisms of STAT3 activation by the two distinct cytokine receptors. IL-22 stimulation was indeed reported to utilize a non-canonical constitutive association of STAT3 with the IL-22 receptor in the absence of cytokines²²². This alternative STAT3 activation is mediated by a constitutive interaction between the coiled-coil domain of STAT3 and the 84 C-terminal amino acids of the IL-22R, which lack tyrosine residues. Therefore, IL-22-dependent STAT3 activation is triggered by a phospho-tyrosine independent mechanism in addition to the conventional (phospho-tyrosine dependent) recruitment of STAT3 to the IL-22R following cytokine stimulation. To test if the MS3-6 binding to the coiled-coil domain of STAT3 as described above is able to perturb IL-22 signaling, we first used Ba/F3 cell lines expressing IL-22R mutants, including a tyrosine-less mutant (where all tyrosines located in the intracellular domain of IL-22R were mutated to phenylalanine), and a C-terminal truncation (IL-22R receptor lacking the last 84 amino acids; Δ C-ter). These IL-22R mutants allowed us to dissect the impact of MS3-6 on the conventional (Δ C-ter mutant) and alternative (tyrosine-less mutant) STAT3 activation. The Y705 phosphorylation status of STAT3 was assessed in cells expressing the different IL-22R mutants by flow cytometry following IL-22 stimulation upon electroporation of the Myc tagged monobodies. MS3-6 strongly decreased STAT3 phosphorylation after IL-22 stimulation in cells expressing the wild-type and tyrosine-less receptor, but not the Δ C-ter receptor, highlighting the impact of the monobody on non-canonical IL-22 signaling (Figure 2.6C; 2.6D). To further corroborate this hypothesis, we tested if MS3-6 prevents the pre-association of STAT3 to the C-terminal part of IL-22R in GST pull-down experiments. After pull-down of different recombinant GST-IL22R intracellular domain mutants, STAT3 was robustly co-purified with GST-IL-22R in cells that expressed the control monobody, as long as the IL-22R contains its C-terminal part (Figure 2.6E). In contrast, expression of MS3-6 resulted in the loss of STAT3 co-

Chapter 2. Results

purification. These results indicate that MS3-6 prevents the binding of STAT3 to the C-terminus of IL-22R. Hence, these data show that MS3-6 is able to specifically block the interaction between the coiled-coil domain of STAT3 and the unstimulated IL-22R, thereby selectively perturbing the alternative, non-canonical IL-22 mediated STAT3 activation.

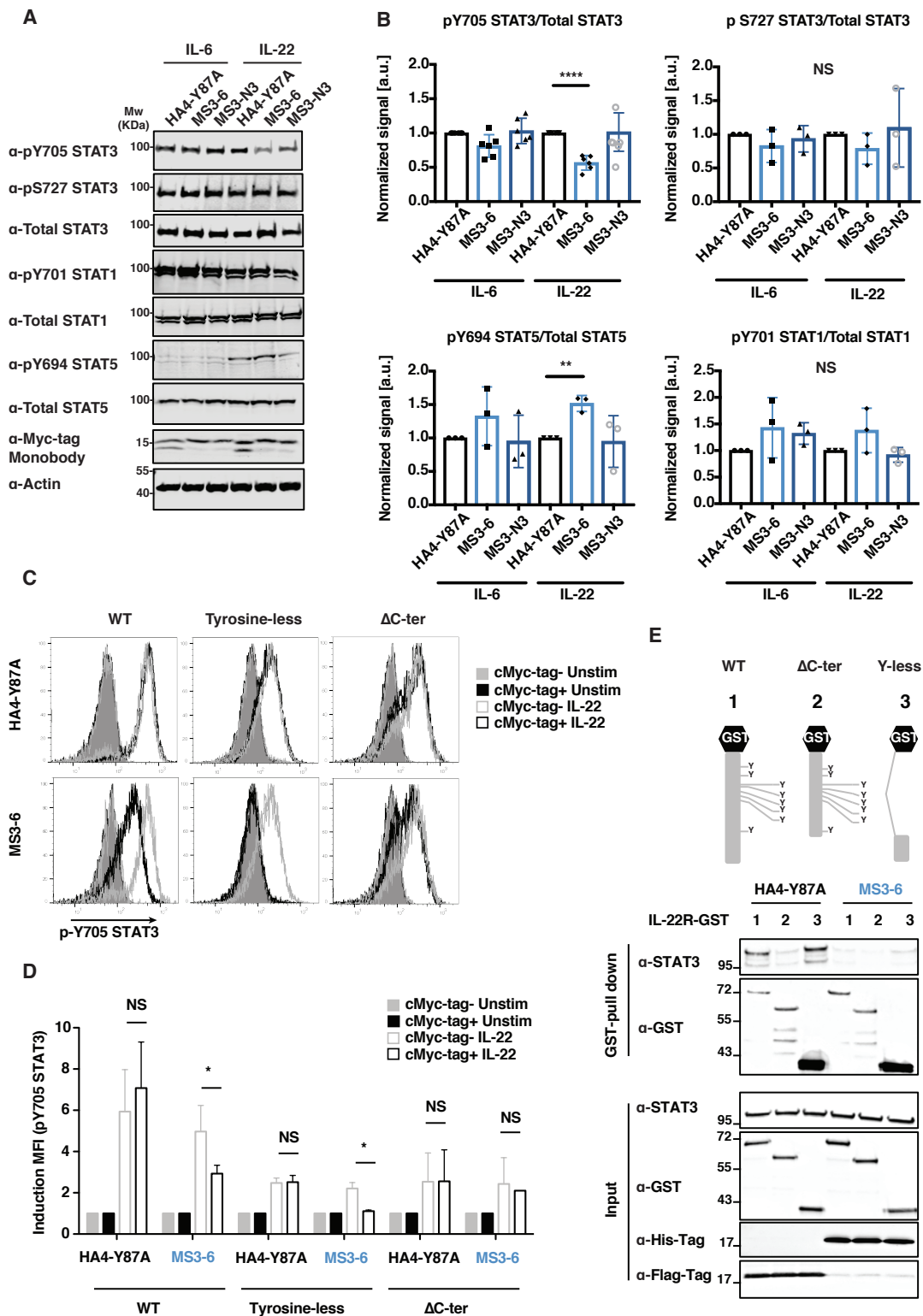
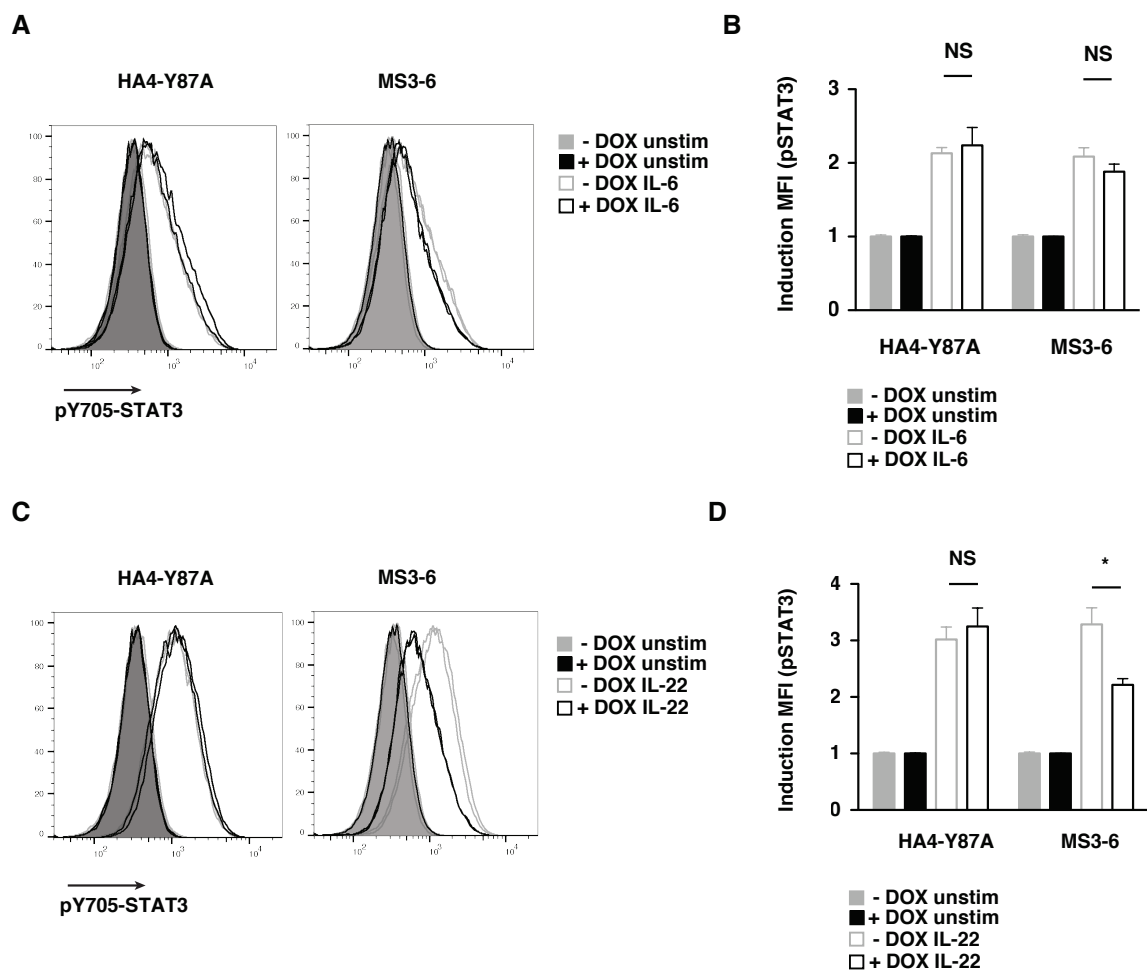


Figure 2.6: see next page for caption.

Figure 2.6: MS3-6 reduces STAT3 Y705 phosphorylation levels upon IL-22 stimulation.

(A) Representative immunoblot analysis of STATs phosphorylation levels following IL-6 and IL-22 stimulation for 15 minutes. (B) Quantification of the normalized phosphorylated STATs normalized to total STAT levels from at least three independent experiments. (C) Flow cytometry analysis on Ba/F3 cells expressing IL-22R. Four hours after electroporation of the monobody (15 μ g), cells were stimulated with IL-22 (500 ng/ml) and staining was performed. A live cells gating strategy was applied and phospho-STAT3 staining was analyzed in cMyc-tag⁺ and cMyc-tag⁻ cells. (D) Quantification of pY705-STAT3 staining from (C). Data are presented as mean \pm SEM of two independent experiments performed in duplicates. (E) Upper panel, schematic representation of GST fusion proteins with intracytoplasmic domain of IL-22R. Lower panel, COS-7 cells were seeded in 6-well plate (4×10^5 cells). The next day, cells were transfected with a vector coding for one of the GST-fusion protein or STAT3. Two days later, cells were lysed. STAT3 was mixed with recombinant monobody (10 μ M) for 8 hours at 4°C before adding IL-22R-GST overnight. Proteins eluted on GST SpinTrap columns as well as input samples were analyzed by western-blot with an anti-STAT3 antibody. Membrane was then re-probed with anti-GST and anti-tag antibodies. Significance according to a Mann Whitney test analysis: * $P \leq 0.05$, ** $P \leq 0.01$, *** $P \leq 0.001$, **** $P \leq 0.0001$. Panels (C), (D) and (E) were obtained from experiments performed by Camille Michiels in the lab of Laure Dumoutier.



Supplementary Figure 2.6: MS3-6 reduces STAT3 p-Y705 levels upon IL-22 stimulation.

(A) and (C) Flow cytometry on A549 with inducible monobody (HA4-Y87A or MS3-6) expression. Cells were treated with control or doxycycline (1 μ g/ml) containing medium to induce monobody expression. After 48 hours, cells were stimulated with IL-6 (100 U/ml) (A) or IL-22 (500 ng/ml) (C) and intracellular FACS staining was performed. The gating strategy was defined on living cells and phospho-Y705 STAT3 levels were assessed (B) and (D). Quantification of phospho-Y705 STAT3 staining from (A) and (C) plotted as mean fluorescence intensities. Data are presented as mean \pm SEM of two independent experiments performed in duplicates. Significance according to unpaired t-test analysis: * $P \leq 0.05$. Graphs obtained from experiments performed by Camille Michiels in the lab of Laure Dumoutier.

2.2. Monobody effects on solid and hematologic cellular cancer cell lines

This chapter contains additional results obtained during my thesis which will serve as ground work for subsequent publications.

2.2.1. Perturbation of STAT3 signaling using monobodies does not lead to several cancer cell lines apoptosis

In addition to investigating the monobody molecular mode-of-action, we were further interested in knowing whether inhibition of STAT3 signaling led to decreased viability in cancer cell lines. In order to identify cancer cell lines that rely on STAT3 signaling to survive, we initially screened for Ruxolitinib (a potent JAK1/2 inhibitor) sensitivity a panel of cell lines described as STAT3-dependent in the literature. Adherent cell lines isolated from human solid tumors (A549, MDA-MB-231, LNCap and DU145) as well as human lymphoblastic cell lines (Karpas, SR786 and SUP-HLU1) were used. In order to follow cell viability over time, cell seeding at different concentrations was performed in a 96 well plate to measure cell growth using real time glo (Figure 2.7A). Initial seeding of 1500 cells ensured that cell confluency remained optimal to assess viability overtime. Next, upon seeding of 1500 cells, titration of Ruxolitinib was performed and cell viability was assessed. Results showed that all cell lines tested had an IC_{50} of $\geq 2\mu M$, suggesting a low sensitivity to JAK inhibition (Figure 2.7B) and are therefore not likely to be strongly functionally dependent on STAT3 signaling. To further investigate whether cells relied on STAT3 for survival, we transfected cells with an siRNA against STAT3, and followed cell proliferation overtime. Despite the effective knockout of the STAT3 protein in A549, MDA-MB-231 and LNCaP cells, no clear effect on cell viability could be seen (Figure 2.7C). We thus next took advantage of NPM-ALK expressing cells from mouse thymoma. Similarly, I initially assessed Ruxolitinib sensitivity in three mouse thymoma cell lines overexpressing the NPM-ALK oncogene: NPM-ALK 144, NPM-ALK 264 and NPM-ALK 361. IC_{50} values were again measured at high μM concentrations ($\sim 2-5\mu M$) in NPM-ALK 264 and 361 cells, while no IC_{50} could be calculated for NPM-ALK 144 cells, as even at the highest concentration of Ruxolitinib, no cell killing was observed (Figure 2.7D). Nevertheless, NPM-ALK mediated tumorigenesis is reported to be dependent on STAT3 activity. Hence, by inhibiting or degrading STAT3 in this context, cell viability was expected to decrease.

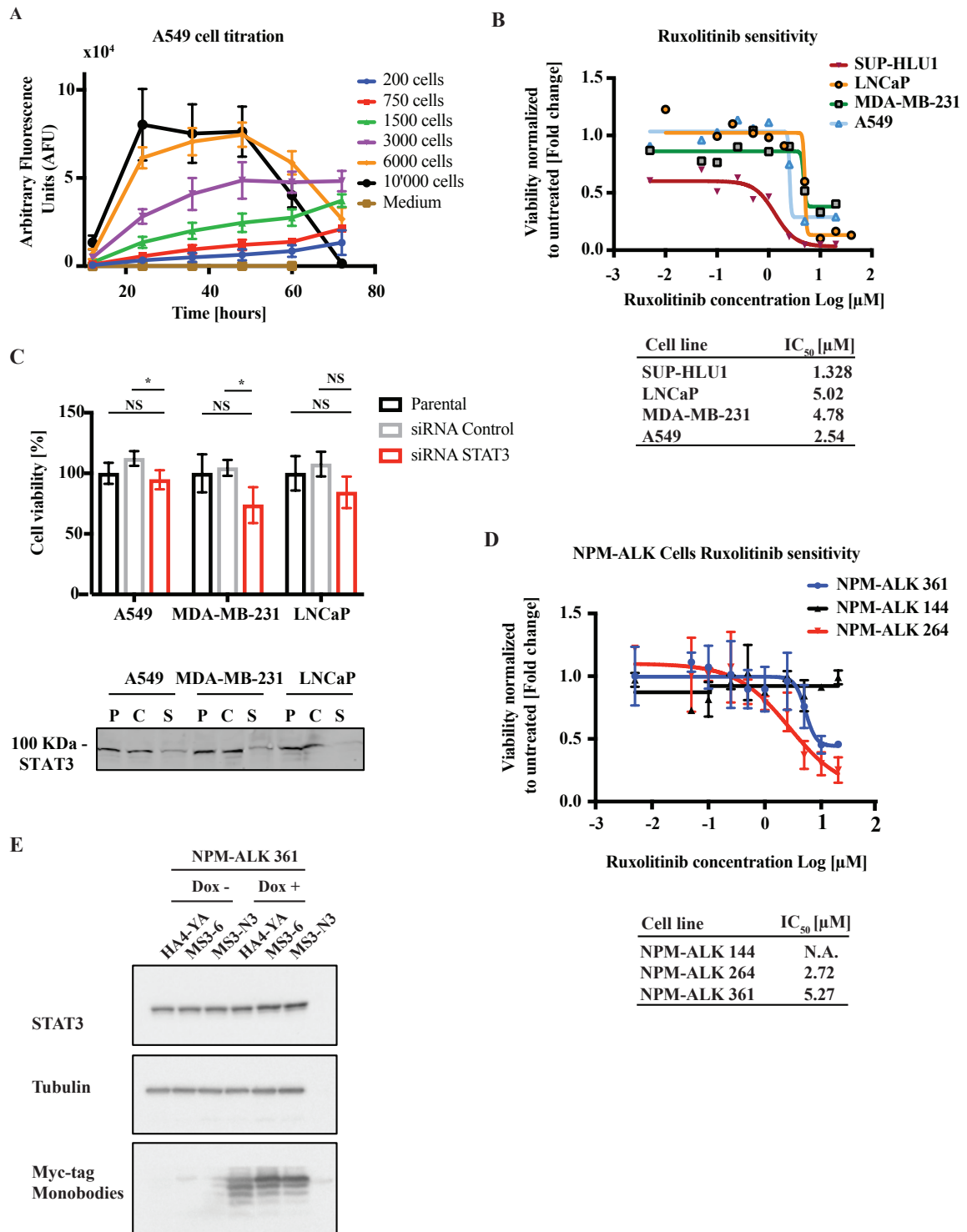


Figure 2.7: Cell lines screening for STAT3 sensitivity.

(A) Representative initial cell titration using cell titer glow to monitor proliferation and viability overtime. Optimal cell density was identified as the one which did not reach over-confluency after 72 hours. 1500 A549 cells were seeded in 96 well plates and monitored overtime. Similar titration curves were performed for all cell lines tested. (B) Ruxolitinib titration curves of adherent cell lines. Means from three technical repeats are shown without SD for clarity. Measured IC₅₀ are indicated on the lower panel. Additional cell lines whose IC₅₀ were measured at >5.1 μM are not shown. (C) Cell lines viability as measured by real time glo 96 hours post transfection of cells with siRNA against STAT3 or control siRNA. Viability is presented normalized to the un-transfected parental cells signal. Data from three

Chapter 2. Results

technical repeats and significance is indicated according to *t*-test: * $P < 0.05$. Successful STAT3 knockdown was monitored by immunoblotting (C – lower panel): P, parental untransfected cells; C, siRNA control; S, siRNA STAT3. (D) NPM-ALK suspension cells sensitivity to Ruxolitinib. Measured IC_{50} are indicated in the lower panel. Means \pm SD are shown from three technical repeats. (E) NPM-ALK 361 cells stable transduction of doxycycline inducible monobody constructs. Successful monobody expression was monitored by immunoblotting upon doxycycline treatment for 48 hours.

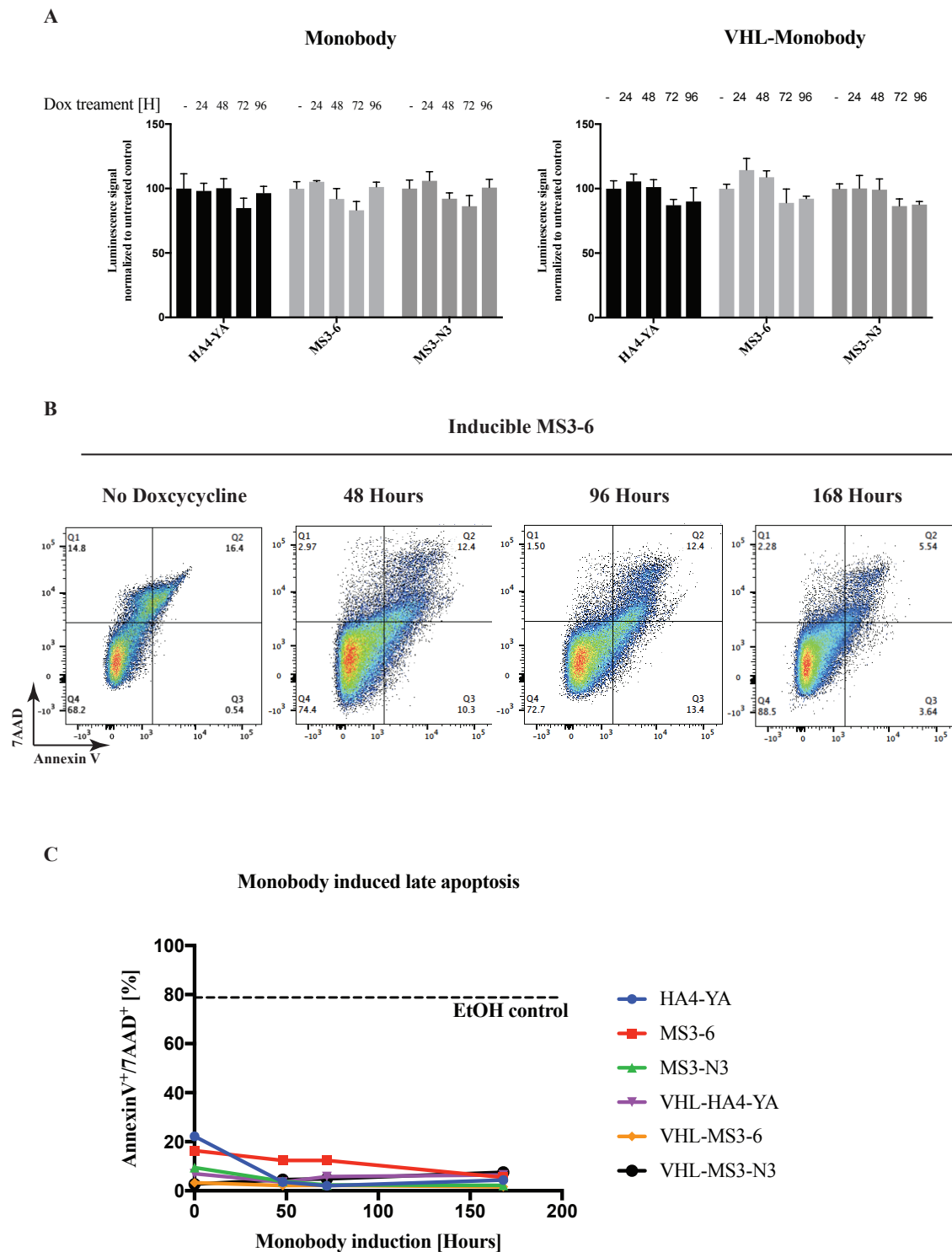


Figure 2.8: see next page for caption.

Figure 2.8: NPM-ALK cell proliferation and viability are not impaired upon monoclonal antibody induction.

(A) Cellular proliferation upon 96 hours of growth in presence or absence of Doxycycline measured by Cell titer glo. (B) Representative FACS plots of NPM-ALK cells viability assessment upon monoclonal antibody expression. (C) Percentage of late apoptosis AnnexinV/7AAD double positive cells induced by the monoclonal antibody or VHL-monoclonal antibody fusion expression.

In order to test our monoclonal antibodies impact on cancer cell viability, I established stable inducible cell lines expressing either the monoclonal antibodies alone or as protein fusion with the VHL ubiquitin ligase to take advantage of the PROTAC inspired targeted degradation of STAT3 described above (see chapter 2.1.2). The successful expression of the monoclonal antibodies and monoclonal antibody-VHL fusions was assessed by western blots (Figure 2.7E and Figure 2.1D respectively). Importantly, a strong dose-dependent degradation of STAT3 was observed using MS3-6 and MS3-N3 as bait (Figure 2.1D; 2.1E). However, no effect on cell viability could be observed using Cell titer glo (Figure 2.8A) and AnnexinV/7AAD staining (representative FACS plots and AnnexinV⁺/7AAD⁺ percentages in Figure 2.8B and 2.8C respectively).

We hypothesized that this result might be explained by the leakiness of the inducible plasmid resulting in the rapid development of monoclonal antibody resistant cells during the 2-3 week of harsh selection for stable inducible cell lines. To test this hypothesis, I monitored cell viability using a constitutive monoclonal antibody expression in an IRES-GFP vector which allowed me to track the percentage of GFP expressing cells overtime. However, no effect of the monoclonal antibodies expression could similarly be observed as measured by GFP⁺ cell percentage or AnnexinV/7AAD staining overtime (Figure 2.9A-C).

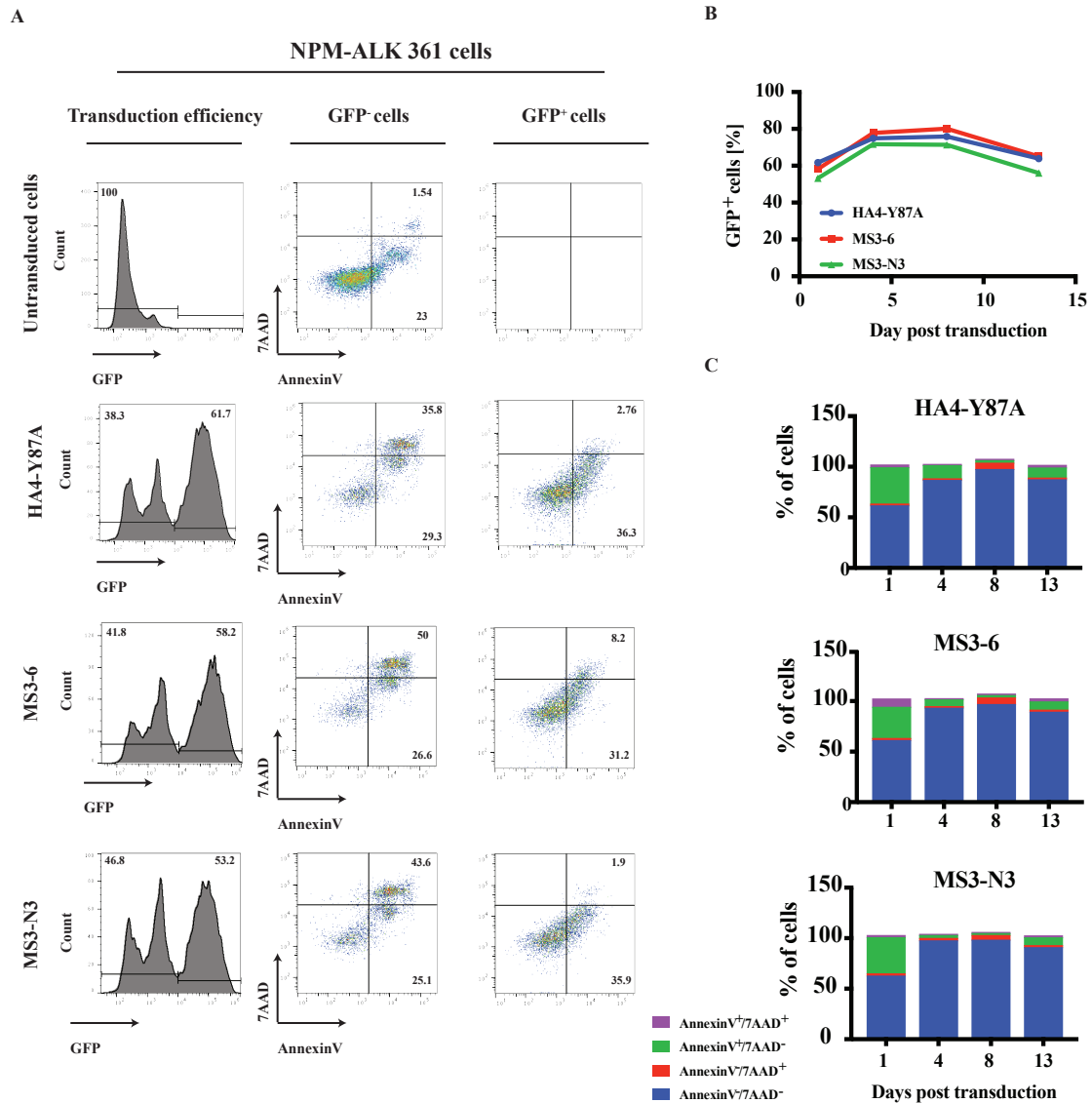


Figure 2.9: Constitutive monobody expression does not lead to NPM-ALK cells apoptosis.

Transduction efficiencies were analyzed by monitoring GFP expression overtime. (A) Representative FACS analysis of GFP expression and AnnexinV/7AAD stainings of the GFP⁺ and GFP⁻ cells. (B) Percentage of GFP⁺ (monobody expressing) cells overtime. (C) Percentage of cells according to their AnnexinV/7AAD profile overtime.

2.2.2. Monobody effects on STAT3 mutants identified in cancer patients

Lastly, we wanted to investigate whether our monobodies reduce the proliferative advantage of oncogenic mutant STAT3 Y640F. To answer this question, we took advantage of hematopoietic progenitor cells overexpressing a STAT3 Y640F mutant, which led to a significant proliferative advantage and colony formation potential as compared to cells expressing STAT3 WT (data not

shown). To test our monobodies in this context, I established stable HPC-7 STAT3-Y640F cell lines expressing a constitutive monobody (HA4-Y87A control, MS3-6 or MS3-N3 together with an IRES GFP). Successful transduction of cells was confirmed by GFP expression which additionally allowed cells to be sorted by FACS. Upon recovery, the expression of monobody was confirmed using western blot analysis, and cell growth was assessed using cell titer glow 72 hours post seeding of 1000 cells. Figure 2.10A shows the relative ATP dependent-luciferase signal following cell growth after 72 hours in the presence of the monobodies. MS3-6 led to a consistent and significant reduction in cell proliferation in presence of various concentrations of stem cell factor (SCF). To further investigate the monobody effect on cellular proliferation, cells were seeded in a 6 well plate and counted to follow cellular proliferation over time. However and surprisingly, no significant effect of the monobodies could be observed in this context (Figure 2.10B). Hence, in view of these contradictory results, further experiments would be required to conclude whether monobodies are decreasing the proliferative advantage provided by the STAT3 oncogenic mutant Y640F.

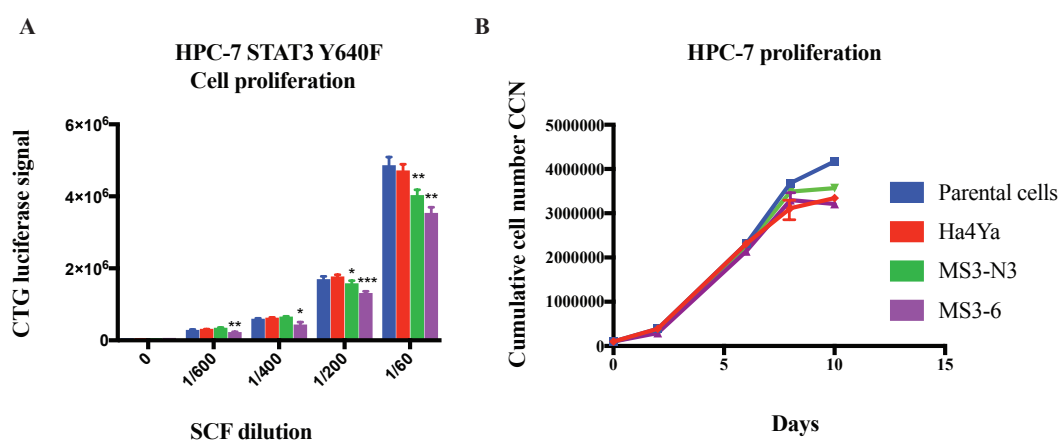


Figure 2.10: Effect of monobodies on the STAT3-Y640F oncogenic mutant driven HPC-7 cells proliferation. (A) Proliferation assessed by Cell titer glow at different stem cell factor (SCF) dilutions. (B) Proliferation assessed by cell counting using FACS in presence of constitutive monobody expression in HPC-7 cells with SCF at a 1/60 dilution.

3. DISCUSSION

3.1. Targeting transcription factors with monobodies: from theory to practice

Transcription factors are considered as essential players in the development of pathological conditions such as cancer. Nonetheless, intrinsic challenges in targeting transcription factors, such as their lack of deep pockets able to fit an antagonistic small molecule inhibitor, or the large number of proteins sharing high sequence and structural homology among transcription factor families, make them difficult proteins to be specifically inhibited. While monobodies have been developed against oncogenic kinases and challenging proteins like RAS GTPases, no monobodies were yet developed to bind and prevent the transcriptional activity of transcription factors.

My work illustrates for the first time that inhibition of specific transcription factors implicated in the development of malignancies and chronic inflammatory diseases can be achieved using monobodies.

The inhibition of key oncogenic transcription factors such as c-MYC or specific STAT family members is considered as highly desirable. Up to date, a lot of efforts towards the therapeutic antagonism of STAT3 in particular was raised among the scientific community. Unfortunately, the targeting of STAT3 remains currently challenging as illustrated by the lack of FDA approved drugs. Nonetheless, with our approach, we have developed the first monobodies binding and modulating the functions of a specific STAT transcription factor family member. A current limitation in targeted therapies remains the off-target toxicity of the low selectivity probes developed. In contrast, our monobodies were found to be highly specific against STAT3 in two physiological intracellular contexts. The high selectivity and affinity of the monobodies developed here serve as proof of concept that the targeting of currently considered “undruggable proteins” can be addressed using state of the art engineered antibody-mimics. Thus, this work opens the door to the use of

monobodies as intracellular inhibitors of transcription factors implicated in pathological tumor growth.

3.2. Impact of individual STAT3 domain blockade using monobodies

Despite the overall JAK/STAT signaling pathway being well described in the literature, little is known in regards to the function of defined STAT domains. Here, we developed monobodies binding to two largely unexplored domains of STAT3. The targeting of the coiled-coil domain led to a strong inhibition of the transcriptional activity of STAT3, while the specific blockade of the NTD mildly impaired its overall transcriptional activity. Below, I detail the molecular mode of action behind the MS3-6 driven STAT3 inhibition and describe potential uses of MS3-N3 as a specific STAT3 NTD binding protein to further dissect the implication of this domain in cellular processes.

3.2.1. MS3-6 mediated STAT3 inhibition relies on cumulative synergistical mechanisms

While most efforts have been currently focused on the inhibition of STAT3 dimerization mediated by the reciprocal interaction of its SH2 domains, the targeting of additional domains and alternative strategies remain to be further investigated in order to preclude pathological STAT3 signaling. In this work, we developed a monobody binding to the previously untargeted coiled-coil of STAT3, which is implicated in essential protein functions. Our data indicate that MS3-6 intervenes at various levels by (I) modulating the STAT3 phosphorylation status specifically upon IL-22 stimulation, (II) reducing the nuclear translocation and (III) interfering with DNA binding as demonstrated *in vitro* by fluorescence polarization assays. Hence, our results suggest that the inhibitory mode of action of MS3-6 relies on the accumulation of distinct mechanisms acting in synergy towards the overall reduction of STAT3 transcriptional activity (Figure 3.1).

The binding of MS3-6 to the coiled-coil domain of STAT3 was investigated by protein crystallography. The crystal structure of the complex led to the understanding that the MS3-6 binding site is located in close proximity to a proposed Nuclear Localization Signal (NLS) in the coiled-coil domain.

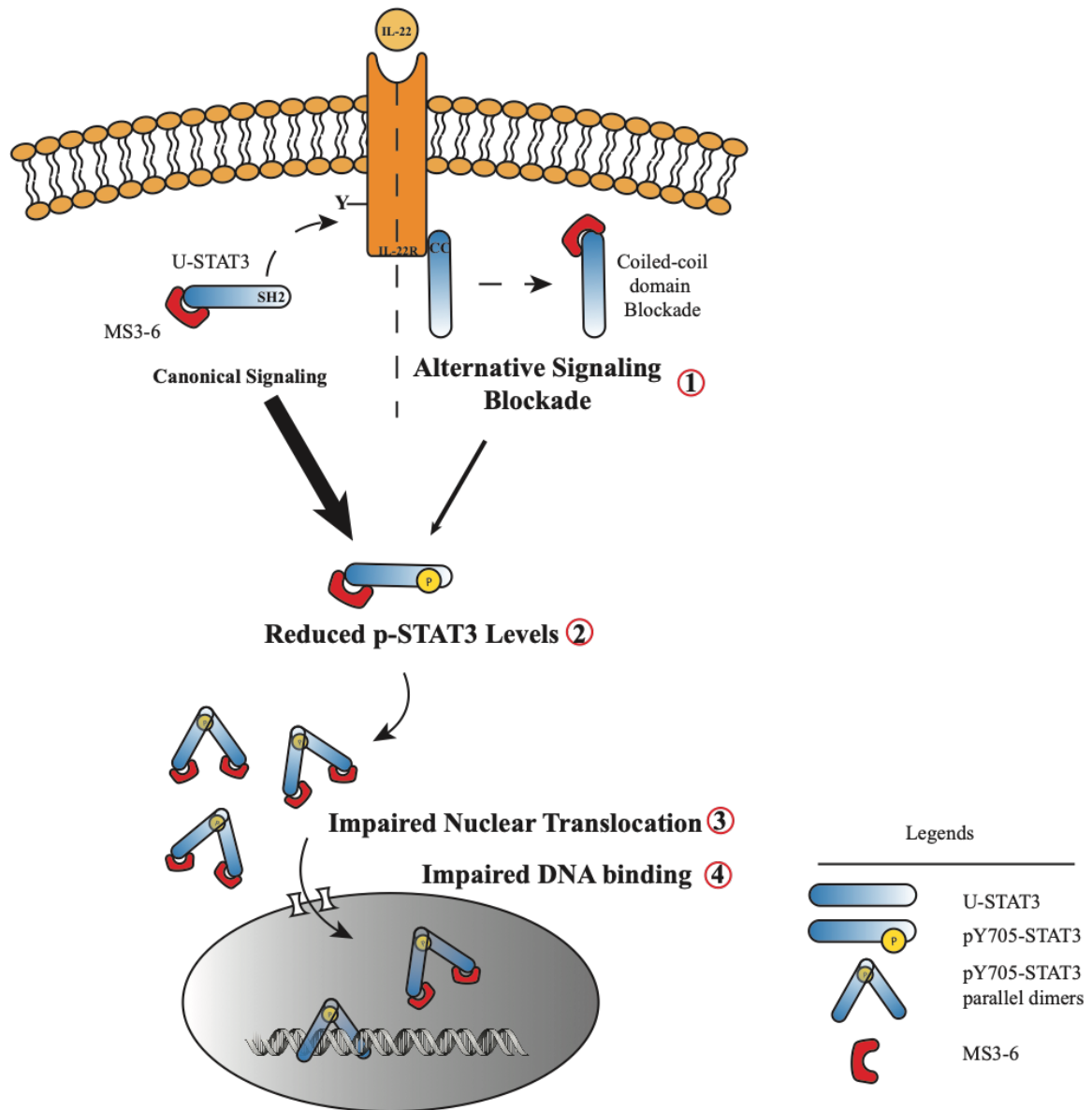


Figure 3.1: Scheme depicting the overall MS3-6 mode of action.

The cumulative influences (labeled 1 to 4) of MS3-6 binding synergistically results in the inhibition of STAT3 transcriptional activity. MS3-6 decreases STAT3 Y705 phosphorylation levels by impairing the binding of STAT3 to the IL-22R cytosolic tail, thus specifically blocking the alternative IL-22R/STAT3 signaling axis (1) and (2). Additionally, MS3-6 leads to the reduction of STAT3 translocation in the nucleus upon cytokine stimulation (3) and decreases STAT3 binding to DNA in vitro (4).

Importantly, our results demonstrate that MS3-6 leads to a reduction of nuclear STAT3 levels upon stimulation. Hence, we stipulated that the binding of MS3-6 interferes with the overall nuclear localization of STAT3. This could be further explained by an impaired recognition of the NLS by the importins responsible for the nuclear translocation of STAT3. Similarly, the binding of MS3-6 led to the bending of the coiled-coil domain tetra helix. This could participate to the impaired

importin recognition due to the strong allosteric effect of MS3-6. Nonetheless, our data show that the nuclear translocation of STAT3 was not fully prevented. Indeed, reduced levels of STAT3 could still be observed in the nucleus despite treating cells with MS3-6. However, our data additionally indicate that MS3-6 led to decreased binding to DNA *in vitro*. MS3-6 may thus additionally interfere with the overall transcriptional activity of STAT3 by reducing the binding to DNA. Furthermore, in a cellular context, STAT3 needs to associate and form large protein complexes with other transcription factors, functional interactors and the overall core transcriptional machinery in order to drive target gene transcription²²³ (Figure 3.2). MS3-6 might additionally interfere with the protein-protein interaction processes required for an efficient transcriptional activity to be held.

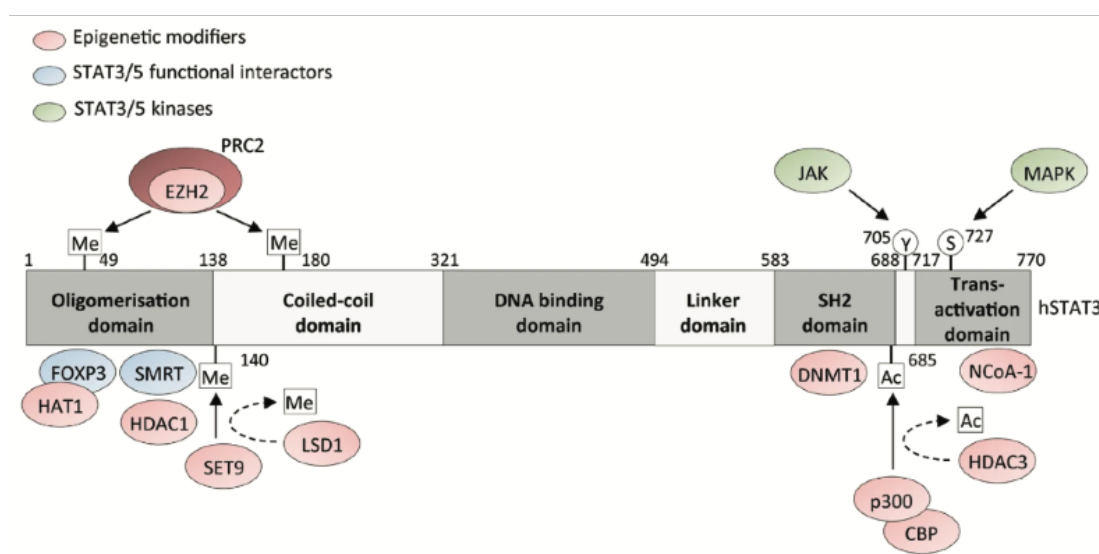


Figure 3.2: Binding sites of proteins physically interacting with STAT3.

STAT3 is required to associate and form high order complexes in order to carry out its transcriptional activity. The proteins labeled in green and blue are respectively required to activate or modulate the transcriptional activity of STAT3. Similarly, proteins in red have been shown to play major roles in modifying the chromatin structure in vicinity to STAT binding sites. Figure adapted from²²³.

3.2.2. STAT3 NTD blockade by MS3-N3 as an innovative inhibitory strategy

In contrast to the strong inhibition of the transcriptional activity of STAT3 by MS3-6, the specific blockade of the NTD by MS3-N3 led to a modest antagonism of the STAT3 canonical activities. Indeed, the transcriptional levels of STAT3 were mildly impacted by MS3-N3 binding as shown by luciferases assays and quantification of the mRNA levels of downstream endogenous genes. Notably, the binding affinity of MS3-N3 to STAT3 was lower than MS3-6. This might explain the

weaker effects of MS3-N3 on the overall STAT3 transcriptional activity. Similarly, as MS3-N3 did not lead to a strong reduction of STAT3 nuclear levels in contrast to MS3-6, its molecular mode of action still remains to be elucidated and could rely on the perturbation of STAT3 oligomerization in the nucleus.

Indeed, the role of the NTD in regards to STAT3 oligomerization, DNA binding and overall transcriptional activity is currently still not well understood. Recent evidence indicated that the NTD favors the recognition of weaker DNA binding sites by STAT3 resulting in the transcription of specific gene sets⁹⁵. Furthermore, STAT3 has been reported to oligomerize in the nucleus once bound to DNA. This oligomerization is mediated by the reciprocal interaction of the NTD between two DNA bound parallel p-STAT3 homodimers^{89,224} (Figure 3.3). Interestingly, because many cancer cells suffer from elevated STAT3 nuclear levels, these oligomers are believed to be more frequent in tumor cells than in healthy cells. Such rationale recently generated a lot of interest in the STAT signaling research community, which is currently investigating the role of the NTD of various STAT family members and the overall benefit from antagonizing the NTD mediated oligomerization. MS3-N3 could thus become a key, state-of-the-art protein antagonist tool that precludes the reciprocal interaction between two STAT3 NTD by physically interfering with their association. Notably, this novel strategy relying on the targeting of the NTD-mediated STAT3 nuclear oligomers could result in reduced toxicity levels as compared to the complete inhibition of STAT3 transcriptional activities.

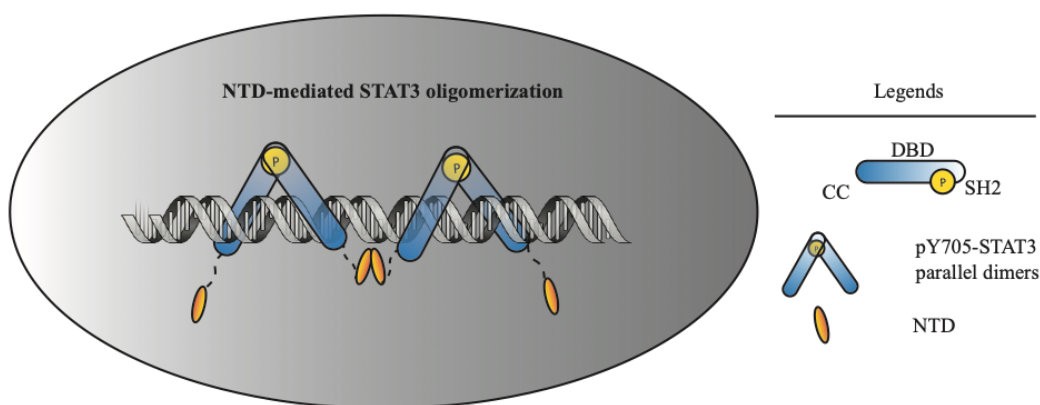


Figure 3.3: NTD-mediated STAT3 oligomerization.

The NTD has been found to favor the oligomerization of STAT3 dimers bound to DNA leading to the creation of STAT3 paracrystals in the nucleus. This causes a prolonged transcriptional activity of STAT3. Such high order oligomers are thought to be relevant in cancer cells suffering from elevated nuclear STAT3 levels. MS3-N3 might represent an interesting approach towards the reduction of nuclear STAT3 oligomers. Scheme adapted from²²⁵.

Additionally, the NTD of various STAT family members have been described to mediate the formation of un-phosphorylated anti-parallel dimers in the cytoplasm⁹³. Due to their high structural and sequence conservation, it is thought that the NTD of STAT3 similarly leads to the formation of an un-phosphorylated STAT3 (U-STAT3) dimer mediated by the reciprocal interaction between the NTD and a dimerization interface between the coiled-coil domain and DBD of two STAT3 monomers. Of note, our crystal structure of the MS3-6/STAT3 complex represents the first crystallographic evidence of such an anti-parallel dimer between two STAT3 monomers. This exciting result similarly suggests that binding of MS3-6 is compatible with anti-parallel STAT3 dimer formation. However, the specific blockade of the NTD using MS3-N3 might represent a unique approach to specifically preclude the formation of un-phosphorylated anti-parallel STAT3 dimers. Hence, this unique feature of MS3-N3 might prove valuable to further study the yet poorly characterized singling roles of U-STAT3.

3.3. Cancer cell viability often does not rely on the STAT3 constitutive signaling

Despite its constitutive activation in various tumor types such as breast cancer, melanoma and leukemias, the tumor cells dependency on STAT3 signaling for survival has not been thoroughly demonstrated in many cases. Current evidences in the literature indirectly linking tumor cell death with STAT3 signaling perturbation rely on the treatment of cancer cell lines with pre-clinical drugs often suffering from an unknown selectivity profile and used at very high concentrations. For example, the preclinical small-molecule inhibitor A69 used at 20 μ M led to A549 lung cancer cell death. Similarly, another compound against STAT3, named S31-201, killed MDA-MB-435, MDA-MB-453 and NIH3T3/v-Src cells when used at 100 μ M. Given that the selectivity of the drugs mentioned above has not been demonstrated, one cannot exclude potential off-target effects resulting in unspecific toxicity, especially when used at such an exaggerated concentration range, often orders of magnitude above the *in vitro* binding affinities to STATs. In all cases, experiments with drug-resistant STAT3 mutants (gold standard in chemical biology/molecular pharmacology to demonstrate on-target inhibition) were not available. Hence, the link between STAT3 signaling and tumor cell survival only remained indirectly observed and is mostly hypothesized due to the transcription of survival and anti-apoptotic genes such as BCL-2, BCL-XL, MCL-1 and survivin among other genes under STAT3 transcriptional control. In our work, we have tested a panel of human cancer cell lines described as “STAT3-dependent” in the literature including the MDA-MB-231 breast cancer cell line, A549 lung cancer cell line and LNCaP and DU145 prostate cancer cell lines, together with SR786, Karpas and SUP-HLU1 lymphoma cells. Nonetheless, all cell lines tested did not show a strong decreased proliferation upon treatment with an siRNA against STAT3.

Similarly, treatment of these cells with Ruxolitinib, a potent low-nanomolar JAK1/2 inhibitor, led to IC₅₀ values >3 μ M, with the exception of A549 cells (2.5 μ M). Hence, these data suggest that the cell lines we tested do not rely on STAT3 for survival. Perturbation of STAT3 signaling in these cells thus was not expected to lead to tumor cell death. Nonetheless, the link between NPM-ALK oncogenic cell transformation and STAT3 signaling has been described in the literature²²⁶. We thus postulated that, since the overall cellular transformation in this context is described to rely on STAT3, our monobodies could lead to tumor cell death, as suggested in the literature. To investigate the impact of our monobodies on NPM-ALK tumor cell viability, we took advantage of mouse thymoma cells isolated in the lab of Veronika Sexl (Vienna). In an initial Ruxolitinib screening, these cells showed IC₅₀ values ~ 2 to 5 μ M. We could nonetheless explain this lack of JAK1/2 inhibition sensitivity as NPM-ALK directly mediates the phosphorylation of STAT3, thus bypassing the need for the JAK upstream kinase. In order to irrefutably demonstrate that NPM-ALK cells were relying on STAT3 for their survival, we aimed to take advantage of shRNAs against STAT3. Unfortunately however, several commercial shRNAs were not able to effectively knock-down STAT3 expression. We nonetheless, decided to investigate whether our monobodies led to NPM-ALK tumor killing as expected from the literature. The NPM-ALK cell lines were engineered with constitutive and inducible expression systems with both MS3-6 and MS3-N3, as well as VHL-monobody fusions. We evaluated the effects of our constructs on cell proliferation and viability as measured by Annexin V and 7AAD staining, however, no effects could be observed. This illustrates how the frequent activation of STAT3, identified in >70% of solid and hematological tumors, may not directly translate into tumor cell dependency for survival, as originally hypothesized by the scientific community.

In line with our observations, a study published in 2019 showed that, out of a panel of nine additional leukemia and nine lymphoma human cell lines not included in our original screening, only one, the MOLM-16 cell line, resulted in strong growth inhibition upon treatment with the potent SI-109 STAT3 PROTAC. These very recent data thus indicated that STAT3 dependency in tumor cell lines is perhaps less frequent than originally believed. As a perspective, it would be interesting to test the effect of MS3-6 in MOLM-16 tumor cell growth in order to validate the repercussions of STAT3 inhibition on cell proliferation and viability.

In this work, we similarly investigated the binding of MS3-6 to known oncogenic STAT3 mutants. MS3-6 binding to STAT3 S614R, Y640F and D661V was measured at low nM affinities in a similar range as the WT protein. This can be explained due to fact that the monobody binding site is located far away from the SH2 domain where the oncogenic mutations are found. Hence the distal monobody binding is not perturbed by the single point mutations of the SH2 domain. These STAT3 oncogenic mutants led to a proliferative advantage and colony forming/replating potential in

hematopoietic stem cells (HPC-7) as compared to WT-STAT3 (Sexl lab, unpublished result). Hence, in order to further investigate the therapeutic opportunities for STAT3 monobodies, I tested their activity on STAT3 Y640F oncogenic mutant that showed the strongest effect. While preliminary data suggested that MS3-6 reduced the HPC-7 STAT3-Y640F cell proliferation as measured by cell titer glo, no effect could be observed upon cell counting. Hence, in view of these contradictory results, further experiments would be required in order to conclude to a beneficial effect of the monobodies in that context. Nonetheless, it is worth noting that HPC-7 cells expressing the oncogenic STAT3 do not survive in total absence of cytokines stimulation (stem cell factor; SCF) suggesting that the oncogenic STAT3-Y640F mutant is rather hyper-reactive to upstream stimulation than constitutively activated on its own. Similarly, no tumor development could be observed in xenograft mice models, suggesting that on its own, STAT3 may act as a weak oncogene and may require additional driving force from an additional oncogene. Therefore, the use of monobodies led to a better understanding of the molecular mechanisms driving the STAT3-mediated tumorigenesis. These exciting experiments are planned to be published independently in a future collaboration with the lab of Veronika Sexl, as monobodies provide a first strategy to inhibit STAT3 oncogenic mutants.

3.4. The use of monobodies as biochemical tools towards the dissection and modulation of STAT3 signaling

Current approaches to study protein functions rely on genetic knockouts or RNAi treatments resulting in the complete loss of the protein. However, these approaches often fail to predict the effects of a specific domain blockade or of the inhibition of a precise catalytic activity as illustrated by several kinases inhibitors who led to unexpected effects in cells. In contrast, monobodies are binding to defined regions in key protein domains and thus provide additional information as compared to the overall genetic loss-of function approaches towards a better understanding of the underlying biology. Our monobodies thus allowed the dissection of STAT3 activity by identifying the implication of the NTD and coiled-coil domains in key cellular functions. Similarly, the targeting of these previously untouched domains opens the door for the development of novel inhibitory approaches.

3.4.1. MS3-6 interferes with alternative IL22-R signaling

In addition to modulating the transcriptional activity of STAT3, the specific blockade of defined domains using monobodies is an interesting approach to further dissect and provide additional

insight towards the characterization of intracellular pathways and protein functions. This is perhaps best illustrated by the non-conventional STAT3 signaling induced by IL-22. The specific blockade of the coiled-coil domain using MS3-6 in this context provided supporting evidence corroborating an alternative IL-22R signaling mechanism.

The IL-22R is a key player in controlling inflammatory responses. IL-22 signaling is importantly implicated in the regulation of pathogenic infections in the gastrointestinal and pulmonary systems. Interestingly, the IL-22R is mostly expressed in epithelial cells, which are responsible for eliciting protective responses. In our work, we have shown that MS3-6 does not prevent STAT3 Y705 phosphorylation upon IL-6 stimulation, but strongly reduces the phosphorylation levels of STAT3 upon IL-22 stimulation. We subsequently demonstrated that this effect was mediated by the specific blockade of the coiled-coil domain of STAT3, which prevents a non-canonical tyrosine independent IL-22R/ STAT3 association (Figure 3.1). Such an alternative receptor/STAT3 association, relying on the C-terminal portion of the cytokine receptor and the STAT3 coiled-coil domain has not been described for the IL-6 cytokine receptor family, which may explain why MS3-6 does not lead to decreased STAT3 phosphorylation levels upon IL-6 stimulation. Indeed, IL-22R is part of the interferon family, which in contrast to the IL-6 cytokine family, do not associate with the gp130 co-receptor. Hence, it is believed that the alternative IL22R-STAT3 signaling has evolved to ensure a strong and rapid activation of STAT3 upon pathological infections to elicit a strong pro-inflammatory response. Nonetheless, while the IL-22 cytokine has beneficial functions when precisely controlled, excess of IL-22 signaling may contribute to the development of pathological diseases such as psoriasis and cancer. Indeed, the link between chronic inflammation and the onset of tumorigenesis has been established and STAT3 is thought to play a pivotal role in linking the two pathologies. The IL-22R mediates STAT3 activation in a pro-inflammatory context, which in turn drives a feedback loop consisting in the transcription of genes implicated in the inflammatory response. Importantly, the local inflammatory conditions trigger the secretion of cytokines, which encourage the neoplastic cell growth in a paracrine fashion. Similarly, stromal cells suffering from accumulated mutations in oncogenes and tumor suppressor genes show increased production of soluble mediators leading to the promotion of tumor development in an autocrine manner. Therefore, the IL-22 signaling drives a fine balance between beneficial and deleterious effects. Hence, a potential therapeutic strategy may rely on the reduction of pathological IL-22 signaling by targeting the alternative IL-22R/STAT3 association using MS3-6. We have shown in this work that the constitutive association of STAT3 to the IL-22R can be prevented by blocking the coiled-coil domain, which leads to a strong reduction of STAT3 activation. We now aim at demonstrating the therapeutic potential of this approach *in vivo* in a psoriasis mouse model in close collaboration with the laboratory of Laure Dumoutier (UCL, Belgium).

As a whole, the use of MS3-6 to further dissect and characterize the IL-22 cytokine receptor alternative mechanism perfectly illustrate the important role of monobodies as protein engineered tools towards the better understanding of intracellular signaling pathways.

3.4.2. Monobody mediated STAT3 targeted degradation

Over the past decade, the targeted degradation of pathogenic proteins has emerged as a powerful alternative to their inhibition. Indeed, the repurposing of the polyubiquitination and proteosomal degradation machinery appeared as an alternative strategy in order to overcome the challenges in inhibiting proteins that lack key catalytic domains. A current limitation of this approach remains the development of molecular probes specific enough to bind a single protein target. A strong advantage of monobodies as compared to small molecular probes consists in the selectivity achievable towards a precise target. Moreover, monobodies can be readily developed to bind to virtually any target of choice. This characteristic opens the door to additional strategies such as a targeted degradation inspired approach. Indeed, the exquisite binding affinity and specificity of monobodies against key undruggable oncoproteins may serve as exceptional warheads to facilitate the target polyubiquitination by E3 ubiquitin ligases.

Until recently, the development of a STAT3 directed PROTAC remained challenging. Recent work demonstrated the feasibility and effectiveness of such an approach against STAT3⁹⁰, leading to complete and long-lasting tumor regression in tumor xenograft mice models. Hence, this work advocates for the development of a high affinity monobody binders capable of specific binding to previously undruggable proteins in order to mediate their targeted degradation. Here, such an approach applied to STAT3 was undertaken to develop a monobody-mediated targeted degradation system against a specific STAT family member. The system developed in this work consisted in the inducible expression of a VHL-monobody fusion upon doxycycline treatment, which led to endogenous STAT3 degradation overtime. The differences of degradation efficiency observed between the VHL-MS3-N3 fusion construct as compared to VHL-MS3-6 may be explained by their relative affinities towards STAT3, together with the local availability of lysines for polyubiquitination. Interestingly, ~20% of the endogenous protein remained. This can be explained by the natural turnover of STAT3 expression, where the STAT3 degraded proteins are rapidly replaced by freshly transcribed STAT3 proteins. Similarly, STAT3 is known to be located in cellular compartments such as in the nucleus or in mitochondria, which may render it inaccessible for binding to the VHL-monobody protein. Nonetheless, this approach led to a strong knockdown of endogenous STAT3 levels in cells.

3.5. Concluding remark and future perspectives

In the past decade, monobodies have emerged as powerful synthetic binding proteins from non-antibody scaffolds. The use of monobodies as state-of-the-art biochemical tools to further dissect and understand key oncogenic signaling has been illustrated in this work by highlighting an alternative IL-22R signaling relying on a constitutive STAT3 association to the receptor. Similarly, the use of monobodies as intracellular inhibitors opens the door for novel strategies to preclude oncogenes whose inhibition still remains currently unexplored. With this work, I have shown that the specific targeting of an intracellular transcription factor, which is commonly regarded as “undruggable”, is in fact feasible using monobodies. With this work, we hope to further push boundaries of the current limitations in cancer targeted therapies and provide new opportunities and approaches to define complex intracellular proteins from “undruggable”, to “not yet drugged.”

Nonetheless, future efforts should be undertaken to determine the overall use of monobodies in a therapeutic context. Indeed, the high affinity binding and selectivity of monobodies were demonstrated *in vitro* and in cells. However, their potential use as *in vivo* therapeutics must be assessed as well. To initially study the delivery and biodistribution in murine models, future work should firstly take advantage of monobodies raised against extracellular targets such as CD20 (a B-lymphocytes antigen implicated in cell maturation) or the Programmed death-ligand 1 (PD-L1) which diminishes the CD8⁺ T cell proliferation and suppresses the immune responses.

Key questions that remain to be addressed are:

- Are monobodies stable in plasma?
- Are the monobodies homogeneously distributed in the body?
- Is there an efficient co-localization with the target?

Common limitations of small biologics, including peptides and antibody fragments consist in low proteolytic stability and fast renal clearance from blood circulation. One should thus first assess the monobody stability and resistance to proteases in plasma *ex vivo*. Previous publications have highlighted the thermal stability of the fibronectin type 3 scaffold with a reported melting temperature (T_m) of $43 \pm 2^\circ\text{C}$. Additionally, this thermal stability could be further improved while maintain high affinity for the target protein as illustrated by a reported T_m of $87 \pm 2^\circ\text{C}$ upon engineering of the FN3 scaffold²²⁷. Hence the thermal stability of the monobody scaffold suggests that they are suitable for a use as protein-based therapeutics in physiological systems. Nonetheless, the resistance of these small proteins against proteases may represent a potential drawback. Should this prove to be an issue, possible ways to increase the plasma half-life include conjugation with

the F_C fragment of antibodies, the non-covalent tethering with albumin binding ligands and pegylation of monobodies. Mass spectrometry analysis could be performed to assess the monobody degradation rate overtime.

While protein stability and protease resistance may not be the major issues towards the use of monobodies *in vivo*, the delivery to specific target cells might be. The characterization of monobodies metabolic and renal clearance rate upon intravenous application in mice could be performed by taking advantage of fluorescent monobodies injected intravenously and measured using flow cytometry. After various time points, washing of the remaining monobodies in blood circulation could be performed by perfusion. Organs including lung, liver, heart, spleen, bone marrow, lymph nodes and kidneys could then be collected. An important fluorescence detection in kidneys would suggest clearance from the bloodstream, while the efficient binding to target cells in specific organs can be assessed by flow cytometry.

The intracellular delivery of monobodies to target cells in cell culture and ultimately *in vivo* is an additional essential step to be studied in order to evaluate the potential of monobodies as intracellular inhibitors. Our lab is very active in that research field and developed several approaches to achieve cytosolic delivery of recombinant monobodies. For example, the polycationic re-surfacing of the monobody scaffold allowed intracellular penetration *in vitro* as observed by fluorescence microscopy. Nonetheless, this approach by itself is not capable of distinguishing target tumor cells from healthy cells. A potential solution might consist in the development of bi-valent monobody fusions, where one monobody targeting an extracellular antigen highly enriched at the surface tumor cells (such as HER2 for example) is fused to a second monobody targeting an intracellular oncogene. This approach could ensure the tumor tropism of the bi-specific monobodies which in turn, provided that their size (20 KDa) is not too large, might penetrate tumor cells preferentially.

An additional strategy developed by our lab consisted in the coupling of a recombinant monobody with a bacterial toxin derived from the Shigella strain. This approach takes advantage of the evolutionary process which ensured that bacterial toxins are intracellularly delivered. Upon binding to the extracellular receptor, which has been found to be highly expressed in certain malignancies such as colon cancer for example, the toxin-monobody fusion is up taken in the cell and evade endosomes resulting in the cytosolic delivery of the monobody. This approach is promising for future therapeutic usage, but suffers from the nature of the bacterial toxin, which might trigger a rapid immune response upon injection in the blood stream. Hence, *in vivo* studies should similarly investigate whether monobody treatment triggers an important anti-monobody immune reaction. This could be performed a week following monobody injections, at the peak of T cell response,

where blood samples could be harvested and T cell populations isolated in order to determine the relative affinity of their TCR towards a given monobody. Typically, this could be assessed by ELISA and should allow to determine whether an effective anti-monobody T cell response was mounted overtime.

In conclusion, I described in this work the development of high affinity, specific monobody binders against previously untargeted domains of STAT3 which resulted in the inhibition of its transcriptional activity. This has been previously regarded as highly challenging by the scientific community. Importantly, the monobodies developed here led to a novel antagonistic mode of action against STAT3 which was previously unexplored. In addition, the specific blockade of the coil-coil domain using MS3-6 provided further evidence for an alternative IL-22 signaling pathway where STAT3 is pre-associated with the cytosolic tail of the cytokine receptor. Hence, altogether, the monobodies developed in this study represent an exciting advance from a drug discovery perspective and allowed at the same time a better understanding and dissection of the STAT3 signaling pathway.

4. MATERIALS AND METHODS

4.1. Antibodies, cell lines and Reagents

Antibodies against STAT1 (No. 9172), pY701 STAT1 (No. 9167), STAT3 (No. 9139), pY705 STAT3 (No. 9145), pS727 STAT3 (No.9134) and pY694 STAT5 (No. 9359) were purchased from Cell Signaling Technology. The antibody against STAT5b (sc-1656) was obtained from Santa Cruz Biothechnology. The anti-Myc tag antibody coupled to Dylight800 was purchased from ThermoFisher (No. MA1-21316-D800). The anti-penta-His antibody was obtained from QIAGEN (No. 34610) and the anti- α -Tubulin antibody (T9026) was ordered from Sigma-Aldrich. Secondary antibody used in western blots were obtained from LiCOR: anti mouse IRDye680 (No. 926-32210), Anti mouse IRDye800 (No. 925-32210), and anti-rabbit IRDye680 (No. 925-68071). Similarly, the secondary mouse or rabbit HRP coupled antibodies were purchased from Cell Signaling Technology (No. 7076 and 7074 respectively). Streptavidin-coupled magnetic beads (Promega #Z5481) were used in the monobody selection process to perform pull-downs of the recombinant biotinylated proteins. K562 and Jurkat cells were purchased from DSMZ (Deutsche Sammlung von Mikroorganismen und Zellkulturen, Braunschweig, Germany). A549 cells were a kind gift from Prof. Etienne Meylan (EPFL). NPM-ALK cells were established from mouse thymoma in the lab of Prof. Veronika Sexl (Vet Med Uni Wien). The cytokines used in this work, human Oncostatin M (O9635) and IL-22 (SRP3089) as well as Human IL-6 (MAN0003501) were purchased from Sigma-Aldrich and Gibco respectively.

4.2. Cloning and plasmids

4.2.1. Conventional cloning

Human STAT3 cDNA was purchased from the Gene Expression Core Facility at EPFL. The NTD [a.a. 1-127] and core fragment of STAT3 [a.a. 129-722] were cloned into a pHFT vector comprising a 6xHis tag, tobaccoetch virus (TEV) protease cleavage site and Avi-tag for biotinylation using the

restriction enzymes BamHI and XhoI. For lentiviral transduction, monobodies and VHL-monobodies fusions were cloned into an inducible pEM24 vector (modified pCW2239 obtained from E. Meylan, EPFL) using InFusion recombinase (Clontech). The lentiviral expression system vectors pCMV-R8_74 (encoding gag and pol proteins) and pMD2_G (encoding VSV-G envelope) were obtained from the Trono Lab at EPFL. Retroviral transduction was performed using a constitutive pRV-NTAP vector containing a 2xProteinG-TEV-xMyc tag. Monobodies were inserted in the pRV-NTAP vector using gateway cloning. Retroviral expression system encoding the VSV-G envelope was obtained from the Superti-Furga lab. Monobody-GFP fusions were introduced into a doxycycline inducible pEBtetD vector using conventional cloning using the BamHI and XhoI restriction enzymes. All DNA constructs were confirmed by DNA sequencing (Microsynth).

4.2.2. Gateway cloning

Gateway compatible human expression vectors were used such as the pRV-NTAP, pEBtetD, hPGK and pCS2 vectors. The original gene sequence were initially elongated with primers encoding gateway compatible overhangs by conventional PCR. The resulting DNA was next introduced into a pDONR201 by performing a BP reaction (BP clonase kit, Invitrogen) followed by the subsequent cloning into the destination vectors by LR reaction (LR clonase kit, Invitrogen). DH5a *E. coli* cells were next transformed with the resulting DNA sequences and plasmids were recovered by Miniprep (QIAGEN).

4.2.3. In-Fusion cloning

Myc-tagged monobodies from the pCS2 vector were further subcloned into the pEM24 vector using in-fusion cloning. To do so, DNA template of the Myc-tagged monobody sequence was amplified by PCR with primers encoding In-fusion compatible overhangs. The target PCR product was isolated in an agarose gel, excised and purified to be further inserted into the pEM24 vector: 50ng of the insert was mixed with 100ng of the target pEM24 vector previously linearized with the restriction enzymes HpaI and PacI, as well as with a 5xfusion mix (Invitrogen). Samples were incubated at 50°C for 15 minutes and the product was transformed into *E. Coli* HB101 strains. Transformed bacteria were plated on an Ampicilin agarose petri dish, single colonies were isolated and DNA was extracted by miniprep (Qiagen). All plasmids were verified by sequencing (Microsynth).

4.2.4. Site directed mutagenesis

Site-directed mutagenesis was performed on the pHFT vector encoding the human STAT3 sequence to generate oncogenic mutants identified in patients suffering from various hematological malignancies. Oligoes encoding oncogenic points mutations were ordered from Microsynth: S614R (5'gattcagtgaagcagGaaagaaggaggcgtc3'), Y640F (5'cagtcctggaacatTcacaagcagcagctg3'), D661V (5'gctataaga- tcatggTtgctaccaatatcctg3'), as well as the negative dominant STAT3 mutant Y705F (5'gtagcgtgccccatTcctgaagaccaagttatc3'). Site directed mutagenesis was performed according to the lab standard operation procedure (SOP). Briefly, 50ng of template pHFT-STAT3 WT DNA was used for PCR reactions consisting in 1 cycle of 30 second at 95°C, followed by 18 cycles at 95°C (30 seconds), 55°C (1 minute) and 68°C (2 minutes/kb of the plasmid). 1µl of DPN1 was added to the PCR solution for 1hr at 37°C to digest the original template vector and transformation of XL-10 Gold cells followed. DNA extraction was performed using the QIAGEN miniprep kit according to the manufacturer's instructions. All plasmids were confirmed by sequencing (Microsynth).

4.3. Monobody selection

Biotinylation of Avi-tagged STAT3 target proteins was achieved *in vivo* by co-transforming BL21 (DE3) E. coli cells with a BirA plasmid as well as with a pHFT plasmid containing the AviTag target protein fusion. Cells were induced with 0.5 mM of IPTG once the OD600 of the expression culture medium between 0.5 and 0.8. Biotin resuspended in DMSO was added to the culture with a final concentration of 50µM. Cells were grown overnight at 18°C, 200rpm before purification. Monobodies were selected according to methods previously described^{54,56,228}. Briefly, four rounds of phage display were followed by the amplification and transformation of yeast cells with the DNA sequences corresponding to binding monobodies. The yeast cells were next sorted using FACS based on a strict gating strategy comprising double positive cells for surface display and binding to biotinylated STAT3 target proteins. Isolated monobody clones were sequenced and inserted into pHFT vectors for further characterization.

4.4. Yeast binding assay

Increasing concentrations of recombinant biotinylated protein targets resuspended in Tris-buffered saline (TBS) with 0.1% BSA were incubated with yeast cells displaying monobodies and a mouse anti-V5 antibody for 30 minutes at room temperature. Three washes with TBS with 0.1% BSA

followed together with incubation for 30 minutes with a streptavidin-DyLight650 and a FITC-coupled secondary anti-mouse IgG at room temperature in the dark for 30 minutes. Samples were analyzed on a Gallios flow cytometer (Beckman Coulter). Data were fitted on a 1:1 binding model using the software Prism (Graphpad) to determine K_D values.

4.5. Recombinant protein expression

Target protein sequences were cloned into the bacterial pHFT-6xHis-avitag vector and transformed in *E. coli* BL21 (DE3) cells (heat shock transformation). Cells were seeded on an agar petri dish in presence of antibiotics to discourage bacterial contamination and grown overnight at 37°C, 200 rpm. Single colonies were isolated from the petri dish and used to seed a 10 ml LB medium pre-culture grown overnight at 37°C. Dishes older than one month were discarded and fresh BL21 cell transformations were performed instead. An overnight pre culture was added to LB medium with an original OD at 0.05 to 0.1 (10ml of the preculture in 1L of LB medium). Cells were grown at 37°, 200 rpm until OD reached 0.5-0.8 and the culture was next induced with 0.5 mM IPTG final concentration. Cells were further grown overnight at 18°C 200 rpm and harvested the next day. Cells were harvested by centrifugation at 6000g for 10 minutes at 4°C and transferred in 50ml falcons to be stored at -80°C or to be immediately processed for protein purification.

4.6. Ni-NTA gravity flow purification

BL21 bacterial cell pellet was isolated as described above and immediately resuspended in 40ml/L of culture in Buffer A [25 mM Tris pH=7.5, 300 mM NaCl, 5% glycerol, and depending on sample, 1 mM DTT] supplemented with proteases inhibitors tablets (Roche) and DNase. Cells were lysed using an Avestin Emulsiflex homogenizer and the soluble proteins were isolated from the cell debris by centrifugation at 41'000g for 30 min at 4°C. The supernatants containing the 6xHis-tagged proteins were incubated with 1ml of Ni-NTA resin for 1-2 hours at 4°C under constant gentle shaking. Proteins of interest were next purified by gravity flow and harvesting of the Ni-NTA resin. After two washing steps with 20ml Buffer A each, the Ni-NTA resin was resuspended in 5ml of Buffer B (same buffer composition as Buffer A, only with 400 mM Imidazole added) and the eluates containing the protein of interest were recovered. Samples of the input, supernatant, wash fraction, and eluate were kept for subsequent SDS-PAGE analysis. The successful protein purification and protein concentration was assessed using the Nanodrop spectrophotometer.

4.7. Size exclusion chromatography

Ni-NTA protein purification was followed by size exclusion chromatography (SEC) to isolate pure protein fractions. Two injection modes were used: often, directly after elution with 5ml Buffer B, samples were injected on a Superdex 200 16/600 GL column using the pump loading system. Alternatively, samples were concentrated to smaller volumes (600µl) and clarified through a 0.22µm filter before loading onto the Akta Avant system (GE) using the injection loop. SEC methods included an initial equilibration phase consisting in 1.2 column volume washing with the gel filtration buffer such as 25mM Tris-HCL pH 7.5, 150mM NaCl, and 5% Glycerol, followed by the protein injection and gel filtration. Peaks corresponding to the protein of interest molecular weight were harvested, concentrated using the Amicon centrifugal filters and stored at -80°C (flash frozen in liquid nitrogen). Protein concentration was measured using the Nanodrop spectrophotometer.

4.8. SDS-page and Coomassie staining

Proteins purified as described above were next analyzed by Sodium dodecyl sulphate Polyacrylamide Gel electrophoresis (SDS-PAGE). Samples were diluted with 4x sample buffer (0.2M Tris-HCL, 8% SDS, 400mM DTT, 40% glycerol and 0.02% bromophenol blue) and boiled at 95°C for 5 minutes to ensure protein denaturation. Samples were next loaded on a polyacrylamide gel (7-15%, depending on the protein molecular weight) and electrophoresis was performed using constant current of 100V in SDS running buffer (0.25M Tris, 1.92M glycine, 1% (w/v) SDS). Resolved gels were used to perform western blots or were directly stained using a coomassie staining solution (10% acetic acid, 50% absolute ethanol and 0.025% coomassie brilliant blue G-250) for 10-15 minutes RT followed by incubation in a destaining solution (10% acetic acid and 20% ethanol) after boiling. Gels were imaged using a Li-Cor Odyssey infrared imaging system and analysed with the ImageStudio software (Li-Cor).

4.9. X-ray crystallography

BL21 (DE3) E. coli cells were transformed with pHFT-monobody and pHFT-STAT3-CF constructs. Following an overnight recombinant protein expression, bacterial cells were harvested by centrifugation at 6000g for 10 minutes at 4°C and resuspended in 40ml/L of culture in Resuspension Buffer [25 mM Tris pH=7.5, 300 mM NaCl, 5% glycerol, 1 mM DTT]. Cells were lysed using an Avestin Emulsiflex homogenizer and the soluble proteins were isolated by

centrifugation at 41'000g for 30 min at 4°C. Proteins of interest were next purified by affinity using a Ni-NTA resin and elution was performed using an Elution Buffer (25 mM Tris pH=7.5, 300 mM NaCl, 5% glycerol, 1 mM DTT and 400mM imidazole). Elutions containing the target proteins were mixed in a 1:1 molar ratio in presence of TEV diluted 1:50 (W:V) and dialyzed overnight at 4°C in Gel Filtration buffer (20mM HEPES pH = 7, 200 mM NaCl, 10mM MgCl₂ and 2mM DTT). The next day, the STAT3/MS3-6 complexes were purified using size-exclusion chromatography with a Superdex 200 16/600 GL column. The complex was then concentrated in Amicon vivaspin tubes to 11mg/ml and 0.6mM dsDNA (forward: TGCATTTCCCGTAAATCT3' and reverse: 5'AAGATTTACGGGAAATGC3') was added to the drop just before crystallization trials in hanging drop plates by mixing 100 nL of protein with 100 nL of buffer conditions. Crystals were optimized in a 24-well plate format (hanging drop) by mixing 1µL of protein with 1µL of buffer. The best crystals and diffractions were obtained in 19% PEG300, 70mM Calcium acetate dihydrate, 100mM imidazole pH = 7 conditions. Data were collected at the beam-line PXIII of the Swiss Light Source (SLS), Villigen, Switzerland. Best crystal formation required addition of DNA to the protein complex despite not appearing in the crystal structure. The crystal structure of the complex was solved using molecular replacement (molrep, CCP4, and PHENIX) by taking advantage of previously published STAT3 structures and of an homology model of the monobody MS3-6. Manual model building and refinement of the structure was performed using Coot and phenix.refine. The final model geometry was with 93% in favored regions with 1.7% of Ramachandran outliers.

4.10. Script used for structure visualization on Pymol

The conformational change of the coil-coil domain upon MS3-6 binding was illustrated using Pymol by measuring the angles between the alpha helices of our STAT3/MS3-6 complex and previously published structures of STAT3 unbound to the monobody. The script below was used to determine orientation vectors for each alpha helices and measuring the angle formed between them.

```
fetch 6TLC, 4e68
show_as cartoon
align 6TLC, 4e88
# select and hide residues outside the CC domain
select to_hide, i. 321-end
hide to_hide
```

```

# split STAT3 and MS3-6 as two structures

create a_copy, 6TLC

# select MS3-6 to isolate it

select to_cut, i. 1-93

cartoon skip, to_cut and 6TLC

orient

cartoon skip, 1. 136-320 and a_copy

# MS3-6 is now an independent structure

color marine, a_copy

set cartoon_highlight_color, blue, a_copy

color grey, 6TLC

color yellow, 4e68

# set distinct cartoon transparencies

set cartoon_transparency, 0.5, a_copy

set cartoon_transparency, 0.2, 6TLC and 4e68

# calculate angle between two alpha helices

run https://raw.githubusercontent.com/speleo3/pymol-psico/master/psico/orientation.py

select hel1, /6TLC//B/136-188/

select hel2, /4e68/A/136-185/

angle_between_helices hel1, hel2

# normal color + black outline

set ray_trace_mode, 1

ray

```

4.11. ITC

Recombinant proteins were dialyzed overnight at 4°C in ITC buffer consisting in 25 mM Hepes (pH 7.5) and 150 mM NaCl and samples were degassed extensively. Total protein concentration was estimated by measuring the 280 nm absorbance using a nanodrop. ITC measurement were acquired on a MicroCalpeaQ (Malvern panalytical) instrument and consisted in the protein titration from the syringe in 16 injections of STAT3 to monobody or vice and versa, with 0.49µL for the first injection followed by 2.49µL for the remaining steps. Protein concentrations used were 100µM

(syringe) titrated to a 10 μ M solution (cell). The MicroCal software was used to determine thermodynamic parameters.

4.12. Fluorescence polarization

A pY-peptide corresponding to the cytosolic tail of the Gp130-Y905 co-receptor was used (5FLU-GMPKS*YLPQTVR-NH₂). A 50 μ l solution consisting in 250nM of the peptide mixed to 1.25 μ M of recombinant STAT3-CF followed by addition of increasing concentrations (0-10 μ M) of recombinant MS3-6 in TBS buffer (50 mM Tris pH 7.5 and 150 mM NaCl). FP measurements were performed in FP compatible dark bottom 96 well plates at room temperature. Wavelength set for data acquisition was 525nm with a filter at 515nm and data were obtained using an M5 plate reader from Molecular Devices. Raw data were normalized to free peptide in solution in TBS in background measurement. Two DNA oligonucleotides sequences corresponding to STAT3 downstream promoter sequences were used: SOCS3 (forward: 5'FAM-GCAGTTCCAGGAATCGG3' / reverse: 5'CGTCAAGGTCCTTAGCC3') and a2M (forward: 5'FAM-AGCAGTAACTGGAAAGTCCTTAATCCTTCTGGGAATTCT3' / reverse: 5'AGAATTCCCAGAAGGATTAAGGACTTTCAGTTACTGCT5'). Oligoes were initially mixed at equimolar concentration in annealing buffer (10mM Tris pH7.5, 50mM NaCL and 1mM EDTA) and annealed by PCR (heat to 95°C for 2 minutes, then slowly decrease to RT over 45 minutes). Once double stranded DNA was obtained, 25 μ l of 10nM dsDNA probes were added to 12.5 μ l of 2 μ M recombinant p-STAT3 dimer and 12.5 μ l of increasing MS3-6 concentrations (final concentrations: 0, 0.5, 1, 2, 5 and 10 μ M) in 50 μ l FP compatible dark bottom 96 well plates. Fluorescence polarization measurements were performed at room temperature. Wavelength set for data acquisition was 485nm with a filter at 528nm and data were obtained using an M5 plate reader from Molecular Devices. Raw data were normalized to free DNA in solution as background measurement.

4.13. Cell culture

Adherent human cell lines including HeLa (human cervical carcinoma), HEK293 (Human Embryonic kidney), HEK293gp, HEK293T, MDA-MB-231 and A549 cells were cultures in Dulbecco's Modified Eagle Medium, DMEM (Gibco) supplemented with 10% fetal bovine serum (FBS, Gibco) and 1% penicillin/streptomycin (P/S, Amimed). Cells were cultures in 10 or 15 cm dishes at 37°C in 5% CO₂ and were split 3x a week upon reaching confluency: cells were washed with PBS and incubated with 1ml Trypsin-EDTA at 37°C for 5-10 minutes. Dilutions of 1/5 ensured

optimal passage to keep cells under culture. Cells were discarded upon reaching passage number 25-28.

Suspension cells, such as K562 and Jurkat T cells were grown in RPMI (Gibco), supplemented with 10% FBS and 1% P/S. NPM-ALK expressing mouse thymoma cells were cultured in RPMI medium supplemented with 0.5mM 2-Mercaptoethanol (Gibco). Suspension cells were split 3x per week by centrifugation, counting using the CASYton cell counter and adjusted to 1×10^5 cells/ml. Experimental titration curves were performed to determine the optimal Blasticidin / Puromycin concentrations for each cell line upon transfections with mammalian expression vectors encoding for antibiotic resistance (A549: 6 μ g/ml blasticidin for 7 days, MDA-MB-231: 10 μ g/ml blasticidin for 7 days, HEK293 cells: 1 μ g/ml blasticidin for 7 days and 1 μ g/ml puromycin for 7 days, NPM-ALK thymoma cells: 20 μ g/ml blasticidin/2 weeks). A doxycycline concentration of 1mg/ml was used to ensure monobody expression in the pEM24 doxycycline inducible vector.

4.14. Mammalian cell transfection

Transient transfection of mammalian expression vectors was performed using the Polyfect reagent kit (QIAGEN) according to the manufacturer's instructions. Briefly, cells were seeded in 10cm culture dishes and were transfected upon reaching 60-80% confluency. 8 μ g of DNA was diluted to a total volume of 300 μ l with antibiotic and serum free medium and 80 μ l of Polyfect reagent was added for a final volume of 380 μ l. The solution was incubated at RT for 15 minutes and resuspended by addition of 1 ml of medium (containing antibiotics and serum) to the polyfect/DNA solution. The total solution was immediately transferred drop by drop to the cells and incubation at 37°C and 5% CO₂ followed.

4.15. Mammalian cell lysate preparation

Adherent cells were washed in cold PBS and lysed by addition of various cold lysis buffer supplemented with protease inhibitors (50mM NaF, 1 mM PMSF (Sigma), 1mg/ml TPCK (Applchem), 10 μ g/ml protease inhibitor cocktail from Roche) and 1mM orthovanadate. Buffer used consisted in Lysis buffer (50mM Tris-HCl, pH7.5, 150mM NaCl, 5mM EDTA, 5mM EGTA, 1% NP-40), RIPA buffer () or STAT3 lysis buffer (50mM Tris pH8, 150mM NaCl, 1% Triton X-100). Cells were scrapped from the culture dish surface using rubber scrappers and transferred in cold Eppendorf tubes. Incubation at 4°C on ice for 10 minutes followed. Lysed cells were then centrifuged for 10 minutes at maximum speed (20000g) and supernatant was transferred to new tubes. Total protein concentration in lysates was estimated using a Bradford solution titration (Bio-

Rad 1:5 dilution in water, OD_{595nm} measurement) and compared to a standard curve of γ -globulin solution.

4.16. Western blot analysis

STAT3 phosphorylation in A549 cells was assessed upon treatment with IL6 or IL22 (500ng/ml) for 15 minutes at 37°C. Total protein extract was immediately recovered using a lysis buffer (50mM Tris pH = 8, 150mM NaCl, 1% Triton X-100) supplemented with 50mM NaF, 1mM Vanadate, 1mM PMSF, 10 μ g/ml TPCK and protease and phosphatase inhibitors (Roche). Protein concentration was measured using Bradford assay (Bio-Rad No. 500-006) or BCA (Thermo scientific No. 23225) and equal amounts of proteins were loaded on a SDS-polyacrylamide electrophoresis (PAGE) gel. Transfer to nitrocellulose membranes was performed using the semi-dry (Bio-Rad) blotting system or to PVDF membranes by overnight wet transfer. Membranes were next incubated overnight at 4°C with primary antibodies followed by 1 hour room temperature incubation with secondary antibodies. Fluorescent or chemiluminescent detection was performed using the LiCOR and Bio-Rad ChemiDoc Imaging systems. Protein expression levels were quantified using the ImageStudio or Image Lab software and their relative amounts with respect to tubulin were calculated. All blots were performed in three independent experiments.

4.17. Mammalian cell transduction

4.17.1. Retroviral infection

Stable K562 and Jurkat cell lines expressing TAP tagged monobodies in the pRV vector were generated by retroviral transduction. Initial transient transfection of the pRV (12 μ g) vector as well as the VSV-G cDNA (4 μ g) was performed by calcium phosphate transfection in HEK298gp cells which stably expressed the MLV gag and pol proteins required for retroviruses production. Plasmids were mixed with 330 μ l of 0.1x Tris-EDTA, 55 μ l 2.5 M CaCl₂ and with water to a total volume of 550 μ l. 550 μ l 2x Hepes Buffered Saline (HBS) were added dropwise while vortexing. Incubation at room temperature for 15 minutes followed. Transfection complexes were then added dropwise to the HEK293gp cells in 10cm dishes. Cells were incubated overnight at 37°C in 5% CO₂ and the medium was discarded and replaced with 6 ml of fresh DMEM medium on the next morning. Medium containing the viruses was recovered 24 hours later. Cell debris was cleared from the supernatant by centrifugation and sterile filtering through a 0.22 μ m filter. Target cell infection occurred following incubation with 2 μ l of polybrene for 5 minutes. 7ml of fresh DMEM medium was again added to the HEK293gp cells and the infection process was repeated a second

time 24 hours later. After incubation overnight, cells stably transfected with the pRV vector expressed the GFP protein which was contained in the vector after an IRES site, which allowed their analysis and sorting by flow cytometry.

4.17.2. Lentiviral infection

Stable expression of the monobodies in a pEM24 dox inducible vector was established in A549 cells using a lentiviral infection. The pEM24 vector encodes a blasticidin resistance gene for selection of cells which successfully integrated the desired DNA. HEK293T cells were initially used for lentiviruses production by co-transfecting plasmids containing the monobodies, the viral envelope and the packaging plasmids using a calcium phosphate protocol described above. Briefly, 11.25 µg construct DNA, 3.95 µg of the envelope plasmid and 7.3 µg packaging plasmid DNA were mixed with 330 µl 0.1x Tris-EDTA, 55 µl 2.5 M CaCl₂ and with water to a total volume of 550 µl. 550 µl 2x Hepes Buffered Saline (HBS) were added dropwise while vortexing. After incubation 15 minutes RT, the transfection complexes were added to HEK293T cells in 10 cm dishes. Cells were incubated overnight at 37°C in 5% CO₂. Similarly to the retroviral transduction protocol, the medium was discarded and replaced by 6 ml of fresh DMEM, which was itself harvested 24 hours later. The first lentiviral infection was performed after filtering of the supernatant through a 0.22 µm. 7 ml of fresh DMEM was added to the HEK293T cells and harvested on the next day for a second infection round. To ensure a successful cell transduction, infected cells were passed into new 10 cm dishes containing DMEM-blasticidin medium and selected over 7 days. A positive control consisting of un-transduced cells ensured that all uninfected cells died after 7 days of antibiotic selection. A monobody induction test upon addition of doxycycline 1 µg/ml was performed to ensure the successful expression of monobodies as determined by western blot analysis.

4.18. Monobody mammalian cell expression and flow cytometry analysis

Ba/F3 cells were washed 3 times in PBS and 10⁷ cells were electroporated with the vector coding for monobody (15 µg) under specific conditions (74 Ω, 280 V, 1500 µF) and used after 4 hours at 37°C. A549-MS3-6 and A549-Ha4YA cells, which stably expressed the monobody, were plated (10⁵ cells) in 6-well plate. The next day, cells were treated with control medium or Doxycycline (Sigma) at 1 µg/ml for 48 hours.

Cells were stimulated with control medium or with human IL-22 (500 ng/ml) or human IL-6 (100 U/ml) for 15 min at 37°C. After incubation with a viability marker (LIVE/DEAD® Fixation Near-IR Dead Cell Stain Kit, Live), cells were fixed in Paraformaldehyde 2% for 10 min at 37°C and

then permeabilized in 90% methanol for 30 min on ice. After 2 washes with PBS-EDTA 1% dFCS, cells were stained with APC labeled anti-phosphorylated STAT3-Y705 (#557815, BD Biosciences) and AF488 labeled anti-cMyc tag (2279, CST) for 1 hour at room temperature. Cells were analyzed on BD FACSVerserTM flow cytometer.

4.19. Luciferase assay

For initial screening of the monobodies inhibitory activity, U3A-Luc cells stably expressing a STAT3 luciferase reporter system obtained from the D. Frank lab (Harvard) were used. 5×10^5 cells were seeded in 6 well plates and transfected upon reaching 60-80% confluency with a pEBTetD-eGFP-monobody vector using Polyfect (QIAGEN). 1 μ g/ml doxycycline was added to induce monobody expression for 48h. Cells were next trypsinized and washed in FACS buffer (PBS, 0.5% BSA) and 8000 cells were directly sorted into 96 well plates in triplicate using a SONY sorter SH800. Cells were then incubated overnight at 37°C in 5% CO₂ in presence of doxycycline to ensure continuous monobody expression. The next morning, cells were stimulated using OSM 10ng/ml for 6 hours and luciferase activity was measured using the Bright Glo luciferase assay system (Promega) according to the manufacturer's instructions. Untransfected cells treated with 6 μ M Ruxolitinib for 7 hours at 37°C were used as positive control.

Additional Luciferase assays relied on 10⁷ BW5147 or Ba/F3 cells which were electroporated with vector coding for the monobody (7,5 μ g), pGL3-Pap1 luciferase reporter plasmid (7,5 μ g) and pRL-TK plasmid (1 μ g), as internal control of transfection, under specific conditions (74 Ω , 270 V, 1200 μ F).

4.20. Quantitative Reverse Transcription-Polymerase Chain Reaction (RT-qPCR)

Total RNA from A549 cells expressing the monobodies for 48 hours upon IL-22 (100ng/ml) stimulation (1 hour at 37°C) was isolated using TRIzol reagent (Ambion, life technologies No. 15596-026). Primers for known STAT3 downstream target genes were obtained from the Etienne Meylan lab (EPFL) and were originally purchased from ThermoFisher (TaqMan Assays). Primer sequence references are as follow: SOCS3 (Hs02330328_s1), BCL3 (Hs00180403_m1), MMP9 (Hs00234579_M1), IL-6 (Hs00985639_m1), Cldn2 (Hs00252666_s1), Actin (Hs01060665_g1) and 18S (Hs99999901_s1). Each PCR reaction contained 1 μ l of cDNA (from a RT-PCR reaction using 1000ng of total RNA) and 0.5 μ l of each 10 μ M primer mix. PCR conditions consisted in 95°C for 5 minutes followed by 35 cycles of 30 sec at 60°C. Actin and 18s were used for

normalization of signals. All RT-qPCR analyses were performed in triplicates from three independent experiments.

4.21. Tandem affinity purification and mass spectrometry

Monobodies cloned into the retroviral TAP tagged vector were used to establish Jurkat and K542 stable cell lines. Cells expressing the IRES-GFP were selected and sorted using FACS. The TAP purification consisted in the lysis of used $2\text{--}3 \times 10^9$ cells. Briefly, the elution of the protein complexes following two steps of affinity purification was performed using 0.1 M hydrochloric acid immediately followed by the neutralization using 0.5 M Triethyl ammonium bicarbonate. Samples were then boiled and 10% of the eluates were resolved by SDS-PAGE (4–20% gel; Bio-rad) and silver stained to assess the efficiency of the pull-down. The rest of the eluates were then separated by SDS-PAGE and stained with R-250Commassie Blue Solution. The entire bands were excised and digested with trypsin in order to extract peptides that were separated and analyzed by reversed-phase chromatography on a Dionex Ultimate 3000RSLC nano UPLC system (Dionex) on-line connected in line with either an Orbitrap Elite or an Orbitrap Q-Exactive Mass Spectrometer (ThermoFischer Scientific). The raw data recovered were processed using the with Proteome Discoverer (v. 1.3) and searched with Mascot against a human database and data were further analyzed using the Scaffold 3 software. In order to analyze data in an unbiased way and filter for unspecific protein contaminant such as keratin and heat shock proteins frequently found in TAPs, a selectivity score was calculated as a function of the number of experiments a given protein was detected in, as compared to the total number of TAP experiments performed. A threshold of $> 75\%$ was applied to determine the likelihood of a protein being a specific monobody interactor. This scoring permits the identification of proteins found in only $< 25\%$ of all the TAPs we performed up to date in our lab, thus allowing unspecific contaminating or highly expressed cytosolic proteins recovered from the pull down to be filtered out.

4.22. GST pull down assay

To monitor the interaction between the different GST-IL-22R mutants generated previously (Dumoutier et al. 2009) and STAT3, the proteins were produced independently in COS-7 cells. Briefly, 4×10^5 COS-7 cells plated in a 6-well plate were transiently transfected using ViaFect™ (Promega), according to the manufacturer's recommendations. Two days later, cells were lysed in 500 μ l of lysis buffer (1% Triton X-100, 10% glycerol, 10 mM Tris (pH 8), 150 mM sodium vanadate, 1 mM sodium fluoride, 5 mM EDTA, 1 mM DTT and cOmplete Protease Inhibitor Cocktail (Sigma)) and cell debris were removed by centrifugation. STAT3 was mixed with

recombinant monobody at 10 μ M for 8 hours at 4°C. Then, GST-proteins were added for 16 hours more. Purification of GST was performed using GST SpinTrap columns (GE Healthcare Life Sciences) according to the manufacturer's recommendations. Input and eluted samples were analyzed by western-blot with an anti-STAT3 antibody (12640, CST). The membranes were then reprobed with anti-GST (RPN1236V, Sigma), anti-Flag tag antibody (F1804, Sigma) anti-His tag antibody (12698, CST).

4.23. Nuclear/cytoplasmic Fractionation and Immunofluorescence (IF)

Nuclear translocation was performed upon stimulation of A549 cells for 15 minutes at 37°C with 100ng/ml of IL-6 and IL-22. Cytosolic fractions were recovered by lysing cells in cytosolic buffer (10mM HEPES pH 7.9, 10mM KCl, 0.1mM EDTA, 0.1mM EGTA supplemented with 2mM DTT, 0,4mM Na-Vanadate, 25mM Na-Fluoride, 1mM PMSF, 20 μ g/ml Leupeptin and 20U/ml Aprotinin). Following extensive washing in PBS, the nuclear pellet was recovered by centrifugation and lysed in nuclear buffer (20mM HEPES pH 7.9, 25% Glycerol, 400mM NaCl, 1mM EDTA and 1mM EGTA supplemented with 2mM DTT, 0,4mM Na-Vanadate, 25mM Na-Fluoride, 1mM PMSF, 20 μ g/ml Leupeptin and 20U/ml Aprotinin). Western blot analysis was next performed as described above. Immunofluorescence was performed using transiently transfected HEK293 cells (Polyfect Qiagen No. 301107) that expressed an inducible GFP-tagged monobody upon doxycycline treatment (1 μ g/ml) for 48 hours. Cells were stimulated with IL-6 (100ng/ml) overnight at 37°C and were fixed in 4% paraformaldehyde (PFA) for 15 minutes at room temperature. Slides were next washed with PBS containing 0.01% of Triton-X and stained for 1 hour room temperature using a primary antibody anti STAT3. Secondary antibody detection was performed using an anti-mouse 568 antibody. Dapi staining was performed for 5 minutes during the last wash. Cells were imaged with a Zeiss LSM 700 confocal microscope. HEK293 cells used for microscopy experiment attached in groups, which decreased the precision of the cellular outline definition by CellProfiler. To counteract this effect, cells were seeded at low density and random acquisition of isolated cells allowed a clearer definition of the cellular compartments. The ratio of nuclear/cytosolic STAT3 was performed with the following CellProfiler workflow: a primary object detection selected a region of interest surrounding the DAPI staining (Nucleus). Secondary object detection was performed by expansion of the GFP signal around the nucleus, which defined the cell outlines. The tertiary object corresponded to the cell outline minus the nucleus outline which defined the cytoplasm. Mean intensity of both GFP and the anti-mouse568 secondary antibody signals (STAT3) were quantified in all objects. Data were presented as a ratio of nuclear STAT3/cytoplasm

STAT3. Around 30 cells from two individual experiments were acquired and quantified. Cells whose detection failed were discarded from final analysis.

4.24. AnnexinV/7AAD Flow cytometry analysis

Stable monobody expressing cell lines of Doxycycline inducible cell lines were assessed for apoptosis induction overtime using FACS by measuring the intensity of AnnexinV and 7AAD staining. AnnexinV binding buffer was prepared according to the manufacturer's instructions (BD) by diluting the 10x stock in sterile water. The annexinV/7AAD master mix was prepared by diluting the Cy5-coupled AnnexinV (BD) 1:50 and 7AAD (BD) 1:20 in 1x AnnexinV binding buffer. Cells were harvested by centrifugation (500g, 4 minutes) and resuspended in FACS tubes for staining. Cells were washed twice with the staining buffer and resuspended in 100µl of the AnnexinV/7AAD staining solution. Incubation for 20 minutes at RT in the dark followed. Cells were analyzed using the Galios flow cytometer (BD) using the 640nm laser and a 670/14nm bandpass filter for detection of Cy5 and the 561nm laser and a 670/30nm bandpass filter for detection of 7AAD. Unstained cells, single stained and double positive (by adding a few drop of ethanol to the cells) controls were included to determine the right compensation settings for each experiments. Data analysis was performed using the FlowJo software.

4.25. Realtime-Glo cell viability kit

Realtime-Glo assay kit from Promega was used to monitor cell growth and viability overtime. Increasing number of adherent or suspension cells were initially seeded in 96 well plate and their growth was monitored up to 72 hours to determine the optimal seeding density which does not lead to over-confluency. 1500 cells were seeded followed by the addition of increasing concentrations of Ruxolitinib (0 to 20µM). Cells were mixed with a solution of the NanoLuc enzyme and the MT viability substrate in accordance to the manufacturer's protocol. Cells were incubates at 37°C in 5% CO₂. Cells viability was assessed ovetimes (after 24, 48, 72 and 96 hours) by measuring luminescence using a M5 plate reader (Molecular devices). A similar protocol was performed upon addition of doxycycline (1µg/ml) into DMEM medium containing monobodies inducible NPM-ALK 361 cells to assess their effects on cell viability overtime. Doxycycline was replaced every 2-3 days.

5. REFERENCES

1. Hanahan, D. & Weinberg, R. A. Hallmarks of Cancer: The Next Generation. *Cell* 144, 646–674 (2011).
2. Sanchez-Vega, F. *et al.* Oncogenic Signaling Pathways in The Cancer Genome Atlas. *Cell* 173, 321–337.e10 (2018).
3. Garraway, L. A. & Lander, E. S. Lessons from the Cancer Genome. *Cell* 153, 17–37 (2013).
4. Vogelstein, B. *et al.* Cancer Genome Landscapes. *Science* 339, 1546–1558 (2013).
5. Vogelstein, B. & Kinzler, K. W. Cancer genes and the pathways they control. *Nat Med* 10, 789 (2004).
6. Lawrence, M. S. *et al.* Discovery and saturation analysis of cancer genes across 21 tumour types. *Nature* 505, 495 (2014).
7. Gao, J., Ciriello, G., Sander, C. & Schultz, N. Collection, integration and analysis of cancer genomic profiles: from data to insight. *Curr Opin Genet Dev* 24, 92–98 (2014).
8. Tomlinson, P. M. I., Novelli, M. & Bodmer, W. The mutation rate and cancer. *Proc National Acad Sci* 93, 14800–14803 (1996).
9. Lawrence, M. S. *et al.* Mutational heterogeneity in cancer and the search for new cancer-associated genes. *Nature* 499, 214 (2013).
10. Alexandrov, L. *et al.* Signatures of mutational processes in human cancer. *Nature* 500, 415 (2013).
11. Lee, E. & Muller, W. J. Oncogenes and Tumor Suppressor Genes. *Cold Spring Harbor Perspectives in Biology* 2, a003236 (2010).
12. Walsh, T. & King, M.-C. Ten Genes for Inherited Breast Cancer. *Cancer Cell* 11, 103–105 (2007).
13. Holstege, H. *et al.* High Incidence of Protein-Truncating TP53 Mutations in BRCA1-Related Breast Cancer. *Cancer Res* 69, 3625–3633 (2009).
14. Saal, L. H. *et al.* Recurrent gross mutations of the PTEN tumor suppressor gene in breast cancers with deficient DSB repair. *Nat Genet* 40, 102–107 (2007).
15. Thien, C. B. & Langdon, W. Y. Cbl: many adaptations to regulate protein tyrosine kinases. *Nature Reviews Molecular Cell Biology* 2, 294 (2001).
16. Blume-Jensen, P. & Nature, H. T. Oncogenic kinase signalling. (2001).
17. Bhagwat, A. S. & Vakoc, C. R. Targeting Transcription Factors in Cancer. *Trends Cancer* 1, 53–65
18. Gr, ori, C., Cowley, S. M., James, L. P. & Eisenman, R. N. THE MYC/MAX/MAD NETWORK AND THE TRANSCRIPTIONAL CONTROL OF CELL BEHAVIOR. *Annu Rev Cell Dev Bi* 16, 653–699 (2000).
19. Bromberg, J. F. *et al.* Stat3 as an oncogene. 98, 295–303 (1999).
20. Levy, D. E. & Darnell, J. STATs: transcriptional control and biological impact. *Nat Rev Mol Cell Bio* 3, 651–662 (2002).
21. Brivanlou, A. & Science, D. J. Signal transduction and the control of gene expression. (2002). doi:10.1126/science.1066355
22. Inukai, S., Kock, K. & Bulyk, M. L.

Transcription factor–DNA binding: beyond binding site motifs. *Current Opinion in Genetics & Development* 43, 110–119 (2017).

23. Rehemtulla, A. *et al.* The basic motif-leucine zipper transcription factor Nrl can positively regulate rhodopsin gene expression. *Proc National Acad Sci* 93, 191–195 (1996).

24. Wang, Z., Malone, M. H., He, H., McColl, K. S. & Distelhorst, C. W. Microarray Analysis Uncovers the Induction of the Proapoptotic BH3-only Protein Bim in Multiple Models of Glucocorticoid-induced Apoptosis. *Journal of Biological Chemistry* 278, 23861–23867 (2003).

25. Abrams, M. T., Robertson, N. M., Yoon, K. & Wickstrom, E. Inhibition of Glucocorticoid-induced Apoptosis by Targeting the Major Splice Variants of BIM mRNA with Small Interfering RNA and Short Hairpin RNA. *Journal of Biological Chemistry* 279, 55809–55817 (2004).

26. Darnell, J. E. Transcription factors as targets for cancer therapy. *Nature Reviews Cancer* 2, 740–749 (2002).

27. Dang, C., Resar, L., Emison, E., Kim, S. & Li, Q. Function of the c-Myc oncogenic transcription factor. *Experimental cell ...* (1999).

28. Whitfield, J. R., Beaulieu, M.-E. & Soucek, L. Strategies to Inhibit Myc and Their Clinical Applicability. *Frontiers Cell Dev Biology* 5, 10 (2017).

29. Lu, B. *et al.* A Transcription Factor Addiction in Leukemia Imposed by the MLL Promoter Sequence. *Cancer Cell* 34, 970–981.e8 (2018).

30. Bradner, J. E., Hnisz, D. & Young, R. A. Transcriptional Addiction in Cancer. *Cell* 168, 629–643 (2017).

31. Spivakov, M. Spurious transcription factor binding: Non-functional or genetically redundant? *BioEssays* 36, 798–806 (2014).

32. Yeh, J. E., Toniolo, P. A. & Frank, D. A. Targeting transcription factors: promising new strategies for cancer therapy. *Curr Opin Oncol* 25, 652 (2013).

33. Frank, D. A. Targeting transcription factors for cancer therapy. *Idrugs Investigational Drugs J* 12, 29–33 (2009).

34. Bushweller, J. H. Targeting transcription factors in cancer — from undruggable to reality. *Nature Reviews Cancer* 1–14 (2019). doi:10.1038/s41568-019-0196-7

35. Padma, V. An overview of targeted cancer therapy. *BioMedicine* 5, 19 (2015).

36. Xu, G. & McLeod, H. Strategies for enzyme/prodrug cancer therapy. *Clin Cancer Res Official J Am Assoc Cancer Res* 7, 3314–24 (2001).

37. Whitfield, M. L. *et al.* Identification of Genes Periodically Expressed in the Human Cell Cycle and Their Expression in Tumors. *Mol Biol Cell* 13, 1977–2000 (2002).

38. Youn, A. & Simon, R. Identifying cancer driver genes in tumor genome sequencing studies. *Bioinformatics* 27, 175–181 (2011).

39. Luo, J., Solimini, N. & Elledge, S. Principles of cancer therapy: oncogene and non-oncogene addiction. *Cell* (2009).

40. Prober, D. & Edgar. Growth regulation by oncogenes—new insights from model organisms. *Current opinion in genetics & development* (2001).

41. Gerber, D. E. Targeted therapies: a new generation of cancer treatments. *Am Fam Physician* 77, 311–9 (2008).

42. Sliwkowski, M. X. & Mellman, I. Antibody Therapeutics in Cancer. *Science* 341, 1192–1198 (2013).

43. Hantschel, O. Unexpected Off-Targets and Paradoxical Pathway Activation by Kinase Inhibitors. *Acs Chem Biol* 10, 234–245 (2015).

44. Verdine, G. L. & Walensky, L. D. The Challenge of Drugging Undruggable Targets in Cancer: Lessons Learned from Targeting BCL-2 Family Members. *Clin Cancer Res* 13, 7264–7270 (2007).

45. Slastnikova, T. A., Ulasov, A.,

- Rosenkranz, A. & Sobolev, A. Targeted Intracellular Delivery of Antibodies: The State of the Art. *Front Pharmacol* 9, 1208 (2018).
46. Russ, A. P. & Lampel, S. The druggable genome: an update. *Drug Discov Today* 10, 1607–1610 (2005).
47. Hopkins, A. L. & Groom, C. R. The druggable genome. *Nat Rev Drug Discov* 1, nrd892 (2002).
48. Hopkins, A. & Groom, C. Target analysis: a priori assessment of druggability. *E Schering Res Fdn W* 11–7 (2003).
49. Hantschel, O. Monobodies as possible next-generation protein therapeutics – a perspective. *Swiss Med Wkly* 147, w14545 (2017).
50. Hantschel, O., Rix, U. & Superti-Furga, G. Target spectrum of the BCR-ABL inhibitors imatinib, nilotinib and dasatinib. *Leukemia Lymphoma* 49, 615–619 (2009).
51. Palve, V., Kuenzi, B. M. & Rix, U. Unraveling the rewired network. *Nat Chem Biol* 14, 746–747 (2018).
52. Makley, L. N. & Gestwicki, J. E. Expanding the Number of ‘Druggable’ Targets: Non-Enzymes and Protein–Protein Interactions. *Chem Biology Drug Des* 81, 22–32 (2013).
53. Koide, A., Bailey, C. W., Huang, X. & Koide, S. The fibronectin type III domain as a scaffold for novel binding proteins | Edited by J. Wells. *J Mol Biol* 284, 1141–1151 (1998).
54. Koide, A., Wojcik, J., Gilbreth, R. N., Hoey, R. J. & Koide, S. Teaching an Old Scaffold New Tricks: Monobodies Constructed Using Alternative Surfaces of the FN3 Scaffold. *J Mol Biol* 415, 393–405 (2012).
55. Sha, F., Salzman, G., Gupta, A. & Koide, S. Monobodies and Other Synthetic Binding Proteins for Expanding Protein Science. *Protein Sci* 26, 910–924 (2017).
56. Wojcik, J. *et al.* A potent and highly specific FN3 monobody inhibitor of the Abl SH2 domain. *Nat Struct Mol Biology* 17, 519–527 (2010).
57. Grebien, F. *et al.* Targeting the SH2-Kinase Interface in Bcr-Abl Inhibits Leukemogenesis. *Cell* 147, 306–319 (2011).
58. Wojcik, J. *et al.* Allosteric Inhibition of Bcr-Abl Kinase by High Affinity Monobody Inhibitors Directed to the Src Homology 2 (SH2)-Kinase Interface. *J Biol Chem* 291, 8836–8847 (2016).
59. Sha, F. *et al.* Dissection of the BCR-ABL signaling network using highly specific monobody inhibitors to the SHP2 SH2 domains. *Proc National Acad Sci* 110, 14924–14929 (2013).
60. Kükenshöner, T. *et al.* Selective Targeting of SH2 Domain–Phosphotyrosine Interactions of Src Family Tyrosine Kinases with Monobodies. *J Mol Biol* 429, 1364–1380 (2017).
61. Schmit, N., Neopane, K. & Hantschel, O. Targeted protein degradation through cytosolic delivery of monobody binders using bacterial toxins. *ACS Chemical Biology* (2019). doi:10.1021/acscchembio.9b00113
62. Spencer-Smith, R. *et al.* Inhibition of RAS function through targeting an allosteric regulatory site. *Nat Chem Biol* 13, 62–68 (2016).
63. Sikorski, T. W. & Buratowski, S. The basal initiation machinery: beyond the general transcription factors. *Curr Opin Cell Biol* 21, 344–351 (2009).
64. Sakamoto, K. M. *et al.* Protacs: Chimeric molecules that target proteins to the Skp1–Cullin–F box complex for ubiquitination and degradation. *Proc National Acad Sci* 98, 8554–8559 (2001).
65. An, S. & Fu, L. Small-molecule PROTACs: An emerging and promising approach for the development of targeted therapy drugs. *Ebiomedicine* 36, 553–562 (2018).
66. Schneekloth, S. *et al.* Chemical Genetic Control of Protein Levels: Selective in Vivo Targeted Degradation. *J Am Chem Soc* 126, 3748–3754 (2004).

67. Ohh, M. *et al.* Ubiquitination of hypoxia-inducible factor requires direct binding to the β -domain of the von Hippel–Lindau protein. *Nat Cell Biol* 2, ncb0700_423 (2000).
68. Lee, T. & Young, R. A. Transcriptional Regulation and Its Misregulation in Disease. *Cell* 152, 1237–1251 (2013).
69. Tisato, V., Voltan, R., Gonelli, A., Secchiero, P. & Zauli, G. MDM2/X inhibitors under clinical evaluation: perspectives for the management of hematological malignancies and pediatric cancer. *Journal of Hematology & Oncology* 10, 133 (2017).
70. Brennan, P., Donev, R. & Hewamana, S. Targeting transcription factors for therapeutic benefit. *Molecular BioSystems* 4, 909–919 (2008).
71. Hagenbuchner, J. & Ausserlechner, M. J. Targeting transcription factors by small compounds—Current strategies and future implications. *Biochem Pharmacol* 107, 1–13 (2016).
72. Turkson, J. & Jove, R. STAT proteins: novel molecular targets for cancer drug discovery. *Oncogene* (2000).
73. Siddiquee, K., Zhang, S. & of the ..., G. W. Selective chemical probe inhibitor of Stat3, identified through structure-based virtual screening, induces antitumor activity. (2007). doi:10.1073/pnas.0609757104
74. Schindler, C., Levy, D. & of Chemistry, D. T. JAK-STAT signaling: from interferons to cytokines. (2007). doi:10.1074/jbc.R700016200
75. Iwamoto, K. *et al.* Inhibition of STAT3 by Anticancer Drug Bendamustine. *PLoS ONE* 12, e0170709 (2017).
76. Buettner, R., Mora, L. B. & Jove, R. Activated STAT signaling in human tumors provides novel molecular targets for therapeutic intervention. *Clinical cancer research : an official journal of the American Association for Cancer Research* 8, 945–54 (2002).
77. Haura, E. B., Turkson, J. & Jove, R. Mechanisms of Disease: insights into the emerging role of signal transducers and activators of transcription in cancer. *Nat Clin Pract Oncol* 2, 315–324 (2005).
78. Miklossy, G., Hilliard, T. S. & Turkson, J. Therapeutic modulators of STAT signalling for human diseases. *Nat Rev Drug Discov* 12, 611–629 (2013).
79. Meraz, M. A. *et al.* Targeted Disruption of the Stat1 Gene in Mice Reveals Unexpected Physiologic Specificity in the JAK–STAT Signaling Pathway. *Cell* 84, 431–442 (1996).
80. Gamero, A. M. *et al.* STAT2 Contributes to Promotion of Colorectal and Skin Carcinogenesis. *Cancer Prev Res* 3, 495–504 (2010).
81. Szabo, S. J., Sullivan, B. M., Peng, S. L. & Glimcher, L. H. MOLECULAR MECHANISMS REGULATING TH1 IMMUNE RESPONSES. *Annu Rev Immunol* 21, 713–758 (2003).
82. Lovett-Racke, A. E., Yang, Y. & Racke, M. K. Th1 versus Th17: Are T cell cytokines relevant in multiple sclerosis? *Biochimica Et Biophysica Acta Bba - Mol Basis Dis* 1812, 246–251 (2011).
83. Nelson, E. A. *et al.* Nifuroxazide inhibits survival of multiple myeloma cells by directly inhibiting STAT3. 112, 5095–5102
84. Yu, H. & Cancer, J. R. The STATs of cancer—new molecular targets come of age. (2004).
85. Sgrignani, J., Garofalo, M., Matkovic, M. & journal of ..., M. J. Structural biology of STAT3 and its implications for anticancer therapies development. (2018).
86. Belo, Y. *et al.* Unexpected implications of STAT3 acetylation revealed by genetic encoding of acetyl-lysine. *Biochimica Et Biophysica Acta Bba - Gen Subj* 1863, 1343–1350 (2019).
87. Ren, Z. *et al.* Crystal structure of unphosphorylated STAT3 core fragment. *Biochem Bioph Res Co* 374, 1–5 (2008).
88. Becker, S., Groner, B. & Müller, C. W.

- Three-dimensional structure of the Stat3 β homodimer bound to DNA. *Nature* 394, 145–151 (1998).
89. Nkansah, E. *et al.* Observation of unphosphorylated STAT3 core protein binding to target dsDNA by PEMS and X-ray crystallography. *Febs Lett* 587, 833–839 (2013).
90. Hu, T. *et al.* Impact of the N-Terminal Domain of STAT3 in STAT3-Dependent Transcriptional Activity. *Mol Cell Biol* 35, 3284–3300
91. Bai, L. *et al.* A Potent and Selective Small-Molecule Degradator of STAT3 Achieves Complete Tumor Regression In Vivo. *Cancer Cell* 36, 498–511.e17 (2019).
92. Chen, X. *et al.* Crystal Structure of a Tyrosine Phosphorylated STAT-1 Dimer Bound to DNA. *Cell* 93, 827–839 (1998).
93. Neculai, D. *et al.* Structure of the Unphosphorylated STAT5a Dimer. *J Biol Chem* 280, 40782–40787 (2005).
94. Zhong, M. *et al.* Implications of an antiparallel dimeric structure of nonphosphorylated STAT1 for the activation–inactivation cycle. *P Natl Acad Sci Usa* 102, 3966–3971 (2005).
95. Braunstein, J., Brutsaert, S., Olson, R. & Schindler, C. STATs Dimerize in the Absence of Phosphorylation. *J Biol Chem* 278, 34133–34140 (2003).
96. Timofeeva, O., Chasovskikh, S. & of Biological ..., L. I. Mechanisms of unphosphorylated STAT3 transcription factor binding to DNA. (2012). doi:10.1074/jbc.M111.323899
97. KRETZSCHMAR, A. K., DINGER, M. C., HENZE, C., BROCKE-HEIDRICH, K. & Friedemann, H. Analysis of Stat3 (signal transducer and activator of transcription 3) dimerization by fluorescence resonance energy transfer in living cells. *Biochem J* 377, 289–297 (2004).
98. O’Shea, J. J., Kanno, Y., Chen, X. & Levy, D. E. Stat Acetylation--A Key Facet of Cytokine Signaling? *Science* 307, 217–218 (2005).
99. Miranda, C., Fumagalli, T., Anania, M. & PLoS ..., V. M. Role of STAT3 in in vitro transformation triggered by TRK oncogenes. (2010).
100. of clinical investigation, B. J. Stat proteins and oncogenesis. (2002).
101. Yuan, J., Zhang, F. & reports, N. R. Multiple regulation pathways and pivotal biological functions of STAT3 in cancer. (2015).
102. of Immunology, M. P. The JAK-STAT signaling pathway: input and output integration. *The Journal of Immunology* doi:10.4049/jimmunol.178.5.2623
103. Bollrath, J., Phesse, T., von Burstin, V. & cell, P. T. gp130-mediated Stat3 activation in enterocytes regulates cell survival and cell-cycle progression during colitis-associated tumorigenesis. (2009).
104. Yu, H., Lee, H., Herrmann, A., Buettner, R. & reviews Cancer, J. R. Revisiting STAT3 signalling in cancer: new and unexpected biological functions. (2014).
105. Huynh, J., Chand, A., Gough, D. & Ernst, M. Therapeutically exploiting STAT3 activity in cancer — using tissue repair as a road map. *Nature Reviews Cancer* 19, 1 (2018).
106. Takeda, K., Noguchi, K. & of the ..., S. W. Targeted disruption of the mouse Stat3 gene leads to early embryonic lethality. (1997). doi:10.1073/pnas.94.8.3801
107. O’Shea, J. J. *et al.* The JAK-STAT pathway: impact on human disease and therapeutic intervention. *Annual review of medicine* 66, 311–328 (2015).
108. Fornek, J., Tygrett, L., Waldschmidt, T. & Blood, P. V. Critical role for Stat3 in T-dependent terminal differentiation of IgG B cells. (2006).
109. Harris, T., Grosso, J., Yen, H. & of ..., X. H. Cutting edge: An in vivo requirement for STAT3 signaling in TH17 development and TH17-dependent autoimmunity. (2007). doi:10.4049/jimmunol.179.7.4313

110. Kortylewski, M., Kujawski, M., Wang, T., Wei, S. & medicine, Z. S. Inhibiting Stat3 signaling in the hematopoietic system elicits multicomponent antitumor immunity. (2005).
111. Nefedova, Y., Huang, M. & of ..., K. S. Hyperactivation of STAT3 is involved in abnormal differentiation of dendritic cells in cancer. (2004).
doi:10.4049/jimmunol.172.1.464
112. Nishihara, M., Ogura, H. & International ..., U. N. IL-6-gp130-STAT3 in T cells directs the development of IL-17+ Th with a minimum effect on that of Treg in the steady state. (2007).
doi:10.1093/intimm/dxm045
113. Wang, T., Niu, G., Kortylewski, M., Burdelya, L. & medicine, S. K. Regulation of the innate and adaptive immune responses by Stat-3 signaling in tumor cells. (2004).
114. Theurich, S., Tsaousidou, E., Hanssen, R. & metabolism, L. A. IL-6/Stat3-dependent induction of a distinct, obesity-associated NK cell subpopulation deteriorates energy and glucose homeostasis. (2017).
115. Zhang, H.-F. & Lai, R. STAT3 in Cancer—Friend or Foe? *Cancers* 6, 1408–1440 (2014).
116. Dewilde, S., Vercelli, A., Chiarle, R. & Poli, V. Of alphas and betas: distinct and overlapping functions of STAT3 isoforms. *Frontiers in bioscience : a journal and virtual library* 13, 6501–14 (2008).
117. Maritano, D., Sugrue, M., Tininini, S. & Nature ..., D. S. The STAT3 isoforms α and β have unique and specific functions. (2004).
118. Yoo, J., Huso, D., Nathans, D. & Cell, D. S. Specific ablation of Stat3 β distorts the pattern of Stat3-responsive gene expression and impairs recovery from endotoxic shock. (2002).
119. Caldenhoven, E. *et al.* STAT3beta, a splice variant of transcription factor STAT3, is a dominant negative regulator of transcription. *The Journal of biological chemistry* 271, 13221–7 (1996).
120. Lee, J., Baldwin, W. M., Lee, C.-Y. Y. & Desiderio, S. Stat3 β mitigates development of atherosclerosis in apolipoprotein E-deficient mice. *Journal of molecular medicine (Berlin, Germany)* 91, 965–76 (2013).
121. Alvarez, J. & biology therapy, F. D. Genome-wide analysis of STAT target genes: elucidating the mechanism of STAT-mediated oncogenesis. (2004).
doi:10.4161/cbt.3.11.1172
122. Vallania, F. *et al.* Genome-wide discovery of functional transcription factor binding sites by comparative genomics: the case of Stat3. *Proceedings of the National Academy of Sciences of the United States of America* 106, 5117–22 (2009).
123. Yeh, J. E. & Frank, D. A. STAT3-Interacting Proteins as Modulators of Transcription Factor Function: Implications to Targeted Cancer Therapy. *ChemMedChem* 11, 795–801 (2016).
124. Laudisi, F., Cherubini, F., Monteleone, G. & Stolfi, C. STAT3 Interactors as Potential Therapeutic Targets for Cancer Treatment. *Int J Mol Sci* 19, 1787 (2018).
125. Ndubuisi, M., Guo, G., Fried, V. & of Biological ..., E. J. Cellular physiology of STAT3: where's the cytoplasmic monomer? (1999). doi:10.1074/jbc.274.36.25499
126. Avalue, L., Camporeale, A. & death and ..., M. G. STAT3 localizes to the ER, acting as a gatekeeper for ER-mitochondrion Ca²⁺ fluxes and apoptotic responses. (2019).
127. ah, Patel, K., Mukhopadhyay, S., Xu, F. & of Biological ..., G. G. Membrane-associated STAT3 and PY-STAT3 in the cytoplasm. (2006).
doi:10.1074/jbc.M508527200
128. Shen, S., Niso-Santano, M., Adjemian, S. & cell, T. T. Cytoplasmic STAT3 represses autophagy by inhibiting PKR activity. (2012).
129. Silver, D., Naora, H., Liu, J., Cheng, W. & research, M. D. Activated signal transducer and activator of transcription (STAT) 3: localization in focal adhesions and function in ovarian cancer cell motility. (2004).
doi:10.1158/0008-5472.CAN-03-3959

130. Wegrzyn, J., Potla, R., Chwae, Y. & ... N. Function of mitochondrial Stat3 in cellular respiration. (2009).
doi:10.1126/science.1164551
131. You, L. *et al.* The role of STAT3 in autophagy. (2015).
doi:10.1080/15548627.2015.1017192
132. Gao, S. & STKE, B. J. Touched and moved by STAT3. (2006).
doi:10.1126/stke.3432006pe30
133. Ng, D. *et al.* Stat3 regulates microtubules by antagonizing the depolymerization activity of stathmin. (2006).
doi:10.1083/jcb.200503021
134. Calon, A., Espinet, E., Palomo-Ponce, S. & cell, D. Dependency of colorectal cancer on a TGF- β -driven program in stromal cells for metastasis initiation. (2012).
135. Aznar, S., Valeron, P. & del biology of ..., R. S. Simultaneous tyrosine and serine phosphorylation of STAT3 transcription factor is involved in Rho A GTPase oncogenic transformation. (2001).
136. Gough, D. J. *et al.* Mitochondrial STAT3 supports Ras-dependent oncogenic transformation. *Science (New York, N.Y.)* 324, 1713–6 (2009).
137. Macias, E., Rao, D., Carbajal, S. & of Investigative ..., K. K. Stat3 binds to mtDNA and regulates mitochondrial gene expression in keratinocytes. (2014).
138. Ziegler, P., Bollrath, J., Pallangyo, C. & Cell, M. T. Mitophagy in intestinal epithelial cells triggers adaptive immunity during tumorigenesis. (2018).
139. Heiden, V. M., Cantley, L. & science, T. C. Understanding the Warburg effect: the metabolic requirements of cell proliferation. (2009). doi:10.1126/science.1160809
140. maria, Giorgi, C., Miano, V. & Congress ..., M. S. A stat3-mediated metabolic switch is involved in tumour transformation and stat3 addiction. (2011).
141. Phillips, D., Reilley, M., Aponte, A. & of Biological ..., W. G. Stoichiometry of STAT3 and Mitochondrial Proteins IMPLICATIONS FOR THE REGULATION OF OXIDATIVE PHOSPHORYLATION BY PROTEIN-PROTEIN (2010).
doi:10.1074/jbc.C110.152652
142. maria *et al.* STAT3 can serve as a hit in the process of malignant transformation of primary cells. *Cell Death and Differentiation* 19, 1390 (2012).
143. Linher-Melville, K. & and cellular endocrinology, S. G. The complex roles of STAT3 and STAT5 in maintaining redox balance: Lessons from STAT-mediated xCT expression in cancer cells. (2017).
144. Sobotta, M., Liou, W., Stöcker, S. & chemical ..., T. D. Peroxiredoxin-2 and STAT3 form a redox relay for H₂O₂ signaling. (2015).
145. Simon, A., Rai, U. & of ..., F. B. Activation of the JAK-STAT pathway by reactive oxygen species. (1998).
doi:10.1152/ajpcell.1998.275.6.C1640
146. Li, L., Cheung, S., Evans, E. & research, S. P. Modulation of gene expression and tumor cell growth by redox modification of STAT3. (2010). doi:10.1158/0008-5472.CAN-10-0894
147. Yuan, Z., Guan, Y., Chatterjee, D. & Science, C. Y. Stat3 dimerization regulated by reversible acetylation of a single lysine residue. (2005). doi:10.1126/science.1105166
148. Lee, H., Zhang, P., Herrmann, A. & of the ..., Y. C. Acetylated STAT3 is crucial for methylation of tumor-suppressor gene promoters and inhibition by resveratrol results in demethylation. (2012).
doi:10.1073/pnas.1205132109
149. Xu, Y. *et al.* STAT3 undergoes acetylation-dependent mitochondrial translocation to regulate pyruvate metabolism. (2016).
150. Nie, Y. *et al.* STAT3 inhibition of gluconeogenesis is downregulated by SirT1. *Nature cell biology* 11, 492–500 (2009).
151. Bernier, M. *et al.* Negative regulation of STAT3 protein-mediated cellular respiration

- by SIRT1 protein. *The Journal of biological chemistry* 286, 19270–9 (2011).
152. Yang, J., Huang, J. & of the ..., D. M. Reversible methylation of promoter-bound STAT3 by histone-modifying enzymes. (2010).
 153. Kim, E. *et al.* Phosphorylation of EZH2 activates STAT3 signaling via STAT3 methylation and promotes tumorigenicity of glioblastoma stem-like cells. (2013).
 154. Iliopoulos, D., Hirsch, H. A. & Struhl, K. An epigenetic switch involving NF-kappaB, Lin28, Let-7 MicroRNA, and IL6 links inflammation to cell transformation. *Cell* 139, 693–706 (2009).
 155. Ambrogio, C., Martinengo, C., Voena, C., Tondat, F. & research, R. L. NPM-ALK oncogenic tyrosine kinase controls T-cell identity by transcriptional regulation and epigenetic silencing in lymphoma cells. (2009). doi:10.1158/0008-5472.CAN-09-2655
 156. Wu, J. *et al.* Kaposi's sarcoma-associated herpesvirus (KSHV) vIL-6 promotes cell proliferation and migration by upregulating DNMT1 via STAT3 activation. (2014). doi:10.1371/journal.pone.0093478
 157. Li, J., Cui, G., Sun, L., Wang, S. & Oncology ..., L. Y. STAT3 acetylation-induced promoter methylation is associated with downregulation of the ARHI tumor-suppressor gene in ovarian cancer. (2013).
 158. Buettner, R., Mora, L. & cancer research, J. R. Activated STAT signaling in human tumors provides novel molecular targets for therapeutic intervention. *Clinical cancer research* (2002).
 159. Kujawski, M. *et al.* Stat3 mediates myeloid cell-dependent tumor angiogenesis in mice. *The Journal of clinical investigation* 118, 3367–77 (2008).
 160. Kortylewski, M. & Yu, H. Role of Stat3 in suppressing anti-tumor immunity. *Current opinion in immunology* 20, 228–33 (2008).
 161. Herrmann, A. *et al.* Targeting Stat3 in the myeloid compartment drastically improves the in vivo antitumor functions of adoptively transferred T cells. *Cancer research* 70, 7455–64 (2010).
 162. Grivennikov, S., Karin, E., Terzic, J., Mucida, D. & cell, Y. G. IL-6 and Stat3 are required for survival of intestinal epithelial cells and development of colitis-associated cancer. (2009).
 163. Sano, S., Itami, S., Takeda, K. & EO ..., T. M. Keratinocyte-specific ablation of Stat3 exhibits impaired skin remodeling, but does not affect skin morphogenesis. (1999).
 164. Arwert, E., Hoste, E. & Cancer, W. F. Epithelial stem cells, wound healing and cancer. (2012).
 165. Cassetta, L. & Discovery, P. J. Targeting macrophages: therapeutic approaches in cancer. (2018).
 166. Jarnicki, A., Putoczki, T. & division, E. M. Stat3: linking inflammation to epithelial cancer-more than a "gut" feeling? (2010).
 167. Phesse, T., Buchert, M., Stuart, E. & Signal ..., F. D. Partial inhibition of gp130-Jak-Stat3 signaling prevents Wnt- β -catenin-mediated intestinal tumor growth and regeneration. (2014). doi:10.1126/scisignal.2005411
 168. Ernst, M., Najdovska, M. & of ..., G. D. STAT3 and STAT1 mediate IL-11-dependent and inflammation-associated gastric tumorigenesis in gp130 receptor mutant mice. (2008). doi:10.1172/JCI34944
 169. Putoczki, T. & of leukocyte biology, E. M. More than a sidekick: the IL-6 family cytokine IL-11 links inflammation to cancer. (2010).
 170. Reynaud, D., Pietras, E., Barry-Holson, K. & cell, M. A. IL-6 controls leukemic multipotent progenitor cell fate and contributes to chronic myelogenous leukemia development. (2011).
 171. crile, Lim, K. & development, C. C. Oncogenic Ras-induced secretion of IL6 is required for tumorigenesis. (2007). doi:10.1101/gad.1549407
 172. Corcoran, R., Contino, G., Deshpande, V.

- & research, T. A. STAT3 plays a critical role in KRAS-induced pancreatic tumorigenesis. (2011). doi:10.1158/0008-5472.CAN-11-0908
173. Liu, S., Tsang, N. & of ..., C. W. Leukemia inhibitory factor promotes nasopharyngeal carcinoma progression and radioresistance. (2013). doi:10.1172/JCI63428
174. Peñuelas, S., Anido, J., Prieto-Sánchez, R. & cell, F. G. TGF- β increases glioma-initiating cell self-renewal through the induction of LIF in human glioblastoma. (2009).
175. Schroeder, A. *et al.* Loss of androgen receptor expression promotes a stem-like cell phenotype in prostate cancer through STAT3 signaling. *Cancer research* 74, 1227–37 (2014).
176. Marotta, L. L. *et al.* The JAK2/STAT3 signaling pathway is required for growth of CD44⁺CD24⁻ stem cell-like breast cancer cells in human tumors. *The Journal of clinical investigation* 121, 2723–35 (2011).
177. Deng, J. *et al.* S1PR1-STAT3 signaling is crucial for myeloid cell colonization at future metastatic sites. (2012).
178. Zhang, W., Pal, S., Liu, X., Yang, C. & one, A. S. Myeloid clusters are associated with a pro-metastatic environment and poor prognosis in smoking-related early stage non-small cell lung cancer. (2013). doi:10.1371/journal.pone.0065121
179. Visvader, J. & reviews cancer, L. G. Cancer stem cells in solid tumours: accumulating evidence and unresolved questions. (2008).
180. Merry, Reeves, A., Wu, J. & cells, C. B. STAT3 is required for proliferation and maintenance of multipotency in glioblastoma stem cells. (2009). doi:10.1002/stem.185
181. Guryanova, O., Wu, Q., Cheng, L., Lathia, J. & cell, H. Z. Nonreceptor tyrosine kinase BMX maintains self-renewal and tumorigenic potential of glioblastoma stem cells by activating STAT3. (2011).
182. Bromberg, J. F., Horvath, C. M., Besser, D., Lathem, W. W. & Darnell, J. E. Stat3 Activation Is Required for Cellular Transformation by v-src. *Molecular and Cellular Biology* 18, 2553–2558 (1998).
183. Avalle, L., Camporeale, A., Camperi, A. & Cytokine, P. V. STAT3 in cancer: A double edged sword. (2017).
184. Pencik, J. *et al.* JAK-STAT signaling in cancer: From cytokines to non-coding genome. 87, 26–36
185. Constantinescu, S., Girardot, M. & Pecquet, C. Mining for JAK–STAT mutations in cancer. *Trends in biochemical ...* (2008).
186. Fasan, A. *et al.* STAT3 mutations are highly specific for large granular lymphocytic leukemia. *Leukemia* 27, 1598 (2013).
187. Kristensen, T. *et al.* Clinical Relevance of Sensitive and Quantitative STAT3 Mutation Analysis Using Next-Generation Sequencing in T-Cell Large Granular Lymphocytic Leukemia. *J Mol Diagnostics* 16, 382–392 (2014).
188. Koskela, H. *et al.* Somatic STAT3 Mutations in Large Granular Lymphocytic Leukemia. *New Engl J Medicine* 366, 1905–1913 (2012).
189. Morgan, E., Lee, M. & Blood ..., D. D. Systematic STAT3 sequencing in patients with unexplained cytopenias identifies unsuspected large granular lymphocytic leukemia. (2017).
190. de la Iglesia, N. *et al.* Identification of a PTEN-regulated STAT3 brain tumor suppressor pathway. *Gene Dev* 22, 449–462 (2008).
191. Schneller, D. *et al.* p19ARF/p14ARF controls oncogenic functions of signal transducer and activator of transcription 3 in hepatocellular carcinoma. *Hepatology* 54, 164–172 (2011).
192. Wang, H. *et al.* Hepatoprotective versus Oncogenic Functions of STAT3 in Liver Tumorigenesis. *Am J Pathology* 179, 714–724 (2011).
193. Musteanu, M. *et al.* Stat3 Is a Negative Regulator of Intestinal Tumor Progression in Apc Min Mice. *Gastroenterology* 138, 1003–

1011.e5 (2010).

194. Laklai, H., Miroshnikova, Y., Pickup, M. & medicine, C. E. Genotype tunes pancreatic ductal adenocarcinoma tissue tension to induce matricellular fibrosis and tumor progression. (2016).

195. Yu, H., Pardoll, D. & reviews cancer, J. R. STATs in cancer inflammation and immunity: a leading role for STAT3. (2009).

196. Xu, D. & in a journal and virtual library, Q. C. Protein tyrosine phosphatases in the JAK/STAT pathway. (2008).

197. Peyser, N. *et al.* Loss-of-function PTPRD mutations lead to increased STAT3 activation and sensitivity to STAT3 inhibition in head and neck cancer. (2015).
doi:10.1371/journal.pone.0135750

198. Kim, D., Tremblay, M. & one, D. J. Protein tyrosine phosphatases, TC-PTP, SHP1, and SHP2, cooperate in rapid dephosphorylation of Stat3 in keratinocytes following UVB irradiation. (2010).
doi:10.1371/journal.pone.0010290

199. Babon, J., Varghese, L. & in immunology, N. N. Inhibition of IL-6 family cytokines by SOCS3. (2014).

200. Krebs, D. & cells, H. D. SOCS proteins: negative regulators of cytokine signaling. (2001). doi:10.1634/stemcells.19-5-378

201. Chung, C. *et al.* Specific inhibition of Stat3 signal transduction by PIAS3. *Science (New York, N.Y.)* 278, 1803–5 (1997).

202. Ma, J. & signalling, C. X. Regulation of Stat3 nuclear import by importin $\alpha 5$ and importin $\alpha 7$ via two different functional sequence elements. (2006).

203. Cimica, V., Chen, H.-C., Iyer, J. K. & Reich, N. C. Dynamics of the STAT3 Transcription Factor: Nuclear Import Dependent on Ran and Importin- $\beta 1$. *Plos One* 6, e20188 (2011).

204. Petrucci, M. *et al.* Cell cycle regulation and induction of apoptosis by IL-6 variants on the multiple myeloma cell line XG-1. *Ann Hematol* 78, 13–18 (1999).

205. von Minckwitz, G. *et al.* Phase I clinical study of the recombinant antibody toxin scFv(FRP5)-ETA specific for the ErbB2/HER2 receptor in patients with advanced solid malignomas. *Breast Cancer Res* 7, R617 (2005).

206. Gadina, M. *et al.* Translational and clinical advances in JAK-STAT biology: The present and future of jakinibs. *J. Leukoc. Biol.* doi:10.1002/JLB.5RI0218-084R

207. Shuai, K. Modulation of STAT signaling by STAT-interacting proteins. *Oncogene* 19, 1203522 (2000).

208. Turkson, J. *et al.* Phosphotyrosyl Peptides Block Stat3-mediated DNA Binding Activity, Gene Regulation, and Cell Transformation. *J Biol Chem* 276, 45443–45455 (2001).

209. Song, H., Wang, R., Wang, S. & Lin, J. A low-molecular-weight compound discovered through virtual database screening inhibits Stat3 function in breast cancer cells. *P Natl Acad Sci Usa* 102, 4700–4705 (2005).

210. Schust, J., Sperl, B., Hollis, A., Mayer, T. U. & Berg, T. Stattic: A Small-Molecule Inhibitor of STAT3 Activation and Dimerization. *Chem Biol* 13, 1235–1242 (2006).

211. Zhang, X. *et al.* Orally bioavailable small-molecule inhibitor of transcription factor Stat3 regresses human breast and lung cancer xenografts. *Proc National Acad Sci* 109, 9623–9628 (2012).

212. Fagard, R., Meteleev, V., Souissi, I. & Baran-Marszak, F. STAT3 inhibitors for cancer therapy. *Jak-stat* 2, e22882 (2013).

213. Guan, Y. *et al.* G-rich Oligonucleotides Inhibit HIF-1 α and HIF-2 α and Block Tumor Growth. *Mol Ther* 18, 188–197 (2010).

214. Jing, N. *et al.* Targeting Stat3 with G-Quartet Oligodeoxynucleotides in Human Cancer Cells. *Dna Cell Biol* 22, 685–696 (2003).

215. Weerasinghe, P. *et al.* Inhibition of Stat3 activation and tumor growth suppression of non-small cell lung cancer by G-quartet

- oligonucleotides. *Int J Oncol* 31, 129–36 (2007).
216. Johnston, P. A. & Grandis, J. R. STAT3 signaling: anticancer strategies and challenges. *Mol Interv* 11, 18–26 (2011).
217. Hbib, A. *et al.* Efficient killing of SW480 colon carcinoma cells by a signal transducer and activator of transcription (STAT) 3 hairpin decoy oligodeoxynucleotide – interference with interferon- γ -STAT1-mediated killing. *Febs J* 276, 2505–2515 (2009).
218. Koide, A. & Koide, S. Monobodies: antibody mimics based on the scaffold of the fibronectin type III domain. *Methods in molecular biology (Clifton, N.J.)* 352, 95–109 (2007).
219. Verdura, S. *et al.* Silibinin is a direct inhibitor of STAT3. *Food Chem. Toxicol.* 116, 161–172
220. Li, X. *et al.* Novel synthetic bisindolylmaleimide alkaloids inhibit STAT3 activation by binding to the SH2 domain and suppress breast xenograft tumor growth. *Oncogene* 1–12 (2018). doi:10.1038/s41388-017-0076-0
221. Ma, J., Zhang, T., Novotny-Diermayr, V. & of Biological ..., A. A novel sequence in the coiled-coil domain of Stat3 essential for its nuclear translocation. (2003). doi:10.1074/jbc.M304196200
222. Dumoutier, L., de Meester, C., Tavernier, J. & Renauld, J.-C. New activation modus of STAT3: a tyrosine-less region of the interleukin-22 receptor recruits STAT3 by interacting with its coiled-coil domain. *J Biological Chem* 284, 26377–84 (2009).
223. Wingelhofer, B. *et al.* Implications of STAT3 and STAT5 signaling on gene regulation and chromatin remodeling in hematopoietic cancer. *Leukemia* 32, 1713–1726 (2018).
224. Droescher, M., Begitt, A., Marg, A., Zacharias, M. & Vinkemeier, U. Cytokine-induced Paracrystals Prolong the Activity of Signal Transducers and Activators of Transcription (STAT) and Provide a Model for the Regulation of Protein Solubility by Small Ubiquitin-like Modifier (SUMO). *J Biol Chem* 286, 18731–18746 (2011).
225. Riebeling, T., Staab, J., Herrmann-Lingen, C. & Meyer, T. DNA binding reduces the dissociation rate of STAT1 dimers and impairs the interdimeric exchange of protomers. *Bmc Biochem* 15, 28 (2014).
226. Chiarle, R., Simmons, W., Cai, H., Dhall, G. & medicine, Z.-A. Stat3 is required for ALK-mediated lymphomagenesis and provides a possible therapeutic target. *Nature medicine* (2005).
227. Porebski, B. T. *et al.* Circumventing the stability-function trade-off in an engineered FN3 domain. *Protein Eng Des Sel* 29, 541–550 (2016).
228. Gilbreth, R. N. & Koide, S. Structural insights for engineering binding proteins based on non-antibody scaffolds. *Curr Opin Struc Biol* 22, 413–420 (2012).

CURRICULUM VITAE

Grégory La Sala

Chemin de Bérée 18b ▪ 1010 Lausanne (VD) ▪ www.linkedin.com/in/gregorylasala
Phone: 079 265 35 02 ▪ Email: gregory.lasala@gmail.com ▪ Born 01. June. 1992 ▪
Swiss/Italian

Profile

- PhD in Molecular Life Sciences EPFL in cancer targeted therapies biology.
- Strong background in Cancer, Immunology and Protein biochemistry.
- Excellent organizational and interpersonal abilities.

Education

PhD in Molecular Life Sciences ISREC : Swiss Institute for Experimental Cancer Research
École Polytechnique Fédérale de Lausanne – EPFL Expected April 2020

Master in Medical Biology Immunology and Cancer 2014 - 2016
University of Lausanne - UNIL

3rd year of BS in Biology International Exchange Program 2013 - 2014
University of Alaska Fairbanks – UAF (USA)

Bachelor of Sciences in Biology 2011 - 2013
University of Neuchâtel - UNINE

Professional experience

EPFL

- **Doctoral Thesis – Molecular life sciences** 2016-2020
Targeting « undruggable » intracellular signaling mechanisms and oncogenic networks using state of the art engineered protein inhibitors

Project director : Prof. Oliver Hantschel

- **Undergraduate Teaching**
Biological Chemistry I and II: Over 300 hours, including exercises and exam supervision

Lecturers : Prof. Oliver Hantschel and Prof. Bruno Coreia

CHUV

- **Master Project – Immuno-oncology** 2015-2016
Development of a novel Human papillomavirus (HPV) vector mediated tumor selective near infrared photodynamic therapy towards immunogenic treatment of bladder cancer

Project director : Dr. Denise Nardelli Haefliger

LICR

- **Master Traineeship – Fundamental T cell immunology** 2014-2015
Regulation of Wnt Receptor expression by CD8 T cells

Project director : Prof. Werner Held

Languages

French : Native Language / **Italian** : Confirmed (C1) - Dante Alighieri Certificate / **English** :
Confirmed (C1) - Cambridge First Certificate / **German** : Written and Spoken (A2-B1)

Curriculum Vitae

Lab-Skills

- **Molecular Biology** : Site-directed Mutagenesis, Conventional, Gateway and InFusion Cloning.
- **Biochemistry** : Protein expression in E.Coli, purification using ÄKTA systems and protein characterization, including SDS-PAGE, Gel filtration, Fluorescence polarization and Protein crystallography.
- **Protein library screening** : Phage and yeast display.
- **Cellular Studies** : Cell culture of adherent and suspension cells, isolation and culture of mice primary cells, transient transfection and transduction using Lenti. and retroviruses (BS2), establishment of constitutive and inducible engineered cell lines.
- **Immuno-staining techniques** : Multicolor Flow Cytometry, Immuno-fluorescence and confocal/Wide Field Fluorescent microscopy and Western blotting.
- **In-vivo studies** : LTK1 module (Training in Animal Experimentation), Xenogen Bio-imaging
- **Project management**: PRINCE2 certification

IT

Statistical software: Graph-Pad Prism
3D protein modeling: Pymol, , Coot
Figures design: Adobe Illustrator

DNA editing softwares: Geneious, SnapGene
Data analysis: ImageStudio, ImageLab, FlowJo
Microsoft office: Word, Powerpoint, Excel

Soft-Skills

Excellent organizational abilities
Problem Solving Skills

Objectivity
Public Speaking

Team Work
Integrity

Honors

EFPL life-sciences faculty Health Hackathon : Best project proposal	2019
Swiss Cancer Center Leman retreat (SCCL) : Best poster prize winner	2019
European Molecular Biology Organization (EMBO) : Short term fellowship	2019
University of Lausanne (UNIL) : Overall grade 5.5/6	2016
University of Alaska Fairbanks (UAF) : Dean's list - Outstanding students	2014
University of Neuchâtel (UNINE) : Academic reference Magna Cum Laude	2014
Maturity thesis (Denis-de-Rougemont) : Academic reference Insigni Cum Laude	2011

Publications

- **G. La Sala, et al.** Selective targeting and inhibition of STAT3 signaling using Coiled-coil and N-terminal domain specific monobodies. 2020.
Nature communications, submitted
- T. Kükenshöner, **G. La Sala, et al.** Modulating the function of the RING E3 Ubiquitin Ligase CBL with Monobodies. 2020.
Manuscript in preparation

Extracurricular activities

President : Association des Doctorant en Science de la Vie (ADSV)	Elected in 2019
Board Member of the ADSV	Promoted in 2018
EPFL PhD representative for Molecular life sciences doctoral school	Elected in 2017
Committee Member of the martial art Vo-Vietnam Club Neuchâtel	2013-2014

